

Aus der Medizinischen Klinik für Kardiologie
und dem
Berliner Institut für Gesundheitsforschung
- Zentrum für Regenerative Therapien
der Medizinischen Fakultät Charité – Universitätsmedizin Berlin

DISSERTATION

Identification of microRNAs promoting proliferation in human induced pluripotent stem cell-derived cardiomyocytes using a functional high-throughput screening

zur Erlangung des akademischen Grades
Doctor rerum medicinalium (Dr. rer. medic.)

vorgelegt der Medizinischen Fakultät
Charité – Universitätsmedizin Berlin

Von

Harsha Vardhan Renikunta
aus Mancherial, Indien

Datum der Promotion: 17.09.2021

TABLE OF CONTENTS

TABLE OF CONTENTS

1. ABBREVIATIONS	1
2. ZUSAMMENFASSUNG	6
3. ABSTRACT	8
4. INTRODUCTION	9
4.1 Ischemic heart diseases	9
4.2 Myocardial infarction and cardiomyocyte loss	9
4.3 Strategies in achieving heart regeneration	10
4.3.1 Cardiomyocyte cell-cycle activity	10
4.3.2 Cell-cycle regulators in cardiac regeneration	13
4.3.3 Hippo/Yap-signalling in cardiac regeneration.....	14
4.3.4 Hypoxia in cardiac regeneration.....	14
4.4 Human induced pluripotent stem cell derived cardiomyocytes for cardiac regeneration.....	17
4.5 MicroRNAs as therapeutics	20
4.5.1 MicroRNA biology	20
4.5.2 Role of microRNAs in cardiac remodelling.....	22
4.5.3 Role of microRNAs in cardiomyocyte proliferation	23
4.6 High throughput screening of libraries	24
5. AIM OF THE STUDY	27
5.1 Project specific aims.....	27
6. MATERIALS	28
6.1 Reagents	28
6.2 Microscopes	29
6.3 PCR Systems	29
6.4 Centrifuges	30
6.5 Buffers and solutions	30

TABLE OF CONTENTS

6.6	Growth Media	31
6.7	Kits	33
6.8	Cells and cell lines.....	33
6.9	Hit candidate microRNAs	34
6.10	List of human primers.....	34
6.11	Primary Antibodies	35
6.12	Secondary Antibodies	36
6.13	Computer Softwares	38
7.	METHODS	39
7.1	Cell Culture-related methods.....	39
7.1.1	Generation of human iPSC cardiomyocytes	39
7.1.2	Human iPSC-cardiomyocytes selection and culture	39
7.1.3	Splitting of human iPSC-cardiomyocytes	39
7.1.4	MiRNA and siRNA transfection of human iPSC-CMs	40
7.1.5	Functional high-throughput screening in human iPSC-CMs	40
7.1.6	High content imaging in human iPSC-CMs.....	42
7.1.7	Image analysis of human iPSC-CMs	42
7.1.8	Data Processing (Z-score)	42
7.1.9	EdU cell proliferation assay in human iPSC-CM.....	43
7.1.10	Lactate dehydrogenase (LDH) cytotoxicity assay.....	43
7.1.11	Isolation and culture of neonatal cardiomyocytes from mouse hearts using MACs cardio isolation procedure.....	44
7.1.12	Transfection of microRNAs in neonatal mouse cardiomyocytes.....	45
7.1.13	Immunocytochemistry.....	45
7.1.14	Coating of plates.....	46
7.2	RNA-related methods.....	46
7.2.1	RNA extraction from hiPSC-CM.....	46

TABLE OF CONTENTS

7.2.2	Reverse Transcription (cDNA Synthesis).....	46
7.2.3	Quantitative Real-Time PCR (qRT-PCR).....	47
7.2.4	Quantification of miRNA by TaqMan microRNA assays (RT-PCR).....	48
7.2.5	qRT-PCR of miRNAs	49
7.2.6	RNA-sequencing.....	50
7.2.7	Image Analysis and data processing	51
7.3	Protein related methods	51
7.3.1	Protein Isolation	51
7.3.2	Immunoblotting (SDS-PAGE).....	52
7.3.3	Western blotting	52
7.4	Image quantification	53
8.	RESULTS.....	54
8.1	Generation and transfection of human induced pluripotent stem cell-derived cardiomyocytes (hiPSC-CMs)	54
8.2	Transient hypoxia enhances proliferative activity in hiPSC-cardiomyocytes after transfection with miRNAs	56
8.3	High throughput screening of human microRNAs	58
8.4	Selective overexpression, but not downregulation of miRNAs induces proliferative activity in human iPSC-CMs as assessed by HTS	58
8.5	Hsa-miR-515-3p, hsa-miR-519e-3p and hsa-miR-371a-3p substantially induce DNA synthesis in human iPSC-CMs	61
8.6	Hsa-miR-515-3p, hsa-miR-519e-3p and hsa-miR-371a-3p induce late G2/Mitosis in human iPSC-CMs	63
8.7	Concentration-dependent EdU Incorporation and toxicity assessment after miRNA-transfection.....	64
8.8	Long-term effects of miRNA-transfections in cardiomyocyte proliferation	68
8.9	MiR-515-3p and miR-519e-3p markedly alter expression of genes involved in proliferation, dedifferentiation and hypertrophy	69

TABLE OF CONTENTS

8.10	Hsa-miR-515-3p, hsa-miR-519e-3p and hsa-miR-371a-3p regulate cell-cycle genes on protein level	72
8.11	The primate specific miRNAs - miR-515-3p and miR-519e-3p are effective in mouse cardiomyocytes	73
8.12	Transcriptome analysis after overexpression of miR-515-3p and miR-519e-3p in human iPSC-CMs reveals substantial changes on structural organization and proliferation pathways	74
9.	DISCUSSION	81
10.	CONCLUSION.....	88
11.	FUTURE PERSPECTIVES.....	90
12.	REFERENCES	91
13.	STATUTORY DECLARATION.....	104
14.	CURRICULUM VITAE	105
15.	ACKNOWLEDGEMENTS	108

LIST OF TABLES

Table 1 Reagents used for cell culture	28
Table 2 Microscope details.....	29
Table 3 PCR systems	29
Table 4 Centrifuge type, model and supplier	30
Table 5 List of solutions	30
Table 6 List of media.....	31
Table 7 List of kits	33
Table 8 Cells and cell-lines	34
Table 9 List of selected microRNAs	34
Table 10 List of human primers for qRT-PCR	34
Table 11 List of primary antibodies for immunofluorescence staining's	35
Table 12 List of primary antibodies for Western blot.....	36
Table 13 List of secondary antibodies for immunofluorescence staining's	37
Table 14 List of secondary antibodies for Western blot	37
Table 15 List of computer software	38
Table 16 List of Reagents and kits for neonatal mouse cardiomyocytes. .	45
Table 17 Reaction mix for cDNA synthesis	47
Table 18 Thermal cycler program (cDNA)	47
Table 19 Components for performing qRT-PCR.....	48
Table 20 Thermal cycler program (qRT-PCR).....	48
Table 21 Composition of RT-PCR master mix.....	48
Table 22 Program for RT-PCR.....	49
Table 23 Composition of qRT-PCR master mix.....	49
Table 24 Program to perform qRT-PCR by fast advanced master mix.	50
Table 25 List of TaqMan miRNA primers and controls.	50

LIST OF FIGURES

Figure 1: Schematic representation of cardiomyocyte cell cycle activity... 11	11
Figure 2: Expression and activity of cell cycle proteins in cardiomyocytes at different stages of cardiac development. 13	13
Figure 3: Comparison of cardiac regeneration and oxidative metabolism across vertebrate species. 15	15
Figure 4: Steps to overcome the hurdles in cardiac regenerative therapy. 18	18
Figure 5: Evolution of translational cardiac regenerative therapies over time. 19	19
Figure 6: MicroRNAs in cardiovascular diseases 21	21
Figure 7: High Throughput screening workflow in hiPSC-CMs 41	41
Figure 8: Efficient generation and transfection of human iPSC-derived cardiomyocytes. 55	55
Figure 9: Transient hypoxia increases miRNA-induced proliferative potential in human iPSC-cardiomyocytes 57	57
Figure 10: High-throughput screening for identification of pro-proliferative miRNAs..... 61	61
Figure 11: Overexpression of hsa-miR-515-3p, hsa-miR-519e-3p and hsa-miR-371a-3p induce DNA synthesis in human iPSC-CM 62	62
Figure 12: Overexpression of hsa-miR-515-3p, hsa-miR-519e-3p and hsa-miR-371a-3p induce late mitosis in human iPSC-CM..... 63	63
Figure 13: Concentration-dependent EdU Incorporation and toxicity assessment after miRNA-transfection 67	67
Figure 14: Prolonged effects of EdU Incorporation, and late G2 mitosis assessment after miRNA-transfection 68	68
Figure 15: Overexpression of hsa-miR-515-3p and hsa-miR-519e-3p modulates genes involved in cardiomyocyte proliferation, hypertrophy and dedifferentiation 71	71

TABLE OF CONTENTS

Figure 16: Overexpression of hsa-miR-515-3p and hsa-miR-519e-3p regulate cell-cycle genes on protein level.....	72
Figure 17: Hsa-miR-515-3p and hsa-miR-519e-3p induce proliferation in mouse cardiomyocytes	74
Figure 18: RNA-Seq reveals a strong regulation of hsa-miR-519e-3p for biological processes involved in cardiac muscle regeneration.....	79

ABBREVIATIONS

1. ABBREVIATIONS

µg	Microgram
µl	Microliter
All stars	Cell Death Control Small interfering RNA
ATF4	Activating transcription factor 4
BSA	Bovine serum albumin
C3H5NaO3	Sodium lactate
CaCl ₂	Calcium chloride
CM	Cardiomyocytes
cTnT	Cardiac Troponin T
cDNA	Complementary DNA
CDKNA	Cyclin-dependent kinase inhibitor
CIP/KIP	Cdk interacting protein/kinase inhibitory protein
DNA	Deoxyribonucleic acid
DGCR8	DiGeorge Syndrome Critical Region 8
dNTP	Deoxyribonucleotide triphosphate
DMEM	Dulbecco's modified eagle medium
dH ₂ O	Distilled water
EdU	5-ethynyl-2'-deoxyuridine
ESC	Embryonic stem cells
FCS	Fetal Calf Serum
FBS	Fetal Bovine Serum
FAM-miR	Carboxyfluorescein (FAM™) Dye-Labeled Pre-miR™

ABBREVIATIONS

g	Acceleration of gravity
g	Gram
GAPDH	Glyceraldehyde-3-phosphate dehydrogenase
HEK	Human embryonic kidney
HEPES	4-(2-hydroxyethyl)-1-piperazine ethane sulfonic acid
HRP	Horseradish peroxidase
H3P	Histone H3 phosphorylated on serine10
HiPSC	Human induced Pluripotent stem cells
HIF1-Alpha	Hypoxia-inducible factor 1-alpha
HTS	High throughput screening
HCS	High content imaging
Hoechst	Trihydrochloride, Trihydrate
Hox-B13	Homeobox protein
h	Hour(s)
IHD	Ischemic Heart Diseases
ICC	Immunocytochemistry
KCl	Potassium chloride
Klf4	Krüppel-like factor
KH ₂ PO ₄	Monopotassium phosphate
KDa	Kilo Dalton
LDH	Lactate dehydrogenase
LATS1	Large Tumour Suppressor Kinase 1
L	Liter

ABBREVIATIONS

M	Molar
Meis 1	Myeloid Ecotropic Viral Integration Site 1
MOB1B	Mps one binder kinase activator 1B
MgSO ₄	Magnesium Sulfate
mg	Milligram
min	Minute
miR	MicroRNA
MI	Myocardial Infarction
ml	Milliliter
mM	Millimolar
mmol	Millimol
ng	Nanogram
mRNA	Messenger RNA
MYL2	Myosin regulatory light chain 2
MYL7	Myosin regulatory light chain 7
MYOM2	Myomesin 2
MYOM3	Myomesin 3
NaCl	Sodium chloride
NaHCO ₃	Sodium bicarbonate
NPPA	Natriuretic Peptide Precursor A
NPPB	Natriuretic Peptide Precursor B
ng	Nanogram
NP40	Nonidet P40

ABBREVIATIONS

Oct-3/4	Octamer binding transcription factor 4
P	Postnatal day
PBS	Phosphate buffered saline
PCR	Polymerase chain reaction
pH	Negative logarithm of hydrogen ion concentration
PMSF	Phenyl methane sulfonyl fluoride
RISC	RNA-induced silencing complex
RAN	RAs-related nuclear protein
RNA	Ribonucleic acid
RNase	Ribonuclease
Rpm	Revolutions per minute
RT	Room temperature
RT-PCR	Reverse transcription followed by polymerase chain reaction
SAV1	Salvador homologue 1
SDS	Sodium dodecyl sulfate
SOX2	SRY-box2
siRNA	Small interfering RNA
S	Second
TBS	Tris-buffered saline
U	Unit
V	Volt
C-myc	V-myc myelocytomatosis viral oncogene homolog
VGEF	Vascular endothelial growth factor

ABBREVIATIONS

W	Watt
WB	Western blot
YAP	Yes associated protein
W/v	Weight/volume
V/v	Volume/volume

2. ZUSAMMENFASSUNG

Bei Erwachsenen führt ein Myokardinfarkt zum Untergang von Kardiomyozyten (CM), woraufhin es zu anschließender Narbenbildung mit Symptomen der Herzinsuffizienz kommen kann. Obwohl neue Behandlungsansätze die Lebensdauer von Patienten mit Herzinsuffizienz verlängern, kann bisher der geschädigte, nicht-kontraktile Herzmuskel nicht geheilt werden. Dies führt zu einer inakzeptabel hohen Prävalenz von Patienten mit Herzinsuffizienz.

Im vorliegenden Projekt haben wir im Labor von Dr. Jakob/Prof. Landmesser ein Transfektionsprotokoll für microRNAs in humanen induzierbaren pluripotenten Stammzellen (iPSC)-Kardiomyozyten mittels einem Lipid-basierten Ansatz etabliert. Zudem haben wir verschiedene Methoden getestet, um eine Hypoxie und Reoxygenierung in vitro nachzuahmen. Diese Protokolle wurden erfolgreich in einem 384-Well-Format transferiert, welches für ein Hochdurchsatz-Screening geeignet ist. Darüber hinaus wurden fluoreszenzbasierte Färbungen zur Detektion von proliferierenden Kardiomyozyten (5-Ethynyl-2'-desoxyuridin (EdU), phosphoryliertes Histon H3 (pH3)) in hiPSC-Kardiomyozyten etabliert. Nach Erreichen dieses wichtigen Meilensteins wurde am Leibniz-Institut für Molekulare Pharmakologie (FMP, Campus Berlin-Buch) das Hochdurchsatzverfahren durchgeführt.

Als Modellsystem verwendeten wir humane iPSC, die in Kardiomyozyten differenziert wurden. Zwei parallele Hochdurchsatz-Screenings zur Identifizierung pro-proliferativer microRNAs (miRNAs) in humanen Kardiomyozyten wurden umgesetzt. Nach individueller Transfektion von 2019 miR-mimics und anti-miRs mittels einer microRNA-Bibliothek wurden Surrogatmarker der Zellproliferation mittels high-content Imaging analysiert.

Die vorliegende Studie hat zum ersten Mal eine Bibliothek aus 2019 anti- und mimic-miRNAs getestet, um microRNAs zu identifizieren, welche eine zentrale Rolle für den Wiedereintritt in den Zellzyklus in humanen iPSC-Kardiomyozyten spielen. Die Überexpression zweier miRNAs – miR-515-3p und miR519e-3p - führte in verschiedenen funktionellen und molekularen Validierungsexperimenten zu einem signifikanten Anstieg der Zell-Proliferation. Da die ausbleibende Zellproliferation der Kardiomyozyten und somit der Verlust des kontraktiven Herzmuskels bei Patienten mit Herzinfarkt die primäre Ursache der Herzinsuffizienz darstellt, bieten die identifizierten microRNAs einen

ZUSAMMENFASSUNG

potenziellen Therapieansatz zur Wiederherstellung des Herzmuskels über eine Anregung der proliferativen Signaltransduktionswege in Kardiomyozyten.

3. ABSTRACT

In adults, cardiac injury results in loss of cardiomyocytes (CM) and subsequent scar formation with heart failure symptoms. Although novel treatment approaches prolonged life span of patients with heart failure, the damaged myocardium cannot be cured, resulting in an unacceptable high prevalence of patients suffering from heart failure.

In the current project, during the last years in the laboratory of Dr. med. P. Jakob/Prof. Dr. med. U. Landmesser, we established a forward microRNA-transfection protocol using a liposome-based approach in human iPSC-cardiomyocytes (iPSC-CMs) that results in a high transfection efficiency. This protocol was successfully transferred to a 384-well format that is suitable for a high-throughput screening. In addition, fluorescent staining protocols for read-out of proliferation markers (5-ethynyl-2'-deoxyuridine (EdU), phosphorylated histone H3 (pH3)) have been performed and optimized in human iPSC-CMs. In addition, a protocol that mimics hypoxia/reoxygenation in human iPSC-CMs has been established. After the accomplishment of these important milestones, we later transferred the protocol to the Screening Unit at Leibniz-Institute for Molecular Pharmacology (FMP, Campus Berlin-Buch) to conduct a functional high-throughput screening.

As a model system, we used human iPSC that were differentiated into cardiomyocytes. Two parallel high-throughput screenings for the identification of pro-proliferative microRNAs (miRNAs) in human cardiomyocytes were performed after individual transfection of 2019 miR-mimics and anti-miRs using a microRNA-library. Surrogate markers of cell proliferation were analyzed by high content imaging.

For the first time, we utilized a library of 2019 anti- and mimic-miRNAs to identify miRNAs that exert a central role in the induction of cell-cycle reentry and enhancement of proliferation in human cardiomyocytes. Of note, overexpression of two miRNAs - miR-515-3p und miR519e-3p - resulted in a significant induction of proliferation as assessed using functional and molecular validation methods. As withdrawal of adult human cardiomyocytes from the cell-cycle is the primary reason for inadequate replenishment and thus for heart failure in patients after myocardial injury, the identified miRNAs may represent novel potential therapeutic targets for the treatment of myocardial injury and ischemic cardiomyopathy.

4. INTRODUCTION

4.1 Ischemic heart diseases

Cardiovascular diseases (CVDs), especially ischemic heart disease (IHD), remain the leading cause of deaths in the world. Annually an average of 17.3 million deaths are accountable due to IHD. ¹ IHD is also referred to coronary heart disease (CHD) or coronary artery disease (CAD). Etiology of IHD includes acute or chronic obstruction of the coronary blood flow to the cardiac muscle. This obstruction happens due to varied reasons, most commonly due to coronary plaque formation and thrombus formation after plaque rupture such as seen in patients with acute coronary syndrome. Once the disease is established, it eventually leads to temporary or permanent loss of oxygenated blood supply thus causing death of cardiomyocytes. Loss of cardiomyocytes results into decreased contractility and hence, reduced cardiac function. ^{2,3} Cardiomyocyte cell death may occur progressively as consequence of constantly reduced oxygen supply or suddenly in patient with myocardial infarction that may result in loss of more than a quarter of heart muscle. Myocardial infarction remains the most common cause of heart failure (HF). Despite progress made over the last decades, heart failure remains the most significant health issue worldwide. Computational analysis predicts that every 42 seconds a citizen suffers from myocardial infarction and 1 out of 7 deaths are caused by coronary heart disease in the United States. ⁴

4.2 Myocardial infarction and cardiomyocyte loss

Myocardial infarction is due to occlusion or narrowing of coronary arteries in the heart. Coronary arteries supply oxygen-rich blood and nutrients to the heart muscle. The narrowing of the coronary artery is a result of deposition of atherosclerotic plaques (cholesterol and fatty deposits) and may be complicated by thrombotic events. ² This deposition of the plaques can cause obstruction of the coronary arteries thereby limiting blood flow to the heart muscle that leads to damage or death of cardiomyocytes (CM). Loss of CMs is most prominent in the course of MI, which leads to inflammatory response, infiltration of neutrophils, hypoxia and formation of fibrous tissue, with subsequent scar formation that ultimately compromise the heart function. ³ The heart is one of the organs with least regenerative capacity compared to other tissue such as skin, liver, skeletal muscle, gut, bladder, lung and bone. There are approximately four billion cardiomyocytes

that build the left ventricle. One billion cardiomyocytes may be wiped out within a few hours post myocardial infarction.⁵ In this regard, it is of utmost importance to prevent the loss of cardiomyocytes, as the damaged myocardium is irreparable. The adult heart was considered as a post-mitotic organ. However, recent studies have reported that few cardiomyocytes may undergo mitosis in the diseased adult heart in an attempt to regenerate the myocardium.⁶⁻⁸ It was also shown that in adolescence, a negligible count of cardiomyocytes within the human heart undergoes cell cycle re-entry.⁹ However, even if cardiomyocyte proliferation does occur, the rate is too low to repair the injured heart. Therefore, novel regenerative strategies to increase cell cycling of human cardiomyocytes with subsequent regeneration of the heart muscle is urgently needed.

4.3 Strategies in achieving heart regeneration

4.3.1 Cardiomyocyte cell-cycle activity

Cardiomyocyte cell cycle activity diminishes during the postnatal heart growth due to the downregulation of pro-mitotic factors such as cyclins and their dependent kinases, which play a crucial role in cardiac regeneration.¹⁰ The fact that proliferation of cardiomyocytes occurs during the early development and for a short time after birth, but is not evident in later stages, makes the transition of cell-cycle withdrawal and re-entry an interesting model to study. The events that occur in a cell leading to its duplication and division, are regulated as part of the cell cycle (**Figure. 1**). There are four discrete phases in the mammalian cell cycle (G1, S, G2 and M). The G1 (Gap) phase is where the cell prepares to divide. Therefore, the cell enters the S phase (synthesis), where the DNA replication occurs. Later the cell moves into G2 (gap) phase where the genetic material is organized, and the cell prepares to divide. The later phase is the M-Phase (Mitosis), where the cell divides into two daughter cells. The M-mitosis phase comprises the division of the nucleus, which is termed karyokinesis, and division of the cytoplasm, which is termed cytokinesis. Mitosis is comprised of five different phases; these include prophase, prometaphase, metaphase, anaphase and telophase. Cytokinesis is the final step in the cell cycle to achieve cell division (**Figure. 1**).^{11, 12} Adult cardiomyocytes fail to achieve cytokinesis leading to multi-nucleation and polyploidization as cell cycle activity is tightly regulated in the cardiomyocytes by the expression of several protein complexes called

INTRODUCTION

the cyclin dependent kinases (CDK Complexes). CDK activities are controlled by cyclin dependent kinase inhibitors such as p21, p27 and p57. ¹²

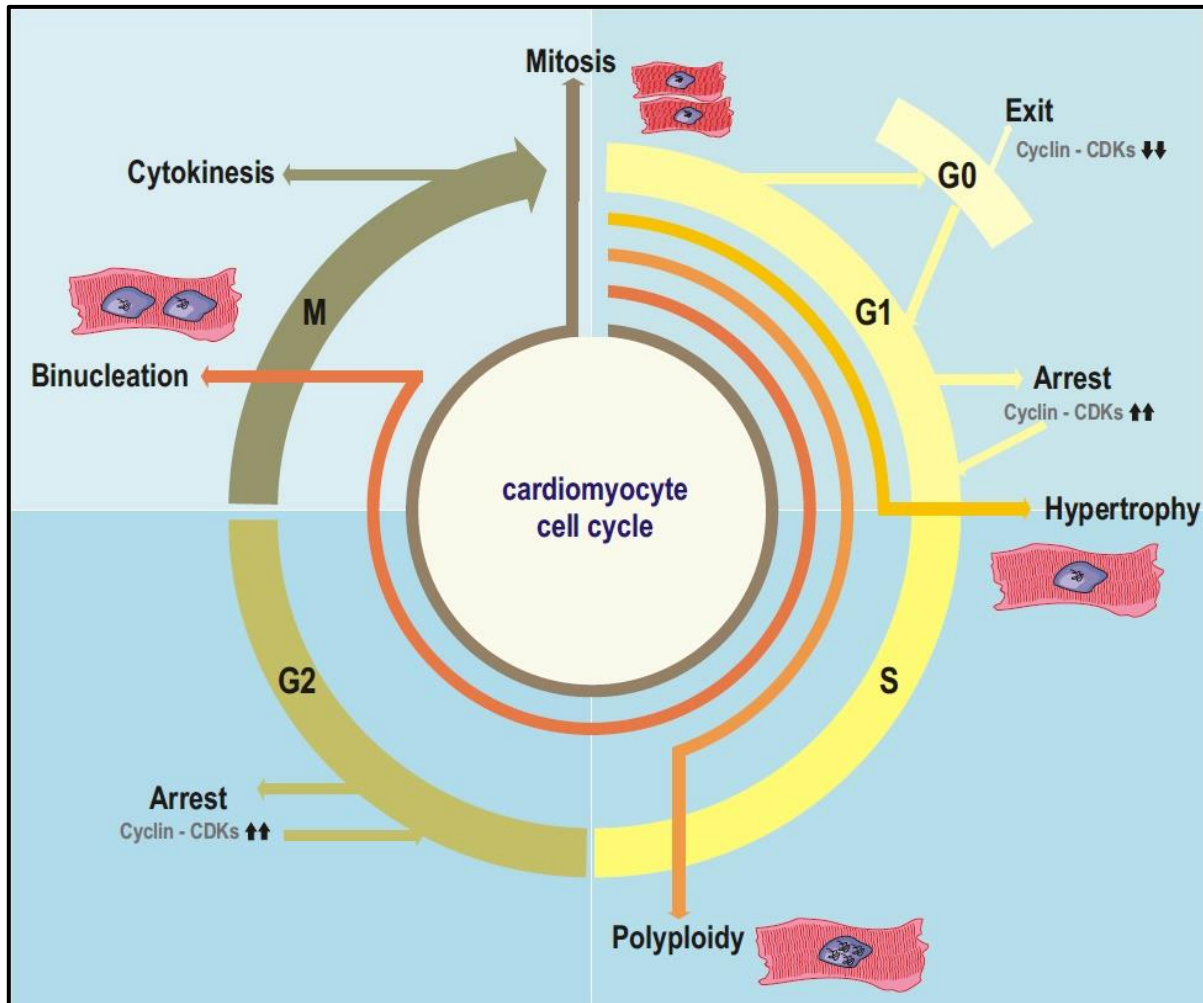


Figure 1: Schematic representation of cardiomyocyte cell cycle activity.

There are four discrete phases in the mammalian cell cycle (G1, S, G2 and M). The word “exit” refers to G0 arrest, due to lack of cyclins and cyclin dependent kinase complexes. The term “arrest” refers to a non-G0 arrest (G1 or G2), caused due to the high levels of cyclin-dependent kinase complexes. Figure adopted from Locatelli. P *et al.*, 2019. ¹³

During cardiac development, the fetal heart grows through proliferation of cardiomyocytes. But shortly after birth, the mammalian cardiomyocytes enter into a terminal state of the cell cycle, resulting in bi-nucleation or poly-nucleation, due to failure of cytokinesis, ^{14, 15} as a consequence of upregulation of cell cycle Inhibitors (e.g. p21, p27, p57, p15, p16 and p18) and by downregulation of cell-cycle activators (e.g., Cyclin A, B, D and E). ^{8, 13, 15} Cell cycle dependent kinases and cyclins are highly expressed in

INTRODUCTION

fetal cardiomyocytes, which help the cells to progress through G1, S, G2 and M-phase to achieve cell division. The levels of these proteins are downregulated significantly in adult cardiomyocytes, resulting in a decline of cardiomyocyte proliferation (**Figure. 2**).¹⁶⁻¹⁸ Therefore some studies have focussed on stimulating the cell cycle activity in the cardiomyocytes either by activating or blocking the cell cycle regulators.¹⁹

Expression /Activity of Major Cell cycle Proteins				
	EMBRYONIC STAGE	MID-GESTATION TO BIRTH	NEONATAL & EARLY POSTNATAL	POSTNATAL & ADULT
Cell Cycle Activators				
Cyclin D	●	●	●	○
Cyclin E	●	●	●	○
Cyclin A	●	●	○	○
Cyclin B	●	●	○	○
CDK1	●	●	○	○
CDK2	●	●	○	○
CDK4	●	●	○	○
CDK6	●	●	○	○
Cdc2	●	●	○	○
Cell Cycle Inhibitors				
p21	○	○	●	●
P27	○	○	●	○
p57	○	○	○	○
P16	○	○	○	○
p18	○	○	○	●
Rb	○	○	○	●
p107	●	○	○	○
p130	○	○	○	○

Figure 2: Expression and activity of cell cycle proteins in cardiomyocytes at different stages of cardiac development.

Dark shades (●) are the indicators for higher expression and lighter shades (● ● ○) for lower activity. Empty circles (○) indicate that the proteins are rarely detectable or undetectable.

Figure adopted from Ponnusamy. M *et al.*, 2017. ¹⁸

4.3.2 Cell-cycle regulators in cardiac regeneration

In an effort to stimulate cardiomyocyte proliferation, the cyclin-dependent kinase (CDK) pathway was targeted. In particular, cell cycle activators such as cyclin D1 and D2 overexpression in the adult heart stimulated DNA synthesis and resulted in regression of the infarct after cardiac injury in mice. ²⁰ It was also shown that cell cycle re-entry of neonatal cardiomyocytes can be achieved through activation of Notch signaling, by targeting cyclin D1. ²¹ Notch signalling pathway plays a crucial role in cell signalling that is mediated by four Notch receptors (Notch1-Notch4). These play a key role during embryonic heart development and are essential for the development of ventricular chamber formation in the heart. ²¹ Another interesting study focussed on the transcription factor Myeloid Ecotropic Viral Integration Site 1 (Meis 1). Meis1-overexpression induced cardiomyocyte cell cycle arrest and blocked the heart regeneration under stress conditions, through transcriptional activation of cyclin-dependent kinase inhibitors p15, p16 and p21. ²² Double knockout of Meis 1 and its co-factor Homeobox protein (Hox-B13) induced cardiomyocyte mitosis and improved systolic left ventricular function post myocardial infarction. ²³ It was also shown that combination of four cell cycle regulators (Cyclin B1, Cyclin D1, Cdk1 and Cdk4) induced post-mitotic cell division in cardiomyocytes in different species such as mice, rats including human induced pluripotent stem cell derived cardiomyocytes (hiPSC-CMs). Combination of these four cell cycle regulators further improved stable cytokinesis and improved cardiac function in mice, suggesting a therapeutic role for activation of cell cycle regulators for cardiac regeneration. ²⁴ In addition to the intrinsic factors, cardiomyocyte cell cycle can also be stimulated by extrinsic signalling mechanisms such as Hippo/Yap signalling and oxidative stress and oxygen metabolism that could play a crucial role in regulating proliferation of

INTRODUCTION

mammalian cardiomyocytes, by inducing cardiac regeneration.²⁵ Therefore, both mechanisms are described in the following paragraphs.

4.3.3 Hippo/Yap-signalling in cardiac regeneration

Hippo/Yap (Yes-associated protein) signalling is an evolutionarily conserved pathway, that plays a crucial role in controlling organ size and cell proliferation.²⁶ The main components of Hippo pathway consist a kinase cascade, such as mammalian STE20-like kinase (MST1 and MST2), large tumour suppressor homologue (LATS1 and LATS2), protein Salvador homologue 1 (SAV1) and its transcriptional coactivators that are downstream effectors YAP and WW-domain-containing transcription regulator 1 (TAZ) that shuttles between nucleus and cytoplasm depending on the response to multiple signals. When the Hippo signalling is activated, YAP is inactive in the cytoplasm where, LATS1 is phosphorelated by MST1, which then further phosphorylates YAP/TAZ. When Hippo is inactivated, YAP/TAZ interacts with members of transcriptional enhancer factor domain (TEAD) and regulates transcription of genes and the nuclear YAP/TAZ promote cell proliferation and de-differentiation of post-mitotic cells.²⁷ Hippo pathway is an important regulator, which controls proliferation of cardiomyocytes and heart size. SAV1 genetic deletion at birth increased cardiomyocyte proliferation.²⁸ Whereas, MST1²⁹ or LATS2³⁰ overexpression resulted in dilated cardiomyopathy and stimulated apoptosis in postnatal heart, which supports an essential key role of this pathway in embryonic and fetal development with the regulation of cardiomyocyte proliferation. Activation of Hippo pathway blocks cardiac regeneration, whereas adult mice with Hippo deficiency induced cardiomyocyte cell cycle re-entry and promoted cytokinesis.³¹ Inactivation of YAP1 in fetal heart resulted in lethal cardiac hypoplasia, while overexpression of YAP1 stimulated postnatal cardiomyocyte proliferation.³² Administration of SAV1 targeted short hairpin RNAs post myocardial infarction improved heart function³³ suggesting that targeting Hippo pathway could be promising therapeutic approach for treating myocardial infarction and enhancing cardiac regeneration.

4.3.4 Hypoxia in cardiac regeneration

Under oxygen deficiency (hypoxia) or anaerobic conditions, the mammalian heart muscle cannot produce enough energy to maintain cellular processes. Therefore, a constant oxygen supply is a vital factor for the viability and function of cardiac cells.³⁴ There is a

INTRODUCTION

strong association between cardiomyocytes proliferative capacity and oxidative metabolism in different species of vertebrates ²⁵ (**Figure. 3**).

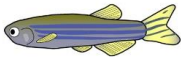
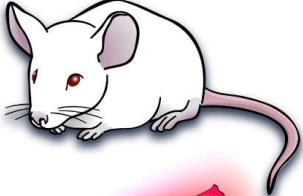
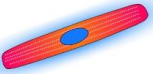
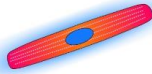
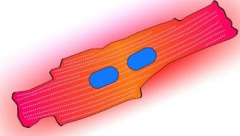
	Adult Zebrafish	Adult Newt	fetal/neonatal Mouse	Adult Mouse
				
Cardiomyocytes				
Injury response	Regenerative	Regenerative	Regenerative	Non-regenerative
Cardiomyocyte growth	Hyperplastic	Hyperplastic	Hyperplastic	Hypertrophic
Cardiomyocyte nucleation	Mononucleated	Mononucleated	Mononucleated	Bi- or Multi-nucleated
Oxygenation state	Low	Low	Low	High
Mitochondrial respiration	Low	?	Low	High
Oxidative stress	Low	?	Low	High

Figure 3: Comparison of cardiac regeneration and oxidative metabolism across vertebrate species.

Figure adopted from Kimura. W *et.al.*, 2017 ²⁵

Embryonic and neonatal cardiomyocytes depend on glycolysis as a source of energy, whereas due to high metabolic needs in postnatal cardiomyocytes, the energy sources utilized by these cells are through mitochondrial respiration. ²⁵ A study described, oxidative metabolism upregulation is the upstream signal, leading to cell cycle arrest of postnatal cardiomyocytes, which is due to the oxygen rich environment. They show, in the heart, especially during the postnatal week, there is a significant increase in the markers for oxidative DNA damage, and DNA damage response (DDR). Rivetingly, either inhibition of DDR or postnatal hypoxemia increases the proliferation potential in postnatal cardiomyocytes, where reactive oxygen species and hyperoxemia shortens the

INTRODUCTION

proliferative window.³⁵ Hypoxia is mainly considered a pathological phenomenon, in fact, the mammalian embryo develops in an environment with low oxygen.³⁶ Hypoxia also plays a major role in differentiation, proliferation and maintenance of embryonic stem cell derived cardiomyocytes (ESC). The molecular mechanism is not well understood, regarding why, low oxygen environments, directs ESCs to differentiate into cardiomyocytes. At the molecular level, hypoxia is mediated by the transcription factor hypoxia inducible factor -1 (HIF-1), and its alpha subunit, hypoxia inducible factor -1 (HIF-1 α) which helps in promotion and oxygen delivery to the regions with hypoxia.

Studies have also shown that exogenous delivery of HIF-1 α in ESCs increased the beating frequency, cardiomyocyte positive cells, increased expression of early and late cardiac markers, such as GATA-binding protein 4 and 6, α - and β -myosin heavy chain and myosin light chain 2. Also promoted cardiogenesis by increased levels of vascular endothelial growth factor (VEGF), suggesting a prominent role of HIF-1 mediated signalling in maturation and cardiomyocyte differentiation.³⁷ HIF-1 α is also necessary for the hypoxic fetal cardiomyocyte proliferation during mid-gestation, and loss of HIF-1 α activated tumour protein p 53 (TP53) and activating transcription factor 4 (ATF4), which inhibited proliferation of cardiomyocytes.³⁸ Furthermore mice exposed to hypoxia conditions re-activated the mitotic cells in cardiomyocytes by decreased ROS production, inhibition of oxidative metabolism and reduced DNA damage.³⁹ Studies performed by Mark T Keating and group, showed that even after 20 % amputation of ventricular heart tissue, the adult zebrafish, was still capable of regenerating the heart in two months through cardiomyocyte proliferation.⁴⁰ The heart of the zebrafish is two chambered with one atrium and one ventricle, that is exposed to hypoxic conditions, due to the mixture of arterial and venous blood,⁴¹ which is also observed, in the fetal circulation system inside the uterus of mammals. Relatively the heart of the zebrafish and fetal heart of the mammals reside in hypoxic environments, which relates to the animal studies describing the positive effects of hypoxia in cardiomyocyte proliferation and cardiac regeneration.^{35,}⁴² However, whether the ambient oxygen changes affect the mammalian cardiomyocyte cell cycle is unknown. It is also shown that moderate levels of hypoxia (15% and 10%) increased cardiomyocyte proliferation in human induced pluripotent stem cell (iPSC)-derived cardiomyocytes (hiPSC-CMs).⁴³ ⁴⁴ Taken together the data highlights that hypoxia stimulation might serve as a potential therapeutic towards human myocardial regeneration.

4.4 Human induced pluripotent stem cell derived cardiomyocytes for cardiac regeneration

Clinical trials using cell-based therapies to improve cardiac function in patients with heart failure yielded only modest effects.^{45 46, 47} Application of cell-based therapies in a clinical setting remains limited due to complicated isolation and culture procedures of adult cardiomyocytes. Therefore, a new source of adult like mature cardiomyocytes is needed. To improve and understand the mechanisms and functionality to achieve cardiac regeneration through cardiomyocyte proliferation.

In 2006, Yamanaka's group for the first time generated induced pluripotent stem (iPS) cells. The iPS were generated by forced expression of four transcription factors, namely Octamer binding transcription factor 4 (Oct-3/4), SRY-box2 (SOX2), V-myc myelocytomatosis viral oncogene homolog (c-Myc), and Krüppel-like factor (Klf4) in mouse embryonic or adult fibroblasts.⁴⁸ These iPS cells express similar properties of embryonic stem cells (hESCs)⁴⁹ and can be differentiated into a variety of cells including cardiomyocytes.^{48, 50} Since the past decade the method is widely applied in the generation of human induced pluripotent stem cells^{51, 52} and their differentiation into functional cardiomyocytes (hiPSC-CMs),⁵³⁻⁵⁵ that are currently being significantly improved to overcome hurdles in achieving cardiac regeneration⁵⁶ (**Figure. 4**). During the last years, by using myocardial ischemic reperfusion model in non-human primates (pig-tailed macaque), the research groups of Laflamme and Murray delivered one billion human embryonic stem cell derived cardiomyocytes (hESCs-CMs) via intra-myocardial injections in the infarcted heart.⁵⁷ The infarcted monkey heart was re-muscularized and cardiac function was improved upon delivery of hESC-CMs. However, during 3-months period, a large number of cardiomyocytes that were engrafted remained immature resulting in non-lethal ventricular arrhythmias.⁵⁷ Similarly, the group from Ikeda, injected induced pluripotent stem cell derived cardiomyocytes in primates that resulted in improved cardiac functionality and contractility.⁵⁸ HiPSC-derived cardiomyocytes were also used in several applications (**Figure. 4**). As the hiPSC-derived cardiomyocytes remain mostly immature, some studies focused on maturation of cardiomyocytes derived from hiPSCs. As it takes several years *in vivo* for the cardiomyocytes to mature,⁵⁹ recent studies described about long term culturing of hiPSC-CMs,⁶⁰ which resulted in mature phenotype in the alignment of myofibril density, with visible sarcomeric structures, a larger

INTRODUCTION

cell size, and the presence of the cardiac maturation genes (e.g. MYH7). Altogether, these studies suggest that cardiac maturation process is still achievable. ^{61, 62}

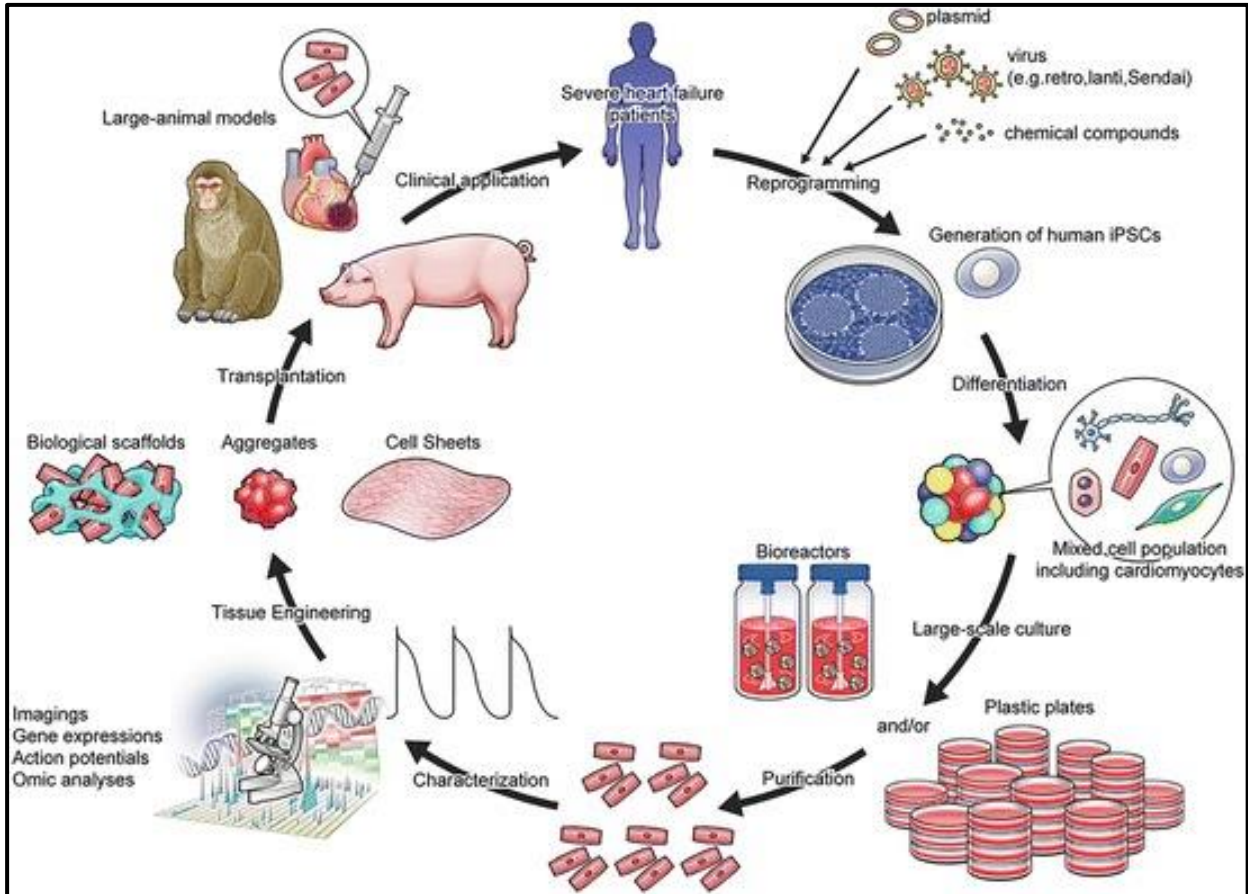


Figure 4: Steps to overcome the hurdles in cardiac regenerative therapy.

(1) Improving the efficiency of cardiomyocyte differentiation. (2) Cultivating cardiomyocytes in large-scale systems, (3) Purification of cardiomyocytes in large-scale systems (4) characterization of electrophysiological properties, (5) Utilizing the state of art techniques to improve tissue engineering and (6) improving the feasibility and safety of using cardiomyocytes in large animal models.

Figure Adopted from Shugo T *et al.*, 2016. ⁵⁶

However, several experiments are still needed to fully understand the maturation and integrity of hiPSC-CMs and resolve the safety and feasibility of transplanted cardiomyocytes derived from hESC and hiPSCs. ⁶³ Indeed hiPSC-CMs can be utilized as a model system in various fields. Such as screening of chemical libraries ⁶⁴,

INTRODUCTION

microRNAs, ^{65, 66} and in drug discovery, ⁶⁷ to assess the effect of drug toxicity. ^{68, 69} Recently, hiPSCs were also used in precision medicine by utilizing patient specific human iPSC derived cardiomyocytes, ⁷⁰ in understanding and to delve mechanisms involved in cardiac diseases ^{60, 71} and in recreating new models for translational cardiac regenerative medicine ^{72, 73} (**Figure. 5**). In addition, growing body of evidence suggests that microRNAs (miRNAs) are pivotal for cardiomyocyte homeostasis and proliferation. ^{74, 75}

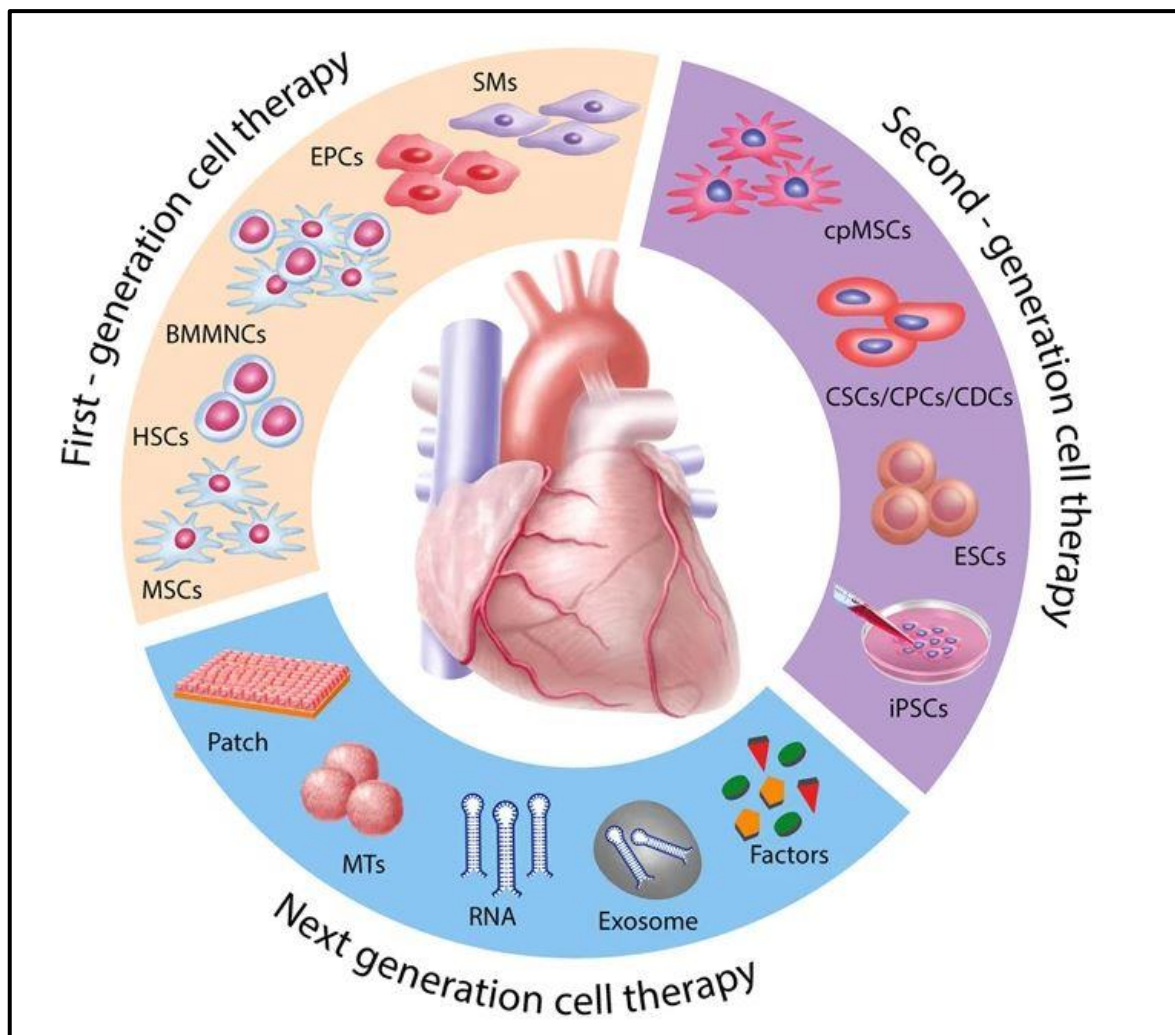


Figure 5: Evolution of translational cardiac regenerative therapies over time.

First generation therapies described safety and feasibility, with limited efficacy in a clinical setting. Cell therapies in the second generation are used to match the target organ such as iPSCs and precision medicine by using patient specific iPSCs. The current and next generation therapies utilized for cardiac repair and regeneration for cell enhancement include, microRNAs, cytokines, 3d cell constructs, biomaterials and cell-free models such as extra-cellular vesicles, non-coding RNAs, growth factors.

Figure adopted from Cambria. E *et al.*, 2017. ⁷³

4.5 MicroRNAs as therapeutics

4.5.1 MicroRNA biology

MicroRNAs (miRNAs) are small non-coding RNAs, with an average of 20-23 nucleotides in length. MiRNAs interfere with messenger RNAs (mRNA) at the post-transcriptional level that results in degradation or translational repression of the targeted mRNAs and thus occupy a central role in gene regulation.⁷⁶ In the year 1993, the groups from Ambros and Ruvkun discovered the first miRNA, termed lin-4, in *Caenorhabditis elegans* (nematode).^{77, 78} Horvitz and his team have previously shown that Lin-4 is a gene that controls the temporal development events in *C. elegans*.⁷⁹ A few years later, Ambros' and Ruvkun's research group discovered that Lin-4 is a small non-coding RNA and not a protein-coding RNA.⁸⁰ This discovery made an important revolution in the field of molecular biology. Most of the miRNAs are transcribed into primary miRNAs (pri-miRNAs), which undergo multistep biogenesis and can be processed into precursor miRNAs (pre-miRNAs) and later into mature miRNAs.⁸¹⁻⁸³

The miRNA fundamental biogenesis factors such as Drosha⁸⁴ and Dicer⁸⁵ are involved in pre-miR splicing. Deletions of these factors are lethal in mouse embryos.^{82, 86} The pri-miRNAs are transcribed by RNA Polymerase II, processed in the nucleus, then cleaved by RNase III enzyme Drosha and the DiGeorge Syndrome Critical Region 8 (DGCR8) protein, known as Pasha, a partner of Drosha to form pre-miRNAs, which are short hairpin RNAs, consisting of around 70 nucleotides.^{87, 88} The pre-miRNA is then exported from the nucleus to the cytoplasm with the help of Ras-related Nuclear protein (Ran), Ran GTPase activating protein (Ran-GTP), Ran-GTP/Exportin 5 mechanism,⁸⁹ and thereafter, the pre-miRNA is processed by Dicer to generate a 22-nucleotide mature miRNA.⁹⁰ The gene silencing induced by miRNAs are processed with the association of a multiprotein complex called RNA-induced silencing complex (RISC).⁸² The mature miRNAs enter into Argonaute containing RISC. Within this complex the gene expression is repressed by the miRNAs through interaction with 3'-untranslated regions.⁷⁶ The 3' untranslated region (3'UTR) of the target mRNA is the most common binding site of the miRNA. However, functional binding sites can also be found in the coding region,⁹¹ and 5'-untranslated region (5'UTR).^{92, 93} The miRNAs are involved in various cellular and biological process such as cell differentiation, cell death, and cell proliferation.^{82, 94}

INTRODUCTION

Intriguingly, one miRNA may target hundreds of mRNAs mostly involved in the inhibition of a common biological pathway such as proliferation or apoptosis. By repression of these mRNAs, the output of a pathway can be profoundly altered. In the recent years, several miRNAs have been tested in animal models of cardiomyocyte hypertrophy, apoptosis and several microRNAs were identified in regulating cardiomyocyte proliferation and cardiac regeneration, which can be used experimentally for treatment of several cardiovascular diseases (**Figure. 6**). Of interest, miRNAs can be therapeutically manipulated and therefore hold exciting opportunities for future clinical therapies.^{95, 96}

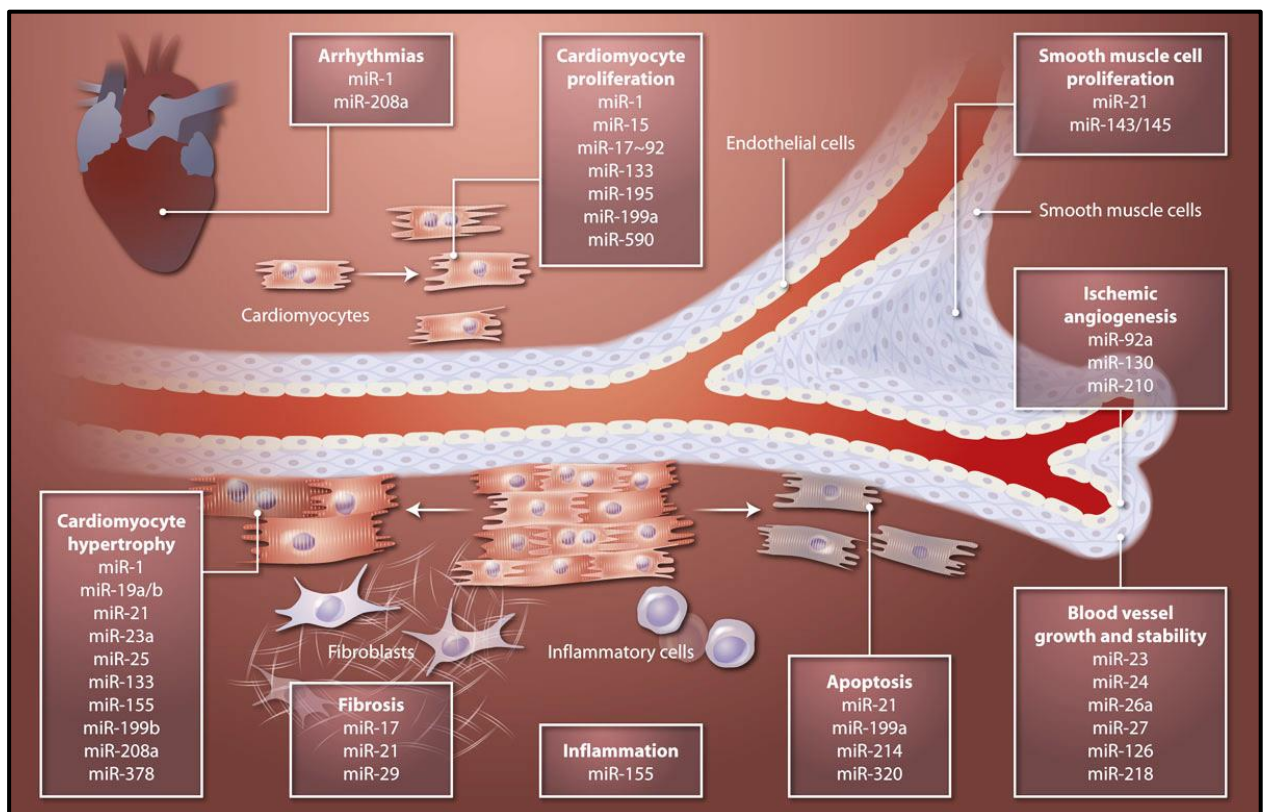


Figure 6: MicroRNAs in cardiovascular diseases

Schematic representation of the list of microRNAs that regulate functions of cardiomyocyte hypertrophy, apoptosis and proliferation. Other microRNAs control pathways related to fibrosis and inflammation. MicroRNAs also acts upon endothelial cells and smooth muscle cells, which play a role in angiogenesis, blood vessel growth and smooth muscle cell proliferation.

Figure adopted from Olson E.N. 2014⁹⁵

4.5.2 Role of microRNAs in cardiac remodelling

MiRNAs play a crucial role in cardiac remodelling and represent a promising treatment strategy for cardiac hypertrophy.⁹⁷ The postnatal heart grows by cardiomyocyte cell enlargement (hypertrophy) in the absence of cardiomyocyte proliferation (hyperplastic).⁹⁷ Cardiac hypertrophy is due to the response from pathological or physiological stress stimuli in the heart, resulting in increased ventricular wall thickness. Importantly, pathological hypertrophy significantly increases the risk of heart failure.⁹⁸ A study demonstrated that microRNA-1 (miR-1) a muscle specific microRNA has a reduced expression in patients with cardiac hypertrophy. To test the effect of the miR-1, miR-1 was overexpressed by using microRNA-mimics in adult rat cardiomyocytes that were exposed to hypertrophic stimuli.⁹⁹ Overexpression of miR-1,⁹⁹ in another study also demonstrated a correlation between miR-1 and miR-133¹⁰⁰ which attenuated cardiomyocyte hypertrophy, by decreasing the expression of β -MHC (myosin heavy chain) and cell surface area of rat cardiomyocytes. Similarly, inhibition of miR-1 by using anti-miR-1 treatment increased the expression of β -MHC and cell surface area of rat cardiomyocytes suggesting that inhibiting miR-1 induced cardiomyocyte hypertrophy.⁹⁹

It has been also shown that miR-133 overexpression is beneficial while inhibition of miR-133 resulted in increased expression of hypertrophy markers and cell size both *in vitro* and *in vivo*. Therefore, miR-1 and miR-133 may be considered as anti-hypertrophic miRNAs. MiR-133 levels are also downregulated in human disease states and linked to myocardial hypertrophy. Therefore, modulation of *miR-133* expression may have a therapeutic clinical potential.¹⁰⁰ In an experimental study investigating miR-199, mice were subjected to pressure overload in the left ventricle for three weeks to stimulate hypertrophy. Treatment with anti-miR-199b for three weeks resulted in reduction of fibrosis and cardiomyocyte hypertrophy with increased cardiac function suggesting that miRNA-199b is a pro-hypertrophic microRNA.¹⁰¹ Taken together, miRNAs can induce either pro-hypertrophic or anti-hypertrophic pathways that influences cardiac remodelling associated with hypertrophy.⁹⁸

Moreover, miRNAs have also been observed as important regulators of the apoptotic signalling pathway in cardiomyocytes that renders them highly attractive for cardioprotective therapy in patients with myocardial infarction. Rane's research group showed that knockdown of miR-199a during hypoxia results in an upregulation of pro-apoptotic genes that trigger apoptosis in myocytes.¹⁰² Another cardioprotective miRNA

INTRODUCTION

is miR-210. In the infarcted mouse heart, delivery of miR-210 minicircle constructs increased myocyte survival and neovascularization.¹⁰³ In contrast to miR-199a and miR-210, miR-320a was shown to be a pro-apoptotic miRNA. Silencing of miRNA-320a by the administration of a miR-320 antagomir resulted in reduced infarct size by de-repression of the cardioprotective heat-shock protein 20. Consistently over-expression of miR-320 in cardiomyocytes exhibited an increased apoptosis and infarct size in transgenic mice carrying the miR-320 mouse DNA.¹⁰⁴ In conclusion, miRNAs are important post-transcriptional regulators of cellular growth and apoptosis in cardiomyocytes.

4.5.3 Role of microRNAs in cardiomyocyte proliferation

MiRNAs are required for modulation of the proliferative capacity of cardiomyocytes, as cardiac deletion of enzymes that are involved in the biogenesis and processing of miRNAs resulted in dilatation of the heart and premature lethality.^{105, 106} Several studies have shown that artificial inhibition or upregulation of miRNAs improved LV-function after myocardial infarction.^{65, 107-114} This miRNA-induced regenerative potential is not only observed in animals during the neonatal phase,¹¹⁰ where the cardiac regenerative potential is preserved,¹¹⁵ but also in the postnatal/adult phase,¹¹¹ where the regenerative response is absent. An important modulating role of miRNAs is further supported by the observation that miRNA-levels change in a spatiotemporal manner during the short phase where the regenerative cardiac potential is preserved in postnatal murine hearts.⁹

As an example, miR-195, a member of the miR-15-family, is highly up-regulated in mouse hearts between day 1 and 10 after birth. Delivery of artificial anti-miRs targeting miR-15-family members in neonatal mice increased cardiomyocyte proliferation by de-inhibition of cell cycle genes^{110, 111}. They further investigated the impact of miR-15 on cardiac regeneration after cardiac injury in postnatal mice. Postnatal myocardial infarction at day 1 resulted in an extensive infarcted area. However, functional recovery was observed at day 21.¹¹¹ Furthermore, pretreatment of adult mice with anti-miR-15 improved cardiac function after induction of myocardial infarction in adult mice.¹¹¹

Another study investigated the miR-302-367 cluster in hearts that suppresses contributors of the Hippo-signalling pathway. This recently discovered conserved pathway regulates cardiomyocyte proliferation.¹¹² Transgenic cardiac or systemic transient over-expression of the miR-302-367 enhanced cardiomyocyte proliferation and improved cardiac function in a mouse myocardial infarction model.¹¹² In recent reports,

INTRODUCTION

the research group from Giacca performed a high throughput screening using a human microRNA library, and identified miRNA-mimics (miR-199 and miR-590), as potential regulators of mouse and rat cardiomyocyte proliferation *in vitro*.⁶⁵ In addition, using a myocardial infarction model in 8-12 weeks old mice, they generated AAV9 (Adeno Associated Virus) vectors which express miR-199 or miR-590, and injected these at the peri-infarct area post myocardial infarction. Post 60 days, administration with one of the vectors, displayed a significant improvement in the cardiac function in the adult mice.⁶⁵ In a very recent study, the same group has injected AAV-mediated microRNA mimics (miR-199 and miR-590) in a pig model,¹¹⁶ also resulted in functional recovery, post injury and increased cardiomyocyte proliferation.^{116, 117}

All these studies^{65, 108, 112, 116} indicate that cell-cycle reentry of cardiomyocytes can be induced by administration of pro-proliferative miRNAs. Most of these miRNAs modulate an important conserved signalling pathway, which regulates tissue and organ size, termed Hippo kinase pathway.^{112, 118, 119} In the heart, inhibition of Hippo pathway augments cardiomyocyte proliferation. Interestingly, Hippo deficiency reverses systolic heart failure after myocardial infarction.³³ Therefore, targeting this pathway using miRNA therapeutics is a promising strategy to treat heart failure after myocardial infarction. Although strong evidence for the use of miRNAs as a regenerative application in murine cardiomyocytes exists,^{65, 107, 112} the support for a miRNA-induced proliferative potential in human cardiomyocytes is scarce.

Of note, the potential future clinical use of miRNA-therapeutics is supported by a clinical phase 2 trial that used systemic miRNA delivery to target Hepatitis C virus infection.¹²⁰ MiRNAs are currently also evaluated for clinical use in cardiovascular diseases to modulate hypertrophy and angiogenesis.^{121, 122}

To address the regenerative potential after miRNA-modulation, in human cardiomyocytes and to develop a miRNA-therapy for remuscularization of the human heart in patients after myocardial infarction; we performed functional high-throughput screening in human iPSC-derived cardiomyocytes (iPSC-CMs).

4.6 High throughput screening of libraries

High throughput screening (HTS) is performed by using automated equipment systems, for testing several thousands of samples for biological activity, at the cellular or molecular level. There are many compound libraries such as antibodies, microRNAs, chemical

INTRODUCTION

cocktails, small molecules that can be tested for several biological processes. HTS is performed using different cell culture microtiter plates such as 96-well plates, 384-plates, and 1536- well formats.¹²³

HTS plays a significant role in drug discovery and the automated platform enables to screen and test several plates in a few weeks. However, due to high number of compounds, there might be false-positive and false-negative readouts from the HTS. Therefore, for robust results, a maximum number of replicates should be considered to minimize the errors. The compounds, identified in the main screen are labeled as “Hit candidates”.

In order to evaluate the efficiency, the hit candidates derived from the main screen are re-tested in a secondary counter screen.¹²⁴ HTS permits to assess many compound libraries, including miRNAs - on their potential to alter biological processes. As miRNAs are crucial regulating proliferative pathways,^{65, 66, 108, 112, 116, 125, 126} a miRNA-targeted therapy to direct human adult cardiomyocytes to cell cycle re-entry and enhance proliferation is of high interest. A potential miRNA-based therapy may aid to compensate for the loss of myocardium after myocardial infarction and ameliorate heart failure.

In the current project, two parallel high-throughput screenings for the identification of proliferative miRNAs in human cardiomyocytes were performed. As a model system, we used human iPSC that are differentiated into cardiomyocytes (iPSC-CMs). Ischemia-reoxygenation was mimicked using a brief period of hypoxia. After individual transfection of 2019 miR-mimics and anti-miRs using microRNA-libraries, surrogate markers of cell proliferation were analyzed by high content imaging. Downregulation of more than two thousand miRNAs using anti-miRs did not result in increased proliferative activity in human iPSC-CMs.

However, overexpression of 28 miRNAs strongly induced cell-cycle re-entry. Intriguingly, three of the candidate miRNAs belong to the primate-specific chromosome 19 miRNA-cluster (C19MC) and two miRNAs to the adjacent miR-372 cluster. Further analysis revealed a strong increase in proliferation after overexpression of hsa-miR-515-3p and hsa-miR-519e-3p in human iPSC-CM, especially under transient hypoxia. These miRNAs further substantially regulated genes involved in the sarcomeric organization, cell-cycle activity and cell division as observed in molecular studies and by performing RNA-sequencing. Altogether, our data suggests that, the identified miRNAs from the screening

INTRODUCTION

may represent interesting novel potential therapeutic targets for the treatment of myocardial infarction and ischemic cardiomyopathy associated with loss of cardiomyocytes.

5. AIM OF THE STUDY

In humans, cardiomyocyte (CM) withdrawal from the cell cycle is observed early after birth. The marginal number of adult CM (<1%) undergoing cell cycle cannot compensate for myocardial loss after cardiac injury. Despite advances in plethora of cell, device and drug-based technologies, the previously observed decrease in cardiovascular mortality has reached a plateau, even in high-income regions. Notably, therapies that may replace damaged heart muscle through the proliferation of cardiomyocytes harbour a potential to reduce cardiac mortality. However, no clinical treatment options are currently available to induce cardiomyocyte proliferation. Thus, it is very important to find potential inducers that efficiently stimulate cardiomyocyte proliferation and regenerate the heart muscle after injury. Therefore, the Ph.D. thesis aimed to detect potential microRNAs (miRNAs) that induce and enhance proliferation of human induced pluripotent stem cell derived cardiomyocytes (hiPSC-CMs) by performing a functional high-throughput screening and high-content imaging.

5.1 Project specific aims

AIM 1: Establishing stable cell culture methods and assess lipid based transfection efficiency and optimizing hypoxia stimulations in human induced pluripotent stem cells (hiPSC)-derived cardiomyocytes (CM) (hiPSC-CM), a hard-to-transfect cell line.

AIM 2: Efficient transfection of hiPSC-CMs with microRNAs to perform immunostaining with fluorescent markers indicative for cell proliferation (e.g. DNA synthesis & G2/Mitosis).

AIM 3: Performing high-throughput screening and high-content imaging of human iPSC-CMs using a human microRNA library, consisting of 2019 microRNA-mimics and 2019 microRNA-Inhibitors.

AIM 4: Validation of positive hit miRNA candidates derived from High Throughput Screening (HTS) to induce cardiomyocyte proliferation *in vitro*.

AIM 5: Performing RNA-sequencing by transfecting hit microRNA candidates and to study relevant microRNA target genes and their role in cardiomyocyte proliferation.

6. MATERIALS

6.1 Reagents

The reagents used in this study are listed in Table 1

Table 1 Reagents used for cell culture

Reagent or Resource	Supplier	Catalogue number
RPMI 1640 mit HEPES mit GlutaMAX	Thermo Fisher Scientific	Cat. no. 72400021
B27 Insulin (Serum Free) (10ml) (50X)	Thermo Fisher Scientific	Cat. no. 17504044
Geltrex (Growth Factor Reduced)	Thermo Fisher Scientific	Cat. no. A1413302
Trypsin /EDTA (0, 25 %/0, 02 %)	Merck Millipore	Cat. no. L2163
Stem pro Accutase cell Dissociation reagent	Thermo Fisher Scientific	Cat. no. A11105-01
Fetal Bovine Serum, SAFC, (FBS)	Sigma-Aldrich	Cat. no. 12103C
Thiazovivin (2µM final)	Merck Millipore	Cat. no. 420220
Collagenase CLS-2 (1 gram)	Worthington	Cat. no. LS004176
DMEM/F-12, HEPES (500ml)	Thermo Fisher Scientific	Cat. no. 113300-32
RPMI 1640 Medium (ATCC modification)	Thermo Fisher Scientific	Cat. no. A10491-01
Dulbecco's phosphate buffer Saline	Sigma-Aldrich	Cat. no. D853
Dimethyl sulfoxide (DMSO) (950ml)	Thermo Fisher Scientific	Cat. no. 20688
Single- use Syringe 10 ml	B. Braun	Cat. no. 4606108V

MATERIALS

Disposable dypoderm needles	B. Braun	Cat. no. 4657519-02
Sterile Filter 0,2 µm (Spritzenfilter)	Carlroth	Cat. no. 272-PA49.1
Cell Strainer (100µm)	Corning	Cat. no. 352360
Annexin binding buffer	BioLegend	Cat. no. 42201
Annexin V Pacific Blue	BioLegend	Cat. no. 640917
Propodium Iodide	BioLegend	Cat. no. 420301

6.2 Microscopes

The microscopes used in this study are listed in Table 2.

Table 2 Microscope details

Microscope	Model	Supplier
Fluorescence	BZ-9000	Keyence
Fluorescence	Operetta (High Content Imaging)	PerkinElmer
Fluorescence	Array Scan XTI(High Content Platform)	Thermo Fisher Scientific
Microscope	AE 2000 (Binocular Inverted Microscope)	Motic
Fluorescent Plate Reader	Infinite 200pro, F200 (Micro plate reader)	Tecan

6.3 PCR Systems

The PCR systems used in the study are listed in Table 3.

Table 3 PCR systems

PCR	Model	Supplier
PCR System	AB ViiA7	Applied Biosystems
Master Cyclor	Nexus	Eppendorf

MATERIALS

6.4 Centrifuges

The centrifuges used in the study are listed in Table 4

Table 4 Centrifuge type, model and supplier

Centrifuge	Model	Supplier
Table top centrifuge	5424	Eppendorf
Multi stage centrifuge	Heraeus IS-R	Thermo Fisher Scientific

6.5 Buffers and solutions

List of Buffers and solutions used in this study are listed in Table 5.

Table 5 List of solutions

Solution	Formulation
Blocking buffer	10% Horse Serum, 1% BSA, 0, 3% Triton, 1X PBS Preparing 100 ml Buffer: <ol style="list-style-type: none">1. 10ml Horse Serum2. 1 Gram BSA3. 300µl Triton x1004. 90ml 1x PBS
Dilution buffer	1% Horse Serum, 1% BSA, 0, 3% Triton, 1X PBS Preparing 100 ml Buffer: <ol style="list-style-type: none">1. 1ml Horse Serum2. 1 Gram BSA3. 300µl Triton x1004. 99ml 1x PBS
10X SDS-running buffer	1000 ml 130g tris

MATERIALS

	144g glycine 10g SDS
TBST buffer (10x)	0.5M NaCl 0.5M tris HCl pH 7.5 20g tween20 (after adjusting pH)
Transfer buffer	20mM tris 159mM glycine 20% MeOH
Blocking Buffer (western blot)	5% milk powder in 1xTBST
Wash Buffer	0.1 % BSA in 1XPBS
Paraformaldehyde 4%	Paraformaldehyde 4% in PBS [v/v]
PBS-0,1% NP40	PBS with 0.1% Nonidet P40
Permeabilization Buffer	PBS with 0.5% Triton-X 100

6.6 Growth Media

List of medium used in this study are listed in Table 6.

Table 6 List of media

Media	Application	Formulation
Cardio digestion medium	Propagation of hiPSC cells	RPME-Glutamax B27 Supplement 10% FBS Thiazovivin (2 μ M)
Cardio culture medium	Culturing of cells	RPME Glutamax B27 Supplement

MATERIALS

Cardio selection medium	Selection of pure cardiomyocytes	500ml RPMI 1640 without Glucose without HEPES 2ml Lactate/HEPES (Stock: 1M) 250mg Albumin, human recombinant 100mg L-Ascorbic Acid 2-Phosphate filter to sterilize
Neonatal cardiomyocyte medium	Culturing and Isolation from Neonatal Mouse hearts	DMEM/F-12 Glutamax medium supplemented with, 1% Pencillin and Streptomycin. 5% FBS
Cardiomyocyte Pre-plating medium	Separation of Non-myocytes harvested from neonatal mice hearts	DMEM/F-12 +GlutaMAX medium supplemented with: 10% [v/v] FBS 1% [v/v] Pen/Strep 2 mM L-Glutamine
Coating medium	Coating for mice cardiomyocytes	0.005 mg/ml Fibronectin
Coating medium	Coating for hiPSC-cardiomyocytes	Geltrex (0.15 mg/ml)
Ischemic medium	Stress trigger for hiPSC-cardiomyocytes	1000 ml distilled water NaCl KCl KH ₂ PO ₄ MgSO ₄ ·7H ₂ O CaCl ₂ ·2H ₂ O NaHCO ₃ C ₃ H ₅ NaO ₃ HEPES (C ₈ H ₁₈ N ₂ O ₄ S)

MATERIALS

Dissociation medium	Dissociation into single cells	Collagenase type 2 (400 Units/ 1 ml of RPME medium)
---------------------	--------------------------------	---

6.7 Kits

List of kits used in this study are listed in Table 7

Table 7 List of kits

Kit	Supplier	Catalogue number
miRNeasy Micro Kit	Qiagen	Cat. no. 217084
LDH Cytotoxicity assay kit	Thermo Fisher Scientific	Cat. no. C20301
Click-iT EdU Cell Proliferation Kit	Thermo Fisher Scientific	Cat. no. C10637
BCA Protein assay Kit	Thermo Fisher Scientific	Cat. no. 23225
High capacity cDNA Reverse Transcription kit	Thermo Fisher Scientific	Cat. no. 4368814
TaqMan miRNA reverse transcription kit	Thermo Fisher Scientific	Cat. no. 4366596
TaqMan miRNA fast advanced master mix	Thermo Fisher Scientific	Cat. no. 4444557
4-20% pre cast Protein gels	Bio-Rad	Cat. no. 4561096
RIPA Lysis Buffer	Santa Cruz	Cat. no. Sc-24948A
High capacity cDNA Reverse Transcription kit	Thermo Fisher Scientific	Cat. no. 4368814

6.8 Cells and cell lines

List of cell lines used in this study are listed in Table 8

MATERIALS

Table 8 Cells and cell-lines

Cell line/Cells	Specification	Supplier
WTD2, Control 1 4- cell lines	HiPSC-Cardiomyocyte	Priv.-Doz. Dr. rer. nat. Katrín Streckfuß-Bömeke
Neonatal Mouse CMs	Mouse Cardiomyocytes	Prof. Dr. Felix B. Engel.

6.9 Hit candidate microRNAs

List of cell lines used in this study are listed in Table 9

Table 9 List of selected microRNAs

MicroRNA	miRNA Sequence
hsa-miR-515-3p	GAGUGCCUUCUUUUGGAGCGUU
hsa-miR-519e-3p	AAGUGCCUCCUUUUAGAGUGUU
hsa-miR-371a-3p	AAGUGCCGCCAUCUUUUGAGUGU
hsa-miR-590-3p	UAAUUUUUAUGUAUAAGCUAGU
hsa-miR-1825	UCCAGUGCCCUCUCUCC
miR-Scrambled (Control)	Negative Control
FAM (Florescent Labeled)	A carboxyfluorescein (FAM™)-labeled RNA oligonucleotide
All stars siRNA (Control)	Short Interfering RNA (Method to assess transfection efficiency)

6.10 List of human primers

List of primers used in this study are listed in Table 10

Table 10 List of human primers for qRT-PCR

MATERIALS

Gene	Forward primer 5'-3'	Reverse primer 5'-3'
GAPDH	GGAGCGAGATCCCTCCAAAAT	GCAAATGAGCCCCAGCCTTC
P21	ATGAAATTCACCCCCTTTCC	CCCTAGGCTGTGCTCACTTC
P27	GGTTAGCGGAGCAATGCG	TCCACAGAACCGGCATTTG
P57	GGCGATCAAGAAGCTGTCC	GACATCGCCCGACGACTT
Cyclin A2	TTATTGCTGGAGCTGCCTTT	CTCTGGTGGGTTGAGGAGAG
Cyclin B1	ACAGGTCTTCTTCTGCAGGG	GAACCTGAGCCAGAACCTGA
Cyclin D2	ATTGAACCATTGTTGGGATGGA	ATGGTGGTGTCTGCAATGAA
LATS1	TCATCAGCAGCGTCTACATCG	TCCAACCCGCATCATTTTCAT
MOB1B	GAGAGTTGTCCAGTGATGTCA	GTCCTGAACCCAAGTCATCA
AURORA B	GGAGAGTAGCAGTGCCTTGG	GAAGTGCCGCGTTAAGATGT
MYL2	TTGGGCGAGTGAACGTGAAAA	TCCGCTCCCTTAAGTTTCTCC
MYL7	GCCCAACGTGGTTCTTCCAA	GCTGAAGGCTTCTTTGAACTCC
MYOM2	GCTTTTGCAGAGAAGAATCGTG	CATGCTGACGTACTTGGCCT
MYOM3	TGAAGCCAGTCTTTGCTCGT	ACCTCAGTAGGCTCCCATCT
NPPA	CAACGCAGACCTGATGGATTT	AGCCCCCGCTTCTTCATTC
NPPB	TGGAAACGTCCGGGTTACAG	CTGATCCGGTCCATCTTCCT

6.11 Primary Antibodies

List of Primary antibodies used in staining of cardiomyocytes used in this study are listed in Table 11

Table 11 List of primary antibodies for immunofluorescence staining's

MATERIALS

Antibody	Company & Catalogue number	Species	Dilution
AIM1	BD Biosciences (611083)	Mouse	1:250
Anti-sarcomeric alpha Actinin	Abcam (ab9465)	Mouse	1:500
Human-Cardiac Troponin T	R & D systems (MAB-1874)	Mouse	1:500
Troponin I	Abcam (Ab56357)	Goat	1:500
Anti-phospho-Histone-H3 (Ser10)	Merck Millipore (06-570)	Rabbit	1:500

List of Primary antibodies used for protein detection in this study are listed in Table 12

Table 12 List of primary antibodies for Western blot

Antibody	Company & Catalogue number	Species	Dilution
AIM1	BD Biosciences (611083)	Mouse	1:250
CDKN1A (P21)	ThermoScientific (MA5-14949)	Rabbit	1:1000
Cyclin A2	Abcam (Ab16726)	Mouse	1:500
YAP	Cell signaling (CS-4912)	Rabbit	1:1000
GAPDH	Merck Millipore (Ab2302)	Chicken	1:500

6.12 Secondary Antibodies

List of Secondary antibodies used in staining of cardiomyocytes used in this study are listed in Table 13

MATERIALS

Table 13 List of secondary antibodies for immunofluorescence staining's

Antibody	Fluorophore	Company
Goat anti-mouse	594	Thermo Fisher Scientific
Goat anti-mouse	488	Thermo Fisher Scientific
Goat anti-rabbit	594	Thermo Fisher Scientific
Goat anti-rabbit	488	Thermo Fisher Scientific
Donkey anti-mouse	594	Thermo Fisher Scientific
Donkey anti-mouse	488	Thermo Fisher Scientific
Donkey anti-rabbit	594	Thermo Fisher Scientific
Donkey anti-rabbit	488	Thermo Fisher Scientific
Donkey anti-goat	594	Thermo Fisher Scientific
Donkey anti-goat	488	Thermo Fisher Scientific

List of Secondary antibodies used for protein detection in this study are listed in Table 14

Table 14 List of secondary antibodies for Western blot

Antibody	Company & Catalogue number	Species	Dilution
Anti-Rabbit IgG, HRP-Linked	Cell signaling (7074)	Goat	1:3000
Anti-Mouse IgG, HRP-Linked	Cell signaling (7076)	Goat	1:3000
anti-Chicken IgG, HRP-Linked	Santa Cruz (sc-2428)	Goat	1:5000

6.13 Computer Softwares

List of software's used in this study are listed in Table 15

Table 15 List of computer software

Software	Application
Microsoft Office Excel, Word, Power Point	Data Analysis, Interpretation and Documentation
Image J, Columbus	Image Analysis
ThermoScientific HCS Studio, Cell omics Scan Version 6.6.0	Image analysis High content Imaging
KNIME Analytics Platform	Data Processing High content screening
Graph Pad 7 Prism	Graphical representation of data and statistical analysis.

7. METHODS

7.1 Cell Culture-related methods

7.1.1 Generation of human iPSC cardiomyocytes

As a model system, human induced pluripotent stem cell (hiPSC)-derived cardiomyocytes (CMs) (hiPSC-CM) were used. Generation of hiPSCs and differentiation into cardiomyocytes were performed in collaboration with the translational stem cell research group of PD. Dr. K. Streckfuss-Bömeke at Universitätsmedizin Gottingen. HiPSCs were generated as previously described.^{127, 128} Female and male donors were used to generate cardiomyocytes, with two different reprogramming based approaches. Two female hiPSC lines were generated with an episomal plasmid based transduction. One female and one male hiPSC line was reprogrammed with the STEMCCA system, which is a humanized excisable lentiviral system containing all four reprogramming factors OCT4, SOX2, KLF4, and c-MYC in a single “stem cell cassette”(pHAGE2-EF1aFull-hOct4-F2A-hKlf4-IRES-hSox2-P2A-hcMyc-W-loxP). The pluripotent clones were expanded up to passage 8. The established iPSCs were proven for their pluripotency by both in vitro studies - the expression of pluripotency markers and differentiation experiments - and in vivo teratoma formation assay.

7.1.2 Human iPSC-cardiomyocytes selection and culture

Post differentiation, cardiac culture medium (RPME 1640 with Glutamax and HEPES, B27 supplement) was aspirated and replaced with cardio selection medium (RPMI 1640 without Glucose, Lactate/HEPES, hAlbumin, human recombinant 100mg L-Ascorbic Acid 2-Phosphate). The medium was exchanged every second day. Post selection, the medium was replaced with cardio culture medium. The iPSCs were effectively differentiated and selected in vitro into > 95% pure cardiomyocytes by using the established technologies.

7.1.3 Splitting of human iPSC-cardiomyocytes

HiPSCs were cultured in T25 flasks. Splitting was performed in 30 to 40 days old cardiomyocytes. Cell detachment was performed using 0.25% trypsin, 0.02% EDTA and Stempro accutase, followed by collagenase diluted in RPME 1640 for cell dissociation. Later, the cells were passed through a 100µm (Micro Meter) cell strainer and counted

METHODS

with a hemocytometer. Cells were mixed very gently and the mixture was passed through a 100µm cell strainer, thereafter counted with a hemocytometer and seeded into cell culture plates.

7.1.4 MiRNA and siRNA transfection of human iPSC-CMs

Lipid based transfection reagent was used for transfection of microRNAs using a standard forward transfection protocol. Medium was replaced with fresh cardio culture medium 24 hours post transfection. 48 hours post transfection; hiPSC-CMs were exposed to hypoxia (0.5% oxygen, 5% CO₂) for 2 hours. 50 hours post transfection, medium was exchanged to cardio culture medium containing EdU, or hiPSC-CMs were fixed and stained with H3P and further proceeded for immunocytochemistry. Assessment of FAM-miR transfected hiPSC-CM was performed 24 hours post transfection using fluorescent imaging or fluorescence activated cell sorting (FACS). For FACS analysis, cells were briefly washed in PBS, trypsinized, and the detached cells were resuspended with freshly mixed staining solution (100-µl Annexin-binding buffer for each sample). The mix was carefully vortexed and measured immediately at an attune flow cytometer. All stars siRNA-cell death control (Qiagen) was used to observe a cell death phenotype in hiPSC-CM 48 hours post transfection.

7.1.5 Functional high-throughput screening in human iPSC-CMs

Human iPSC-CMs were seeded in 384-well plates (Falcon), coated with Geltrex that was aspirated prior to the cell seeding. A washer dispenser (BioTeK EL406) with an automated liquid handling was used to dispense the cells, and to perform medium exchange, washer dispenser was placed in a laminar flow work cabinet to avoid contamination. A high-throughput (HT) screening by using a miRNA-library (Ambion; mirVana Human Library v19.0; 2019 miR-mimics and miR-inhibitors) was performed in two parallel screenings. For the HT screen, a forward transfection protocol was used. Human iPSC-CMs were plated into Geltrex coated 384-well plates (BD Falcon). Each individual miRNA of the library (miR-mimic or miR-inhibitor, 60nM) was robotically transferred using a Freedom EVO liquid handling workstation (Tecan) after complexing with the transfection reagent. The mixture was slowly added drop by drop. MiRNA transfected hiPSC-CMs were incubated for 24 hours at 37 °C in 5% CO₂. Medium exchange was performed by a robotic dispenser after 24 hours. 48 hours post transfection; hiPSC-CMs were exposed to hypoxia (0.5% oxygen, 5% CO₂) for 2 hours. Thereafter, cells were replaced with cardio culture medium containing EdU and incubated

METHODS

for 48 hours. Three days post transfection; cells were fixed and processed for immunofluorescence analysis (**Figure. 7**).

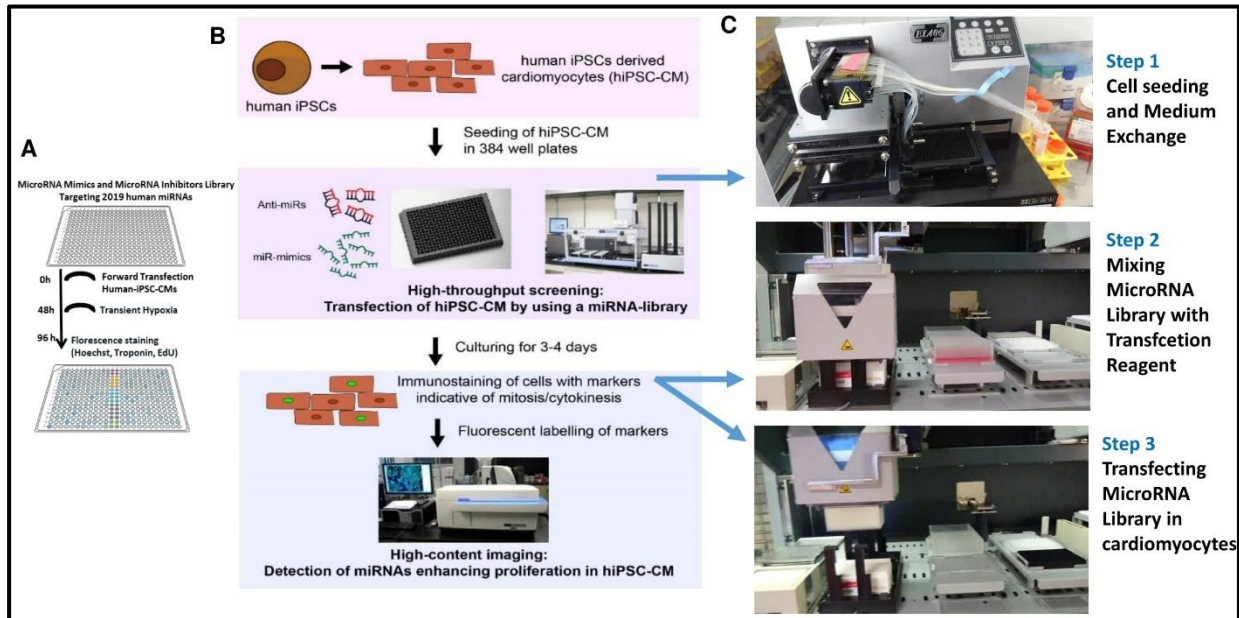


Figure 7: High Throughput screening workflow in hiPSC-CMs

Figure 7A: Graphical illustration of the high-throughput (HT) screening workflow. **Figure 7B:** hiPSC-Cardiomyocytes were seeded in 384 well formats suitable for screening, MicroRNA-mimics and Anti-miRs were transfected using robotic-based platform, 3 to 4 days post transfection cells were fixed and processed for immunofluorescence staining. **Figure 7C:** Series of Steps involved in usage of Robotic platforms in HTS, based screening.

METHODS

7.1.6 High content imaging in human iPSC-CMs

Human iPSC-CMs were fixed and stained. The immunofluorescence imaging was performed by ArrayScan XTI High Content Screening Platform (ThermoScientific). 20X magnification objective was used, with a camera mode of 1104x1104 Pixel. Three imaging channels were used: channel 1 was represented as Hoechst (Nucleus marker), channel 2 as Troponin T (Cardiac specific Marker), and channel 3 as EdU (Marker for DNA synthesis). 36 individual images from each channel were obtained from a single well of 384 well plate, approximately covering the entire area of a well.

7.1.7 Image analysis of human iPSC-CMs

ThermoScientific HCS Studio Cellomics Scan Version 6.6.0 was used to analyze the images acquired from the ArrayScan XTI High Content Screening Platform. Object identification and selection parameters are mentioned below. The first parameter was to identify the cell objects, where the primary object was selected as channel 1 (Nuclei), and channel 3 (EdU) for identification of DNA synthesis in the nuclei. Primary Object Identification Mask (Region of Interest = ROI) from channel 1 (Nuclei) was carried over to channel 3 without modification. EdU-positive nuclei/cells were selected based on the average intensity in the ROI being >2000. Object selection was based on channel 1 and channel 3, as human iPSC-CMs were positive for channel 2 (cardiomyocyte-specific marker). The two used criteria for image output was 1) number of valid objects from nuclei per well and 2) % of EdU-positive objects per well (related to the number of valid objects (nuclei)).

Object Identification

	Method Value	IsodataThreshold	
Object Selection Parameter		Min	Max
ObjectAreaCh1		100.92	4048.77
ObjectShapeP2ACh1		0.1	2.5
ObjectShapeLWRCh1		0.1	3.01
ObjectAvgIntenCh1		0	16380
ObjectVarIntenCh1		0	32767
ObjectTotalIntenCh1		0	1000000000000

7.1.8 Data Processing (Z-score)

Once the required imaging analysis was obtained, the data was processed using the KNIME analytics platform (KNIME). Z-score is represented as standard deviations from

METHODS

being above or below the mean of data points. Negative or below a Z-score represents that the acquired data is below the mean average and positive or above a Z-score represents that the acquired data is above the mean average of the data. For plate-wise normalization, the Z-Score for each miRNA on the plate was calculated from the % of EdU-positive nuclei using robust statistics (Median and MAD (Median Absolute deviation)) as follows:

$$x.zscore = (x - median(x [subset]))/mad(x [subset]).^{124}$$

Where x is the % of EdU-positive nuclei in the well, median(x [subset]) is the median from all candidate wells in the plate and mad(x [subset]) the median absolute deviation of all candidate wells in the plate. The mean for the results from the two replicates then was calculated using the following formula: $(Z\text{-Score } R1 + Z\text{-Score } R2)/2$ and used for the final candidate ranking.

7.1.9 EdU cell proliferation assay in human iPSC-CM

Human iPSC-CM or mouse cardiomyocytes were seeded in 96 or 384 well plates and transfected with either scrambled-miR or miR-mimic-515-3p or miR-mimic-519e-3p or miR-mimic-371. Medium exchange was performed 24 hours post transfection. EdU (5-Ethynyl-2'-deoxyuridine) was diluted in fresh medium and added to the cells for 48 hours to 72 hours. The cells were then fixed and stained with Click-it Plus EdU proliferation Kit, according to manufacturer protocols.

7.1.10 Lactate dehydrogenase (LDH) cytotoxicity assay

LDH assay was performed with the LDH assay kit (Pierce) according to the manufacturer protocols. LDH is a cytosolic enzyme present in many cells. Upon damage to the plasma membrane in a cell, LDH is released into the medium. This allows to measure treatment-induced cytotoxic effects. Cells were plated in 96 or 384-well plates and transfected with either scrambled-miRNA or miRNAs with several concentrations ranging from 20nM to 100 nM to assess toxicity. 24 hours post transfection, medium was carefully collected and placed in a 384 well plate. LDH start reagent was added onto the cells and incubated for a period of 30 minutes. Thereafter, LDH assay stop solution was added to stop the reaction. Tecan fluorescent plate reader at 490nm and 690nm absorbance was used for measurements.

METHODS

7.1.11 Isolation and culture of neonatal cardiomyocytes from mouse hearts using MACs cardio isolation procedure

The experiments were performed as a part of collaboration with Prof. Dr. Felix B Engel, from the group of Experimental Renal and Cardiovascular Research, University Hospital Erlangen, Department of Nephropathology, Erlangen, Germany. Pregnant mice ((C57BL/6) were ordered from Charles River Laboratories. This mouse strain is widely used for its high degree of uniformity in response to the experimental treatments. The experiments have been performed under the license number TS-9/2016 Nephropatho. “The investigation conforms with the guidelines from Directive 2010/63/EU of the European Parliament on the protection of animals used for scientific purposes. Extraction of organs and preparation of primary cell cultures were approved by the local Animal Ethics Committee in accordance to governmental and international guidelines on animal experimentation (protocol TS-9/2016 Nephropatho).

Mice were decapitated at postnatal day 3 (P3), the chest was opened, and hearts were removed with a curved forceps. Isolated hearts (10 to 20) were placed in a Petri dish containing PBS without Ca²⁺ and Mg²⁺ with 50 µl 2M D-Glucose on ice. Using a scalpel blade, the aorta and atria were removed. The ventricles were placed on a dry Petri dish and were minced as small as possible using a scalpel blade. The minced heart tissue was transferred to a c-tube (up to 20 hearts in 1 tube), containing 5 ml of enzyme mix. For the isolation of cardiomyocytes, minced hearts were digested using gentleMACS Octo Dissociator (Miltenyi Biotech) according to the manufacturer’s instruction. For cardiomyocyte enrichment, cells were incubated with pre-plating medium (DMEM/F-12 +GlutaMAX; supplemented with: 10% [v/v] FBS 1% [v/v] Pen/Strep 2 mM L-Glutamine). After 90 minutes, the non-attached, enriched P3 cardiomyocytes were collected in 50 ml falcon tubes. After centrifugation, cells were resuspended in neonatal culture medium (DMEM/F-12 Glutamax medium supplemented with, 1% Penicillin and Streptomycin and 5% FBS, 2% Horse serum (HS)), counted using hemocytometer and plated at appropriate density. After 24 hours, medium was replaced with fresh neonatal culture medium and cells were used for transfections.

Reagent or Kit	Company	Catalogue
----------------	---------	-----------

METHODS

gentleMACS Octo Dissociator	Macs Miltenyi Biotech	130-095-937
Red blood cell lysis solution (10x)	Macs Miltenyi Biotech	130-094-183
GentleMACS M Tubes	Macs Miltenyi Biotech	130-093-236
Neonatal heart dissociation Kit	Macs Miltenyi Biotech	130-098-373
MACS BSA Stock Solution	Macs Miltenyi Biotech	130-091-376
MACS Rinsing Solution	Macs Miltenyi Biotech	130-091-222

Table 16 List of Reagents and kits for neonatal mouse cardiomyocytes.

7.1.12 Transfection of microRNAs in neonatal mouse cardiomyocytes

For transfection experiments, 96 well plates were pre-coated with fibronectin. Lipofectamine RNAiMAX was used to transfect P3 mouse cardiomyocytes, according to the manufacturer protocols. The transfection reagent was mixed together with microRNA and reduced serum medium (Opti-MEM) and mixture was slowly added dropwise to the cells. Medium exchange was performed 24 hours post transfection followed by incubation with EdU or staining with H3P.

7.1.13 Immunocytochemistry

Cardiomyocytes were fixed with 3.7% formaldehyde (Sigma) at RT for 15 min. Cells were washed three times with PBS and permeabilized, with 0.5 % Triton X-100 in PBS for 20 min and washed three times in PBS. The cells were blocked for 1 hour at RT with blocking buffer (10% Horse serum, 1 % BSA, 0.3 % Triton) in PBS and incubated with primary antibodies in dilution buffer (1x PBS, 1% BSA, 1% Donkey or horse serum, 0, 3% Triton) overnight at 4 °C. Subsequently, cells were washed three times with 0.1 % Nonidet P40 in PBS, and incubated with corresponding secondary antibodies conjugated with Alexa Fluor 488/ 594 (1:500 Life technologies) for 1 hour at RT. Cells were thereafter washed three times with 0.1% BSA.

EdU incorporation assay was performed by incubating cells with Click it reaction mix cocktail kit, according to manufacturer protocols (Life Technologies, Invitrogen C10637, C10337) for 30 min. The cells were washed three times with 0.1% BSA in PBS, followed

METHODS

by incubation with respective secondary antibodies for 1 hour at RT. Cells were thereafter incubated with Hoechst and washed three times with PBS.

7.1.14 Coating of plates

For human iPSC-CMs, plates were coated with Geltrex diluted in DMEM/F12 medium for 2 h at 37 °C. Cells were seeded immediately after aspiration of the coating medium. For neonatal mouse cardiomyocytes, plates were coated with fibronectin.

7.2 RNA-related methods

7.2.1 RNA extraction from hiPSC-CM

Total RNA was isolated from human iPSC-CMs using the RNeasy Kit (Qiagen). Kits were used according to the manufacturer instructions. Human iPSC-CM were seeded and transfected in 24- or 48-well cell culture plates. 48 hours and 72 hours post miRNA-transfection, cell culture medium was aspirated and cells were washed three times with sterile DPBS. DPBS was aspirated, QIAzol lysis reagent (350 to 700 μ l) was added onto cells and incubated for 5 minutes at RT. The resulting cell lysates were collected in 1.5 ml nuclease free reaction tubes (Eppendorf). MiRNeasy RNA extraction kit (Qiagen) was used to isolate the RNA according to the manufacturer instructions. The RNA concentration was measured using Nano drop at 260/280 nm. The isolated RNA was dissolved in 14 μ l of RNase-free water and stored at -80 °C or continued for reverse transcription.

7.2.2 Reverse Transcription (cDNA Synthesis)

Isolated RNA was used for reverse transcription of mRNA into complementary DNA (cDNA) by using the enzyme reverse transcriptase. A concentration of 1 μ g RNA was used for cDNA synthesis. High-capacity cDNA reverse transcription kit (Table 5) was used according to the manufacturer instructions.

The following reaction mix for cDNA synthesis by reverse transcription was listed in Table 17

Ingredients	Volume (μ l)
10X RT Buffer	2
25XdNTP Mix (100 mM)	0.8

METHODS

10X RT Random Primers	2
RNAse Inhibitor (20 U/ μ L)	0.5
Reverse transcriptase enzyme (50 U/μL)	1

Table 17 Reaction mix for cDNA synthesis

The reaction mix was performed in the thermal cycler by using the following program according to High-Capacity cDNA kit was listed in Table 18 .

	Step 1	Step 2	Step 3	Step 4
Temperature ($^{\circ}$C)	25	37	85	4
Time	10 min	120 min	5 min	∞

Table 18 Thermal cycler program (cDNA)

7.2.3 Quantitative Real-Time PCR (qRT-PCR)

cDNA was generated as described in section 7.2.1 and 7.2.2. Syber green detection method was used for performing qRT-PCR. The qRT-PCR was performed in 384 well plates and was analyzed by Vii7 real-time PCR system (Applied Biosystems). The following reaction mix and primers were used to prepare one well in a 384 well plate.

Reaction mix for qRT-PCR. Triplicates were pipetted for each sample in the 384 well plates, details are listed in Table 19. The following program was used according to the manufacturer instructions.

Components	Volume (μ l)
SYBR Green	5 μ l
Forward Primer (1.5 μ M)	0.5
Reverse Primer (1.5 μ M)	0.5
Nuclease free H ₂ O	2
cDNA	2

METHODS

Table 19 Components for performing qRT-PCR

Steps	Hold	Cycles (40 cycles)	
		Denature	Annealing
Temperature	95.0 °C	95.0 °C	60.0 °C
Time	10 min	15 sec	1 min

Table 20 Thermal cycler program (qRT-PCR)

The changes in the gene expression were analyzed by the relative quantification of mean Ct value of a housekeeping gene (GAPDH) which served as a normalizing control. Using the reference gene, the relative expression of cDNA was calculated by $2^{-\Delta\Delta CT}$ method.

7.2.4 Quantification of miRNA by TaqMan microRNA assays (RT-PCR)

MiRNA-mimics (hsa-miR-1825) and MiR-inhibitor (hsa-miR-195-5p) were transfected in 24- or 48-well cell culture plates. 48 hours post transfection, cells were collected for RNA isolation as mentioned above. TaqMan MicroRNA reverse transcription kit was used to perform reverse transcription and miRNA qRT-PCR. The master mix (1x) was prepared by mixing the following components provided in the kit. The details of kits were described above (Table 7).

Components	Volume (μ l)/reaction
100 mM dNTPs	0.075
MultiScribe™ reverse transcriptase, 50 U/ μ L	0.5
10x reverse transcription buffer	0.75
RNase inhibitor, 20 U/ μ L	0.095
Nuclease-free water	2,08

Table 21 Composition of RT-PCR master mix

METHODS

To this master mix, 3 μ l of 5x RT primer provided in the TaqMan MicroRNA assay and 5 μ l of 2ng RNA were added. All the components were gently mixed and centrifuged. RT master mix was kept on ice until the PCR reaction was prepared.

The reverse transcription PCR was programmed on a thermal cycler setting up the following parameters.

	Step 1	Step 2	Step 3	Step 4
Temperature ($^{\circ}$ C)	16	42	84	4
Time	30 min	30 min	5 min	∞

Table 22 Program for RT-PCR

7.2.5 qRT-PCR of miRNAs

qRT-PCR was performed in 384-well format using ViiA 7 System (Applied Biosystems). TaqMan MicroRNA fast advanced master mix and TaqMan microRNAs primers were used (Table 5). RNU-48 was used as an endogenous control for normalizing.

The components constituting a 10- μ l reaction/well consist of the following components

Components	Volume (μ l)/reaction well
TaqMan [®] Fast Advanced Master Mix	5
Nuclease-free water	3.75
TaqMan [®] MicroRNA assay	0.5
cDNA template	0.75

Table 23 Composition of qRT-PCR master mix

All the samples were loaded in triplicates in the 384-well plate including the endogenous controls. Null-template controls were used to verify the contaminations and accuracy of the PCR. The 384-well plate was briefly centrifuged, sealed with an adhesive film and loaded into the instrument.

METHODS

The experiment was set up in the ViiA 7 with the following parameters:

Steps	Hold	Hold	Cycles (40 cycles)	
			Denature	Annealing
Temperature	50 °C	95 °C	95.0 °C	60.0 °C
Time	2 min	2 min	1 sec	20 sec

Table 24 Program to perform qRT-PCR by fast advanced master mix.

7.2.5.1 TaqMan MicroRNA Primers

MicroRNA Primers	Company
hsa-miR-195-5p	Thermo Fisher Scientific
hsa-miR-1825	Thermo Fisher Scientific
RNU48 (Internal Control)	Thermo Fisher Scientific

Table 25 List of TaqMan miRNA primers and controls.

7.2.6 RNA-sequencing

MiRNA-scrambled, hsa-miR-mimic-515-3p and hsa-miR-mimic-519e-3p were transfected into human iPSC-CM as described above. 72 hours post transfections, cells were washed with DPBS three times. Thereafter QIAzol (Qiagen- MiRNeasy RNA extraction) was added. Resulting lysates were collected in 1.5 ml nuclease free reaction tubes (Eppendorf). RNA Sequencing and analysis was performed by ArrayStar (Arraystar, Inc., USA). The RNA concentration was measured using Nano drop at 260/280 nm. As previously described by the methodology from Array star, 1~2 µg of total RNA was used to prepare the sequencing library. Briefly, mRNA was isolated from total RNA using mRNA magnetic isolation module. Alternatively, rRNA is removed from the total RNA with a RiboZero Magnetic Gold Kit. Later, the enriched mRNA or rRNA depleted RNA was used for RNA-seq library preparation, using KAPA Stranded RNA-Seq Library Prep Kit (Illumina). Which incorporates dUTP into the second cDNA strand and renders the RNA-seq library strand-specific. The completed libraries were qualified with Agilent 2100 Bioanalyzer and quantified by absolute quantification qPCR method. To sequence the libraries on the Illumina HiSeq 4000 instrument, the barcoded libraries were mixed,

METHODS

denatured to single stranded DNA in NaOH, captured on Illumina flow cell, amplified in situ, and subsequently sequenced for 150 cycles for both ends on Illumina HiSeq instrument.

7.2.7 Image Analysis and data processing

Image analysis and base calling was performed using the Solexa pipeline v1.8 (Off-Line Base Caller software, v1.8). Sequence quality was examined using the FastQC software. The trimmed reads (trimmed 5', 3'-adaptor bases using cutadapt) were aligned to reference genome using Hisat2 software (v2.0.4).¹²⁹ The transcript abundances for each sample was estimated with StringTie¹³⁰ (v1.2.3), and the FPKM¹³¹ value for gene and transcript level were calculated with R package Ballgown (v2.6.0).¹³² The differentially expressed genes and transcripts were filtered using R package Ballgown. The novel genes and transcripts were predicted from assembled results by comparing to the reference annotation using StringTie and Ballgown. Principle Component Analysis (PCA) and correlation analysis were based on gene expression level, Hierarchical Clustering, Gene Ontology, Pathway analysis, scatter plots and volcano plots were performed with the differentially expressed genes in R, Python or shell environment for statistical computing and graphics.

7.3 Protein related methods

7.3.1 Protein Isolation

Human iPSC-CMs were cultured on 6-well cell culture plates (400,000 cell/well) and transfected with individual miRNAs. The medium was aspirated and the cells washed three times with DPBS. RIPA (Radioimmunoprecipitation) lysis buffer (1 ml) was freshly mixed with 15 µl Phosphatase Inhibitor, 10 µl Sodium Orthovanadate and 10 µl PMSF (Protease Inhibitor-phenylmethylsulfonyl fluoride). Freshly mixed cocktail (100 µl/well) was added onto the cells. After incubation for 5 minutes on ice, the cells were scraped with cell scrapers and the cell lysates were collected in 1.5 ml Eppendorf tubes. Cell lysates were centrifuged at 13000 rpm for 20 minutes at 4°C. The supernatants from each tube was collected and the pellet was discarded. BCA protein assay kit (Pierce) was used to determine the concentration of protein. 10 µl of standards and cell lysates were loaded in duplicates in 96-well plates. 100 µl of BCA protein assay mix reagents A and B were

METHODS

prepared in a ratio of 50:1, vortexed and loaded on to the 10 µl standards and cell lysates. After incubation for 30 minutes at 37°C, protein concentration was assessed photospectroscopically at 562 nm. Protein lysates were stored at -80°C until use.

7.3.2 Immunoblotting (SDS-PAGE)

4-20% Pre cast protein gels (Bio-Rad) with 15 well combs were used for the separation of proteins according to their electrophoretic mobility. Loading dye was mixed with the protein samples. The samples were heated up to 95°C for 10 minutes. The gels were placed in the gel running modules. 1X SDS running buffer was added into the apparatus. Equal amount of the denatured protein samples was loaded into the gels. A protein ladder was loaded on either corner of the gels, which gives the corresponding bands to a particular molecular weight on the gels while running. The apparatus was closed and was set to run at 30 mA current and constant voltage.

7.3.3 Western blotting

A western blot apparatus was used to transfer the proteins from SDS-polyacrylamide gel onto a polyvinylidene difluoride (PVDF) membrane. The membrane was activated using 100% methanol for 1 minute, washed twice with ddH₂O and placed in transfer buffer. Thereafter, the pre cast gel was taken out very carefully from the apparatus.

The stacking gel was separated from the resolving gel and discarded. Resolving gel was taken for the protein transfer. Whatmann filter papers were soaked in semidry transfer buffer. The filter papers, membrane, and gel was arranged in semidry transfer apparatus. The transfer was performed for 90 min at a current and constant voltage of 70 mA for 1 gel and 140 mA for 2 gels. The membrane was washed for 10 min in TBST and blocked for 1 h in 5% BSA/TBST at room temperature with mild shaking. Subsequently, the membrane was later incubated in the primary antibody solution overnight at 4°C. The membrane was later washed three times in TBST, transferred into a new 50 ml tube containing secondary antibody solution and incubated for 1h at room temperature. The membrane was washed three times with TBST, transferred onto a thin polythne foil, and placed on an even surface. The chemiluminescent substrate Supersignal westDura Extended solution was prepared by mixing both solutions in 1:1 ratio and added on to the membrane and incubated for about 5 minutes. The solution was taken out and the membrane was developed under chemiluminescence to detect the antibody labeled protein (INTAS Detection System).

7.4 Image quantification

For immunofluorescence analysis, imaging was acquired using ArrayScan XTI High Content Screening platform (Thermo fisher scientific) or with Operetta CLS High-Content Analysis System (PerkinElmer).

For 384-well plate 36 images and for 96-well plate, 64 images per well from all three channels were acquired, Cell nuclei and EdU/H3P-intensities were quantified using Cellomics Scan Version 6.6.0. For the HTS (Figure **10**) 384-well plate, for mimic-screen per replicate > 3000 Cardiomyocytes (CMs) nuclei positive for Cardiac TroponinT and for inhibitor-screen, per replicate > 2500 CMs nuclei positive for Cardiac TroponinT were analyzed. For follow up experiments (Figure **9, 11-14, & 17**), 96-well plates were used per replicate, > 8000 CMs nuclei positive for Cardiac TroponinT were analyzed.

8. RESULTS

8.1 Generation and transfection of human induced pluripotent stem cell-derived cardiomyocytes (hiPSC-CMs)

As a model system, human cardiomyocytes (hiPSC-CM) generated from skin fibroblasts of healthy probands were used (**Figure. 8A**). HiPSC-CMs were used for experiments after 30 to 40 days in culture. We established a liposome-based transient transfection method to efficiently transfect miRNAs into hiPSC-CM (**Figure. 8B-D**). First, fluorescent-labeled miRNAs (FAM-miR) were transfected into hiPSC-CM (**Figure. 8B**) showing a high incorporation. FAM-microRNA transfected hiPSC-CMs further underwent FACS-analysis that confirmed efficient transfection (**Figure. 8C-D**). Furthermore, transfection with death inducing silencing RNAs (siRNAs) resulted in reduced survival of hiPSC-CMs. These are potent siRNAs ubiquitously target genes that are indispensable for cell survival; knockdown of these genes induces a high degree of cell death, which is visible by light microscopy. This method is widely used to quickly assess the transfection efficiency (**Figure. 8E**).

RESULTS

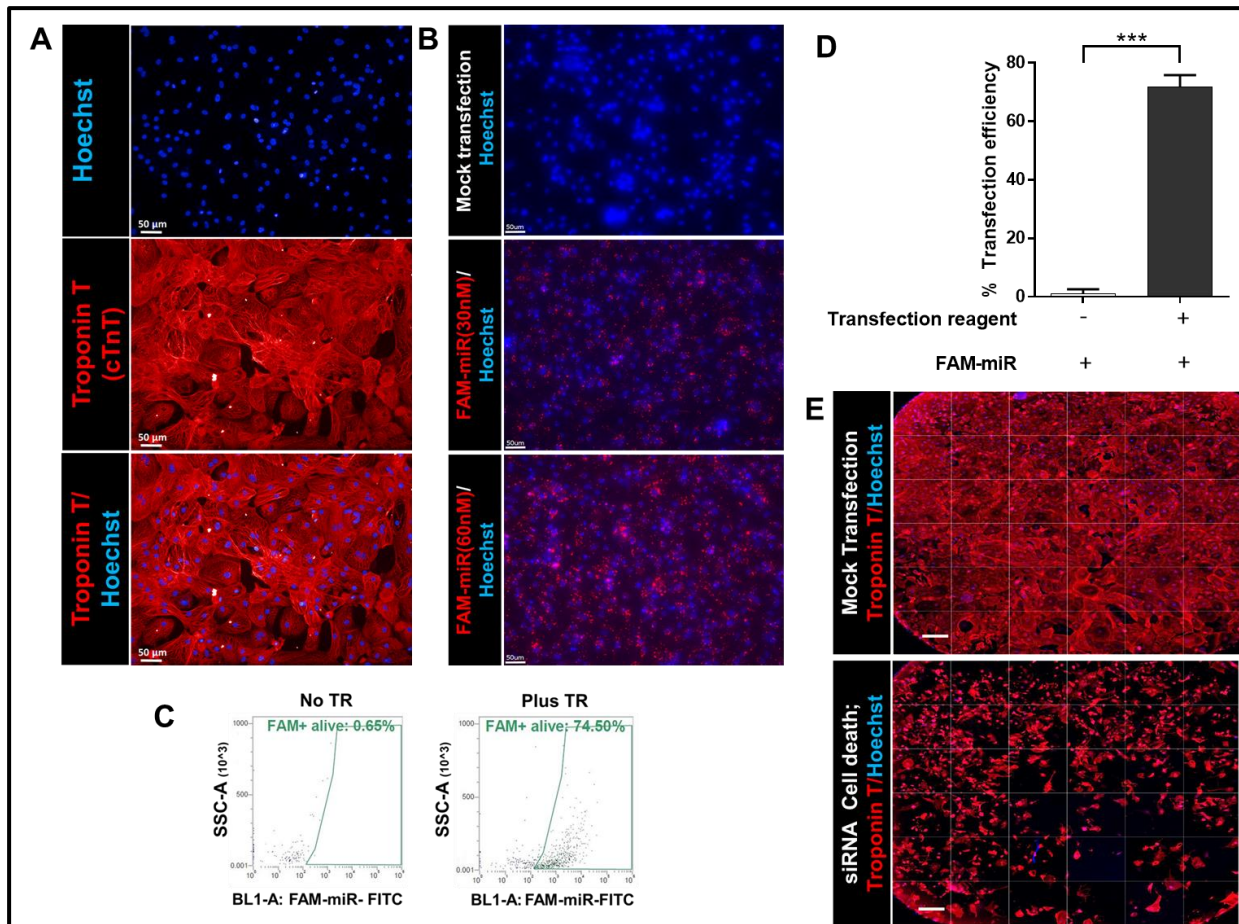


Figure 8: Efficient generation and transfection of human iPSC-derived cardiomyocytes.

Figure 8A: Immunofluorescence images showing Hoechst (blue, nuclei), cardiac troponin T (red) positive hiPSC-CMs. **Figure 8B:** Representative images of mock-transfected (upper image) and fluorescently labeled pre-miRNA (FAM-miR) transfected hiPSC-CMs at 24 hours post transfection (30nM, middle; 60 nM, lower image). **Figure 8C:** Shown are representative flow cytometry plots, Fluorescence-activated cell sorting (FACS), was utilized and samples were gated for side scatter (SSC) versus FITC (Attune channel BL1; Excitation: Blue laser 488nm, Emission filter (nm): 530/30 nm). Left image, hiPSC-CMs were transfected with FAM-miR (Fluorescent labelled microRNA) without any Transfection reagent (TR), whereas right image depicts hiPSC-CMs transfected with TR and FAM-miR; only in the presence of TR, there is an efficient increase of FAM-miR expression in the cells shown as FITC-positive cells. Human iPSC-CMs transfected with fluorescently labeled FAM-miR were analyzed using fluorescence-activated cell sorting (FACS) 24 hours after transfection. **Figure 8D:** shown are the percentage of cells, which are positive for fluorescently labelled microRNA analyzed by FACS analysis (n=3); ***, P < 0.001 vs. Control. **Figure 8E:** Representative images of human iPSC-CMs after mock-transfection (top) and transfection with cell death-inducing siRNAs (bottom) showing a high induction of a cell-death phenotype at 48 hours post transfection, Cardiomyocyte specific marker was used, Cardiac troponin T (red), Hoechst (blue, nuclei). **Scale bar: A, B: 50 μ m. E: 500 μ m**

RESULTS

Statistical Analysis for Figure 8D:

Bars represent average of three biological experiments; data analysis conducted using Graph pad 7 software. Student's t-test, two-tailed was used for the analysis. Values are presented as mean \pm s.e.m. ***P < 0.001 relative to Control. A value of P \leq 0.05 was considered as statistically significant.

8.2 Transient hypoxia enhances proliferative activity in hiPSC-cardiomyocytes after transfection with miRNAs

Once we were able to transfect the cells, we later used miR-1825, a miRNA previously reported to induce proliferation in murine cardiomyocytes,⁶⁵ to test proliferative capacity in human iPSC-CMs (**Figure. 9**). In order to first verify the overexpression or downregulation of microRNA in hiPSC-CMs, we transfected microRNA-mimic-1825 and anti-miR-195, respectively, and performed microRNA-qRT-PCR, which showed significant increase of miR-1825 abundance after overexpression (**Figure. 9A**) and downregulation of endogenous miR-195. MiRNA-195 belongs to mir-15 family and inhibition of anti-miR-195 is known to stimulate cardiomyocyte proliferation,¹¹⁰ this was used to evaluate the transfection and downregulation after anti-miR-195 treatment in hiPSC-CMs as a positive control (**Figure. 9B**). Transfection with miR-1825-mimic increased DNA synthesis assessed by incorporation of 5-Ethynyl-2-deoxyuridin (EdU) in a dose dependent manner (**Figure. 9C-D**). Immunocytochemistry was performed and the representative immunofluorescence images show the increase in EdU positive hiPSC-CMs after transfection with miR-mimic-1825 (60nM) (**Figure. 9D**). Furthermore, a protocol that mimics ischemia/reperfusion in hiPSC-CMs *in vitro* by using transient hypoxia, resulted in increased cell-cycle reentry after miR-1825 mimic transfection, but failed to do so after miR-scrambled transfection (**Figure. 9F**). Of note, transfection of miR-1825-mimic did not enhance toxicity in hiPSC-CMs, as assessed by LDH release (**Figure. 9E**).

RESULTS

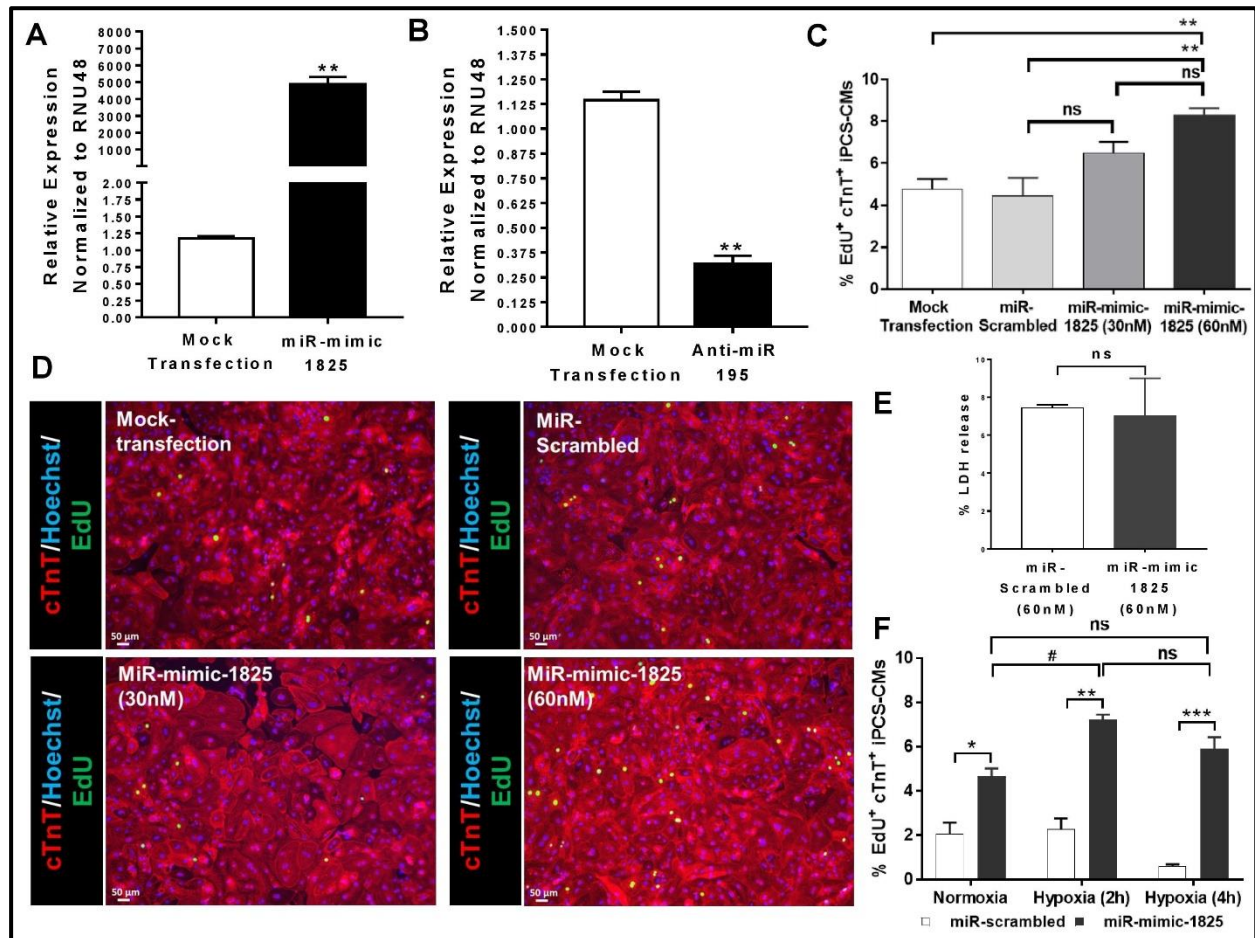


Figure 9: Transient hypoxia increases miRNA-induced proliferative potential in human iPSC-cardiomyocytes

Figure 9A: MiRNA-expression in hiPSC-CMs after transfection with **2A)** miR-mimic-1825 **2B)** anti-miR-195. (n=3); **, P < 0.01 vs. Mock Transfection.

Figure 9C: Incorporation of EdU in hiPSC-CMs treated with transfection reagent (Mock 4.07% ±0.5 %) and after transfection with miRNA-scrambled (4.4% ±0.8%), miR-mimic-1825 ((30nM) (6.4% ±0.5%) and miR-mimic-1825 (60nM) (8.3% ±0.3%). (n=3); **, P < 0.01 vs. Mock or miR-scrambled. (Mock vs. miR-mimic-1825(60nM) **P = 0.005**); (miR-scrambled vs. miR-mimic-1825(60nM) **P = 0.003**).

Figure 9D: Representative immunofluorescence images of EdU-uptake in mock transfected hiPSC-CMs and after transfection with miRNA-scrambled, miR-mimic-1825 (30nM and 60nM)). Hoechst (blue, nuclei), cardiac troponin T (red) and EdU (green). **Scale bar: 50 μm.**

Figure 9E: Lactate dehydrogenase (LDH) release of hiPSC-CMs after transfection with miR-scrambled and miR-mimic-1825 (60nM). Supernatants were collected 24 hours post transfection. (n=3).

RESULTS

Figure 9F: Incorporation of EdU in hiPSC-CMs transfected with miR-scrambled- Normoxia (2.03% \pm 0.5%), Hypoxia 2h (2.29% \pm 0.4%), Hypoxia 4h (0.16% \pm 0.08%) or miR-mimic-1825 under Normoxia (4.69% \pm 0.3%), or after transient hypoxia for two hours (7.21% \pm 0.2%) and four hours (5.9% \pm 0.5%). EdU-positive hiPSC-CMs were assessed 96 hours post transfection. *, miR-scrambled vs. miR-mimic-1825; #, miR-mimic-1825 normoxia vs hypoxia (n=3). *, #; P < 0.05, **; P < 0.01; ***; P < 0.001. **(MiR-scrambled VS. miR-mimic-1825: Normoxia P = 0.012; Hypoxia (2h) P=0.0012; Hypoxia (4h) P=0.0009).**

Statistical Analysis for Figure 9:

Bars represent average of three biological experiments; data analysis conducted using Graph pad 7 software. For **9A, 9B, 9E** Student unpaired t test (Mann-Whitney test). For **9C**, one-way ANOVA using Tukey and for **9F**, two-way ANOVA using Bonferroni's multiple comparisons test was used for the analysis. Values are presented as mean \pm s.e.m. *P < 0.05, **P < 0.01, ***P < 0.001 relative to Control. A value of P \leq 0.05 was considered as statistically significant.

8.3 High throughput screening of human microRNAs

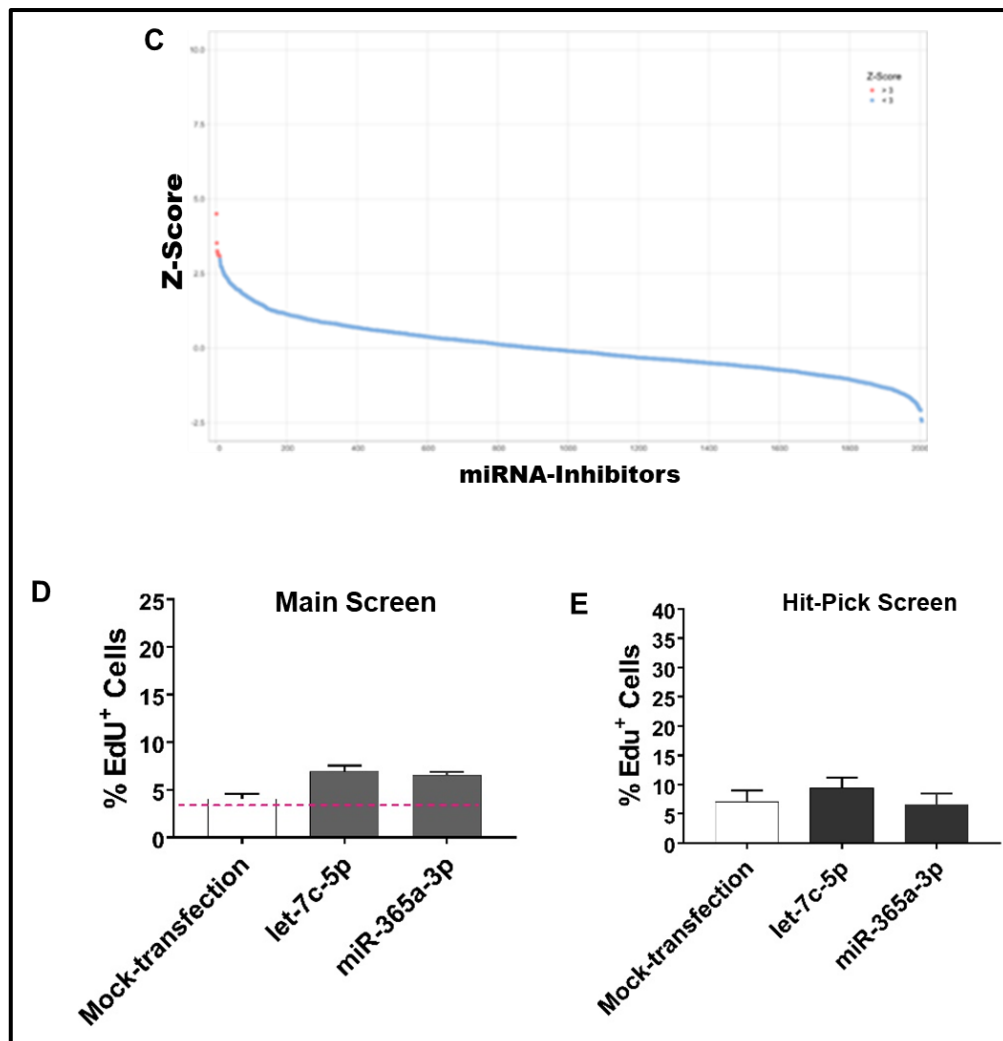
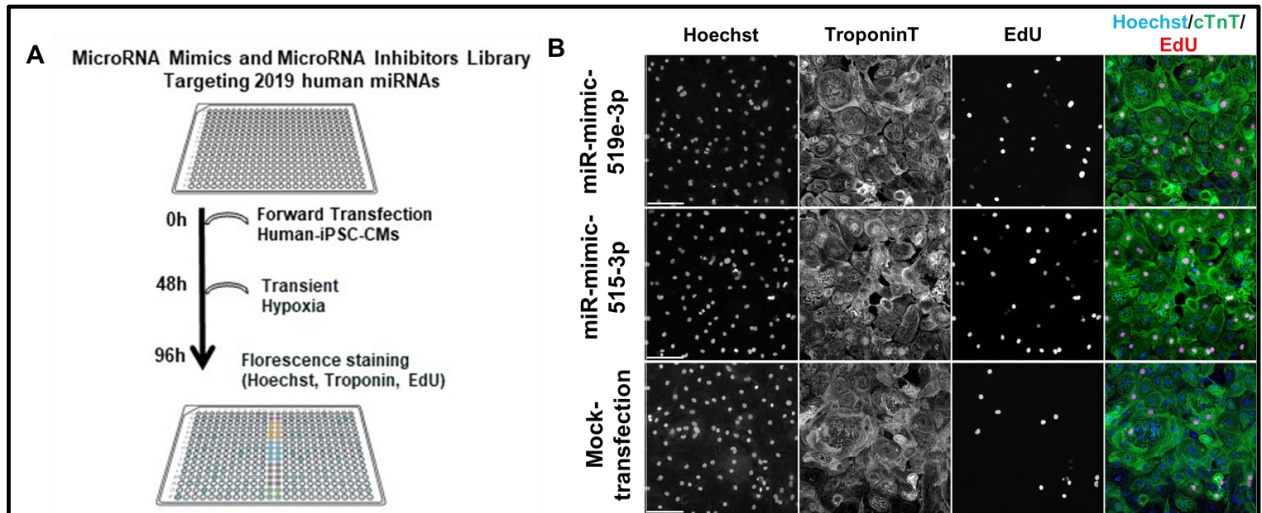
We next performed a high-throughput screening (HTS) by using a miRNA-library consisting of 2019 miR-mimics and miR-inhibitors (Ambion; mirVana Human Library v19.0) in parallel screenings (**Figure. 10**). For the high-throughput screening, each miRNA of the library (miR-mimic or miR-inhibitor) was robotically transferred to a 384-wells pre-plated with hiPSC-CMs. Individual forward transfection of miRNAs was performed with the established protocol and human iPSC-CMs were transiently exposed to hypoxia. Using a high-content imaging system, image segmentation was performed in order to detect proliferating cardiomyocytes by using Hoechst for nuclei staining and troponin as a cardiomyocyte specific marker (**Figure. 10A-B**).

8.4 Selective overexpression, but not downregulation of miRNAs induces proliferative activity in human iPSC-CMs as assessed by HTS

Proliferation of miRNA-transfected human iPSC-CMs was assessed by EdU (**Figure. 10A-B**). Downregulation of 2019 miRNAs yielded only two miRNAs (let-7c-5p and miR-365a-3p) that increased proliferation (Z-Score >3 in both duplicates), as assessed by EdU-positive cells (**Figure. 10C-D**). However, the increase of EdU-positive cardiomyocytes was modest (let-7c-5p: 6.9 \pm 0.3%, miR-365a-3p: 6.5 \pm 0.1%) as compared to mock transfected human iPSC-CMs (Mock; 5.1 \pm 0.5%, **Figure. 10D**) and a Hit-pick

RESULTS

screening did not confirm a significant increase in cell-cycling iPSC-CMs after treatment with anti-let-7c-5p and anti-miR-365a-3p (**Figure. 10E**). Conversely, transfection of miRNA-mimics identified twenty-eight miRNAs that induced proliferative activity in human iPSC-CMs (z-factor > 3 in both duplicates) (**Figure. 10F-G**). A Hit-pick screening confirmed the proliferative potential of candidate miRNA-mimics (**Figure. 10H**).



RESULTS

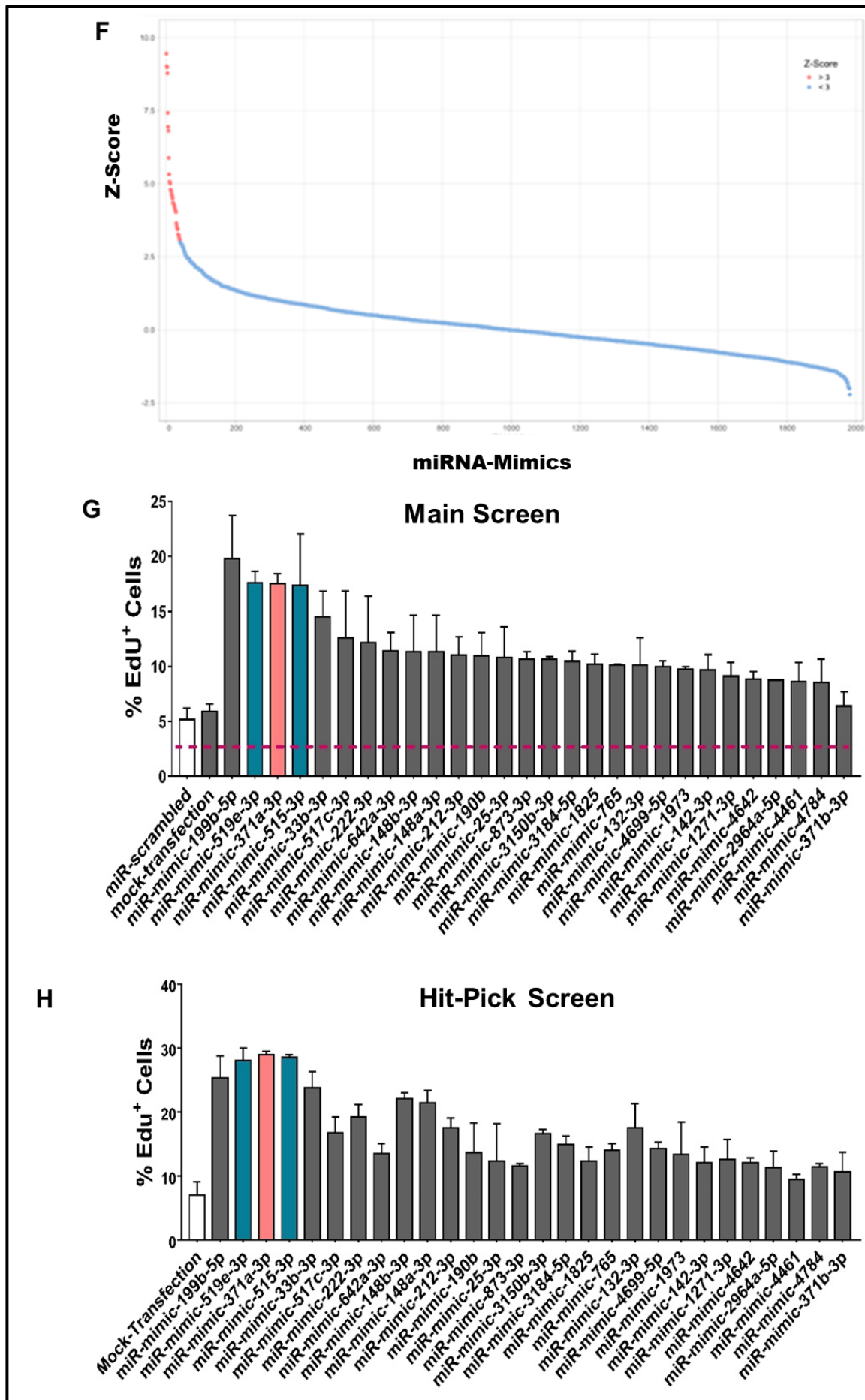


Figure 10: High-throughput screening for identification of pro-proliferative miRNAs

Figure 10A: Graphical illustration of the high-throughput (HT) screening workflow. A miRNA-library was used for overexpression (miR-mimics) and inhibition (anti-miRs) of 2019 miRNAs. HT screen was performed in duplicates. **Figure 10B:** Immunofluorescence images of hiPSC-CMs showing Hoechst (blue, nuclei), cardiac troponin T (green) and EdU (red) after transfection with miR-mimic-519e-3p, miR-mimic-515-3p and mock transfection. **Scale bar: 5 μ m.** **Figure 10C:** EdU-incorporation into hiPSC-CMs was assessed after individual transfection with 2019 miRNA-inhibitors (anti-miRNAs). Data plot indicates EdU-incorporation (%). A Z-factor > 3 in both replicates, indicated by red dots, was used to delineate a significant increase in EdU-uptake. **Figure 10D:** Two anti-miRNAs, let-7c-5p and miR-365-3p significantly increased EdU-uptake in hiPSC-CM. The horizontal dotted line indicates the mean EdU-incorporation of hiPSC-CMs. **Figure 10E:** Validation of anti-miRNAs let-7c-5p and miR-365-3p in a second screen. However, transfection of hiPSC-CM with anti-let-7c-5p and anti-miR-365-3p did not significantly increase EdU-uptake as compared to mock transfected hiPSC-CMs. **Figure 10F:** EdU-incorporation into hiPSC-CMs was assessed after individual transfection with 2019 miRNA-mimics. Data plot indicates EdU-incorporation (%). A Z-factor > 3 in both replicates, indicated by red dots, was used to delineate a significant increase in EdU-uptake. **Figure 10G:** Twenty-eight miRNA-mimics significantly increased EdU-uptake in hiPSC-CM. The horizontal dotted line indicates the mean EdU-incorporation of hiPSC-CMs. Colored bars highlight members of the miR-515-family and members of the miR-371–373 Cluster. **Figure 10H:** Validation of miRNA-mimics in a secondary screen. Screen was performed in duplicates, shown is the mean EdU-uptake of two screens.

8.5 Hsa-miR-515-3p, hsa-miR-519e-3p and hsa-miR-371a-3p substantially induce DNA synthesis in human iPSC-CMs

First, we validated our findings derived from the high-throughput screening. Transfection of hiPSC-CMs with miR-515-3p, miR-519e-3p and miR-371a-3p-mimic substantially increased incorporation of EdU in human iPSC-CMs as compared to miR-scrambled transfected hiPSC-CMs (**Figure. 11A**). In addition, we exposed miR-mimic transfected hiPSC-CMs to transient hypoxia (0.5% O₂ for 2 hours). Interestingly, a brief period of hypoxia further increased proliferative activity after treatment with miR-515-3p and miR-519e-3p (**Figure. 11B**). Immunocytochemistry was performed for the representative immunofluorescence images showing the increase in EdU positive hiPSC-CMs after transfection with miR-mimic-515-3p, miR-mimic-519e-3p and miR-mimic-371a-3p, followed by transient hypoxia (**Figure. 11C**).

RESULTS

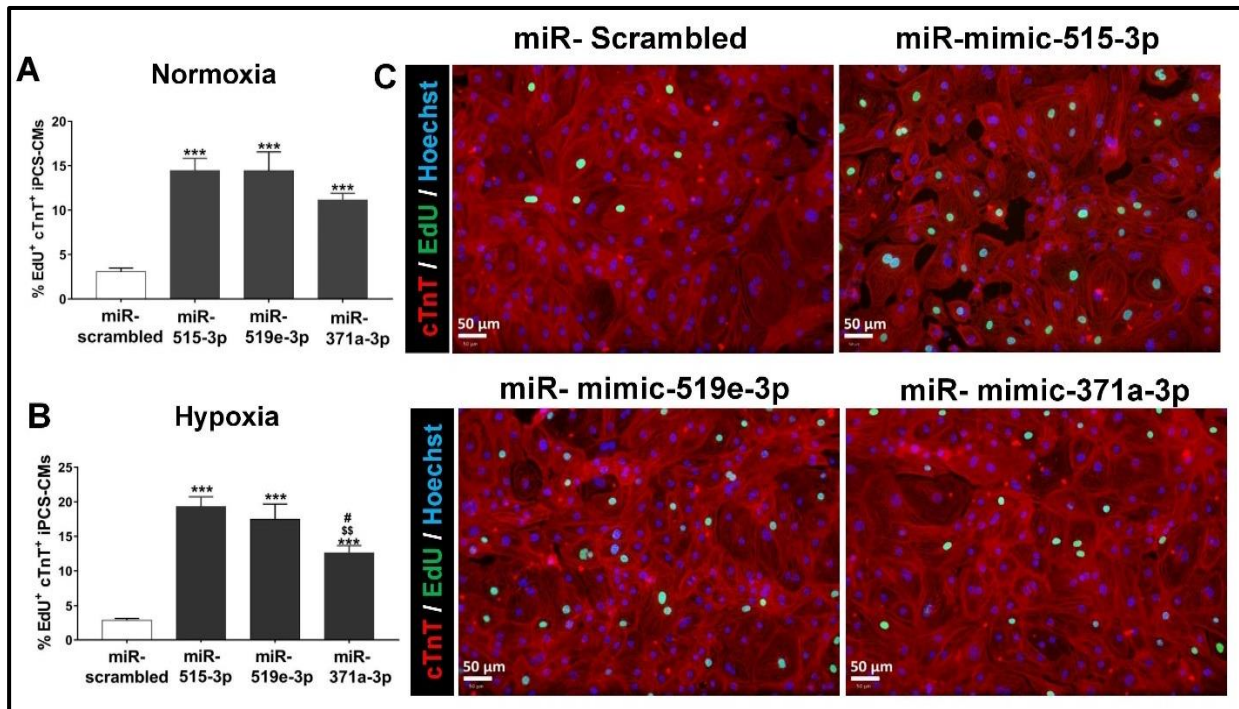


Figure 11: Overexpression of hsa-miR-515-3p, hsa-miR-519e-3p and hsa-miR-371a-3p induce DNA synthesis in human iPSC-CM

Figure 11A: Incorporation of EdU in hiPSC-CMs transfected with miR-scrambled, miR-mimic-515-3p, miR-mimic-519e-3p and miR-mimic-371a-3p under normoxia. (n=3). ***; $P < 0.001$ vs. miR-scrambled.

Figure 11B: Incorporation of EdU in hiPSC-CMs transfected with miR-scrambled, miR-mimic-515-3p, miR-mimic-519e-3p and miR-mimic-371a-3p after transient hypoxia. (n=3). *, miR-scrambled vs. miR-mimic-515, 519 & 371; \$, miR-515 vs. 371; #, miR-519 vs. miR-371. #; $P < 0.05$, \$\$; $P < 0.01$, ***; $P < 0.001$. **Figure 11C:** Representative immunofluorescence images of hiPSC-CMs after transfection with miR-mimic-515-3p, miR-mimic-519e-3p and miR-mimic-371a-3p, followed by transient hypoxia. Hoechst (blue, nuclei), cardiac troponin T (red) and EdU (green). **Scale bar: 50 μ m.**

Statistical Analysis Figure 11:

Bars represent average of three to five biological experiments; data analysis conducted using Graph pad 7 software. Two-way ANOVA with Tukey multiple comparisons test was used for the analysis. Values are presented as mean \pm s.e.m. * $P < 0.05$, ** $P < 0.01$, *** $P < 0.001$ relative to Control. A value of $P \leq 0.05$ was considered as statistically significant

RESULTS

8.6 Hsa-miR-515-3p, hsa-miR-519e-3p and hsa-miR-371a-3p induce late G2/Mitosis in human iPSC-CMs

Furthermore, we analyzed the mitosis marker histone H3 phosphorylated on serine10 (H3PS10), a marker of late G2 mitosis (**Figure. 12**). Similarly, treatment with miR-515-3p, miR-519e-3p and miR-371a-3p-mimic increased H3PS10-positive hiPSC-CM as compared to miR-scrambled treated hiPSC-CMs in Normoxia conditions (**Figure. 12A**). In addition, a transient hypoxia, as compared to normoxia, increased further the number of H3PS10-positive hiPSC-CM in miR-515-3p and miR-519e-3p-mimic transfected hiPSC-CMs (**Figure. 12B**). Immunocytochemistry was performed for the representative immunofluorescence images showing the increase in H3P positive hiPSC-CMs after transfection with miR-mimic-515-3p, miR-mimic-519e-3p and miR-mimic-371a-3p, followed by transient hypoxia (**Figure. 12C**). These results indicate that miR-515-3p, miR-519e-3p and miR-371a-3p induce cardiomyocyte proliferation. As miR-515-3p and miR-519e-3p showed a more pronounced induction of proliferative activity under hypoxic conditions as compared to miR-371a-3p, we further focused our study on these two miRNAs.

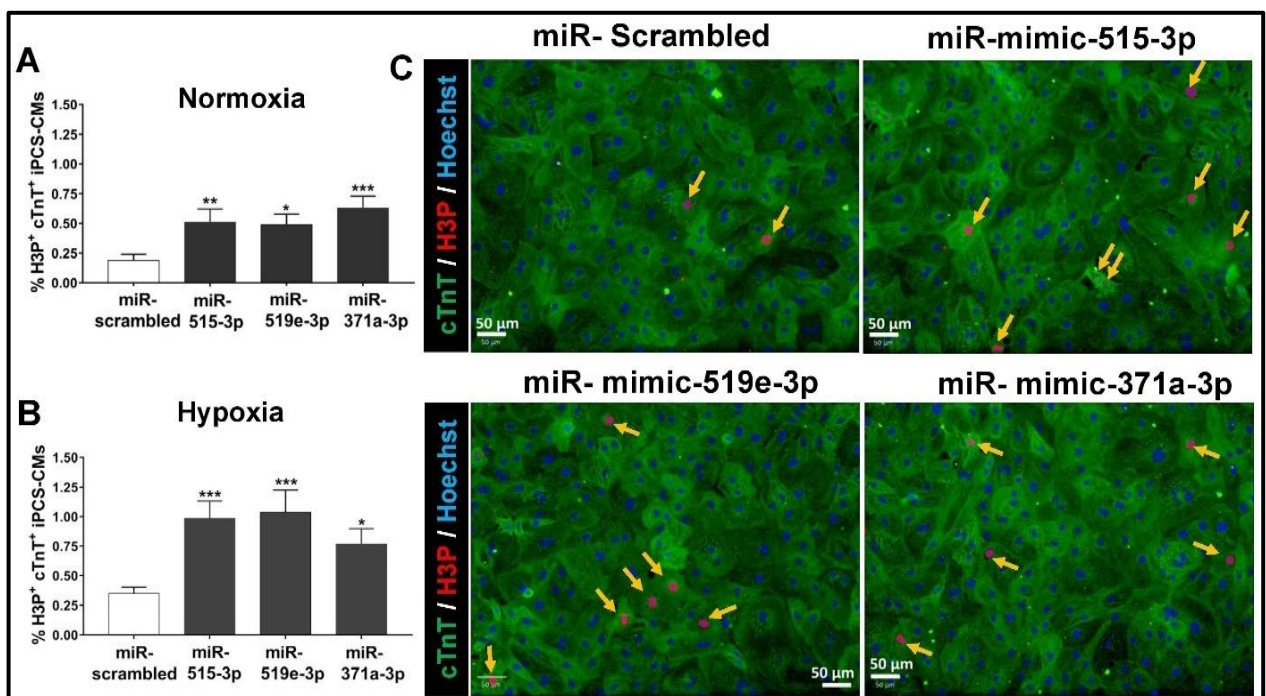


Figure 12: Overexpression of hsa-miR-515-3p, hsa-miR-519e-3p and hsa-miR-371a-3p induce late mitosis in human iPSC-CM

RESULTS

Figure 12A: Analysis of mitosis in hiPSC-CM, as assessed using phosphorylated histone H3 (H3P). H3P-positive hiPSC-CM after transfection with miR-scrambled, miR-mimic-515-3p, miR-mimic-519e-3p and miR-mimic-371a-3p under normoxia. (n=5). *, P < 0.05, **, P < 0.01; ***, P < 0.001 vs. miR-scrambled. **Figure 12B:** H3P-positive hiPSC-CM after transfection with miR-scrambled, miR-mimic-515-3p, miR-mimic-519e-3p and miR-mimic-371a-3p after transient hypoxia. (n=5). *, P < 0.05, ***, P < 0.001 vs. miR-scrambled. **Figure 12C:** Representative immunofluorescence images of hiPSC-CMs after transfection with miR-scrambled, miR-mimic-515-3p, miR-mimic-519e-3p and miR-mimic-371a-3p, followed by transient hypoxia. Yellow arrows represent the cells, which are positive for Phospho histone H3 (H3P) a marker for G2/mitosis. Hoechst (blue, nuclei), cardiac troponin T (green) and EdU (red). (n=5). **Scale bar: 50 μ m.**

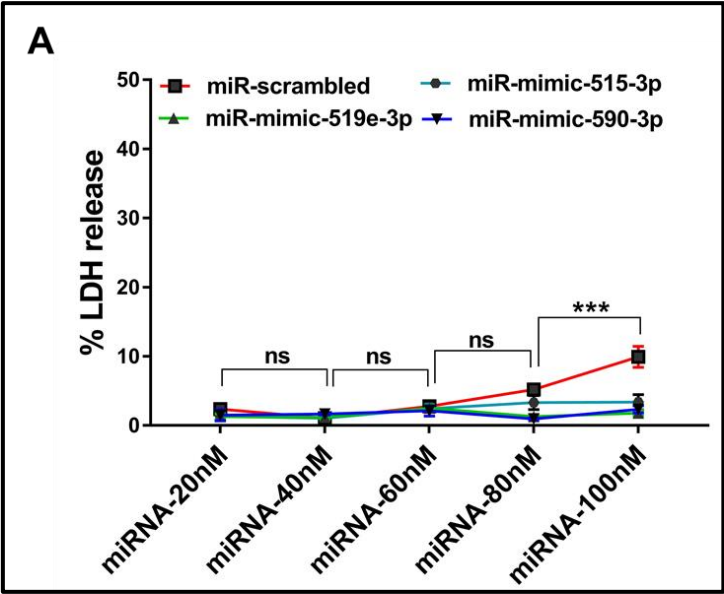
Statistical Analysis Figure 12:

Bars represent average of five biological experiments; data analysis conducted using Graph pad 7 software. Two-way ANOVA with Tukey multiple comparisons test was used for the analysis. Values are presented as mean \pm s.e.m. *P < 0.05, **P < 0.01, ***P < 0.001 relative to Control. A value of P \leq 0.05 was considered as statistically significant

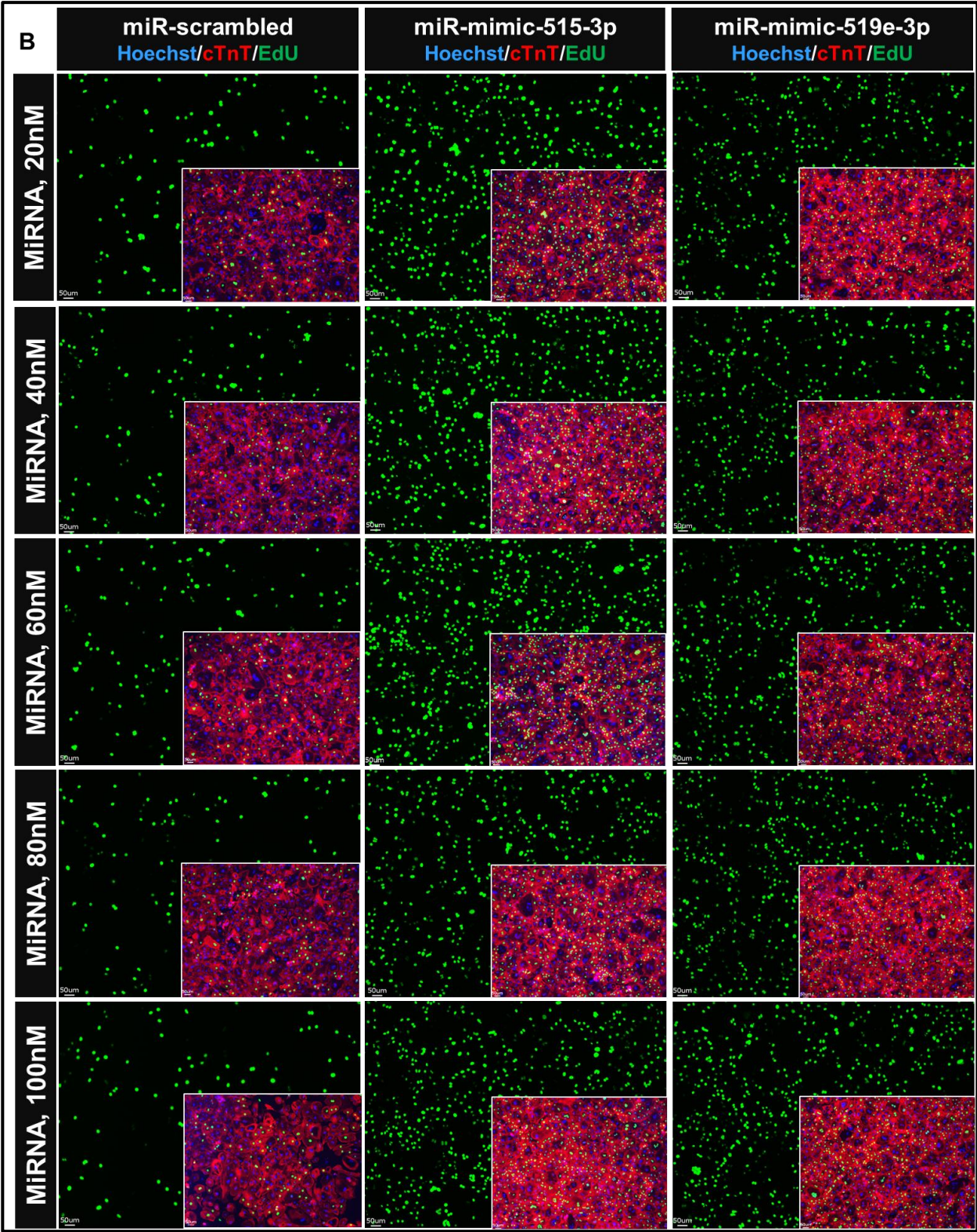
8.7 Concentration-dependent EdU Incorporation and toxicity assessment after miRNA-transfection

In order to define efficacy and toxicity effects, miRNAs were transfected with increasing concentrations, whereby transfection with 60nM induced proliferative activity significantly above lower concentrations (**Figure. 13A-C**) without affecting toxicity, as assessed by LDH assay (**Figure. 13A**). DNA synthesis (EdU) was significantly improved after miR-transfections (**Figure. 13B-C**). Immunocytochemistry was performed for the representative immunofluorescence images showing the increase in EdU positive hiPSC-CMs after transfection with miR-scrambled, miR-mimic-515-3p, miR-mimic-519e-3p and miR-mimic-590-3p (**Figure. 13B**). Of note, transfection of hsa-miR-590-3p that was reported to induce cardiomyocyte proliferation in murine cardiomyocytes,^{65, 114} did not result in enhanced EdU incorporation in human iPSC-CM.

RESULTS



RESULTS



RESULTS

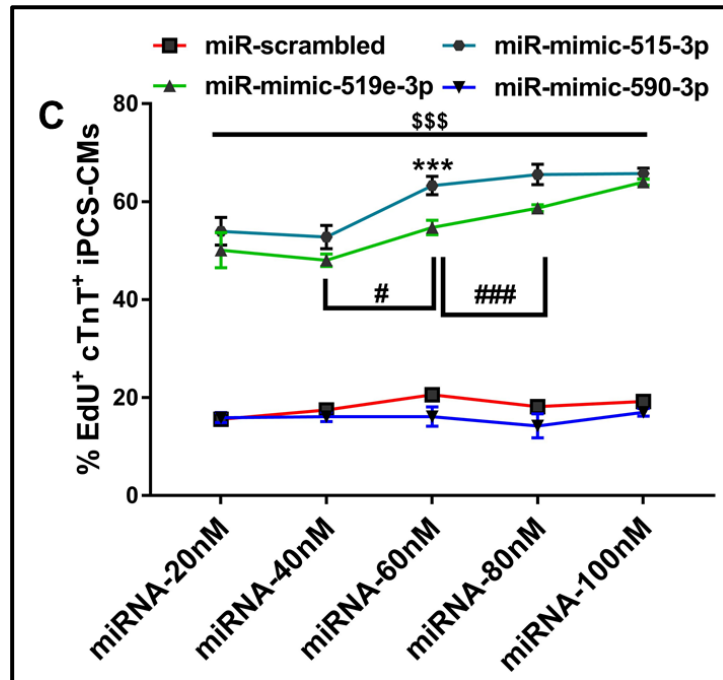


Figure 13: Concentration-dependent EdU Incorporation and toxicity assessment after miRNA-transfection

Figure 13A: Incorporation of EdU in hiPSC-CMs after transfection with increasing miRNA-mimic concentrations (20, 40, 60, 80 and 100 nM). \$, miR-scrambled (20nM- 100nM) vs. miR-515 and miR 519 (20nM-100nM). *, vs. miR-515 in between different miRNA-concentrations (20nM-100nM). #, vs. miR-519 in between different miRNA-concentrations (20nM-100nM). (n=3). \$; P < 0.05, **; \$\$; P < 0.01; ***; \$\$\$; ### P < 0.001. **Figure 13B:** Representative immunofluorescence images of hiPSC-CMs showing Hoechst (blue, nuclei), cardiac troponin T (red) and EdU (green). **Scale bar: 50 μ m.** **Figure 13C:** Analysis of cytotoxicity, as assessed by LDH release of hiPSC-CMs after transfection with miR-mimic-515-3p, miR-mimic-519e-3p and miR-mimic-590 using different miRNA-mimic-concentrations. (n=3). *, treatments within miRNA-scrambled (20 nM vs. 40nM; 40nM vs. 60nM; 60nM vs.100 nM). ***; P < 0.001.

Statistical Analysis for Figure 13:

Bars represent average of three biological experiments; data analysis conducted using Graph pad 7 software. Two-way ANOVA with Tukey multiple comparisons test was used for the analysis. Values are presented as mean \pm s.e.m. *P < 0.05, **P < 0.01, ***P < 0.001 relative to Control. A value of P \leq 0.05 was considered as statistically significant.

RESULTS

8.8 Long-term effects of miRNA-transfections in cardiomyocyte proliferation

In addition, we analyzed EdU-incorporation and positive staining for H3PS10 over a period of six days after transfection (Figure. 14A-B). Whereas hiPSC-CMs showed highest EdU-incorporation at day five (Figure. 14A), H3PS10-positive hiPSC-CMs peaked at day two-post transfection (Figure. 14B). Of note, miR-515-3p and miR-519e-3p transfection was effective in hiPSC-CMs from both, female or male human iPSC-cardiomyocytes (Figure. 14C-D).

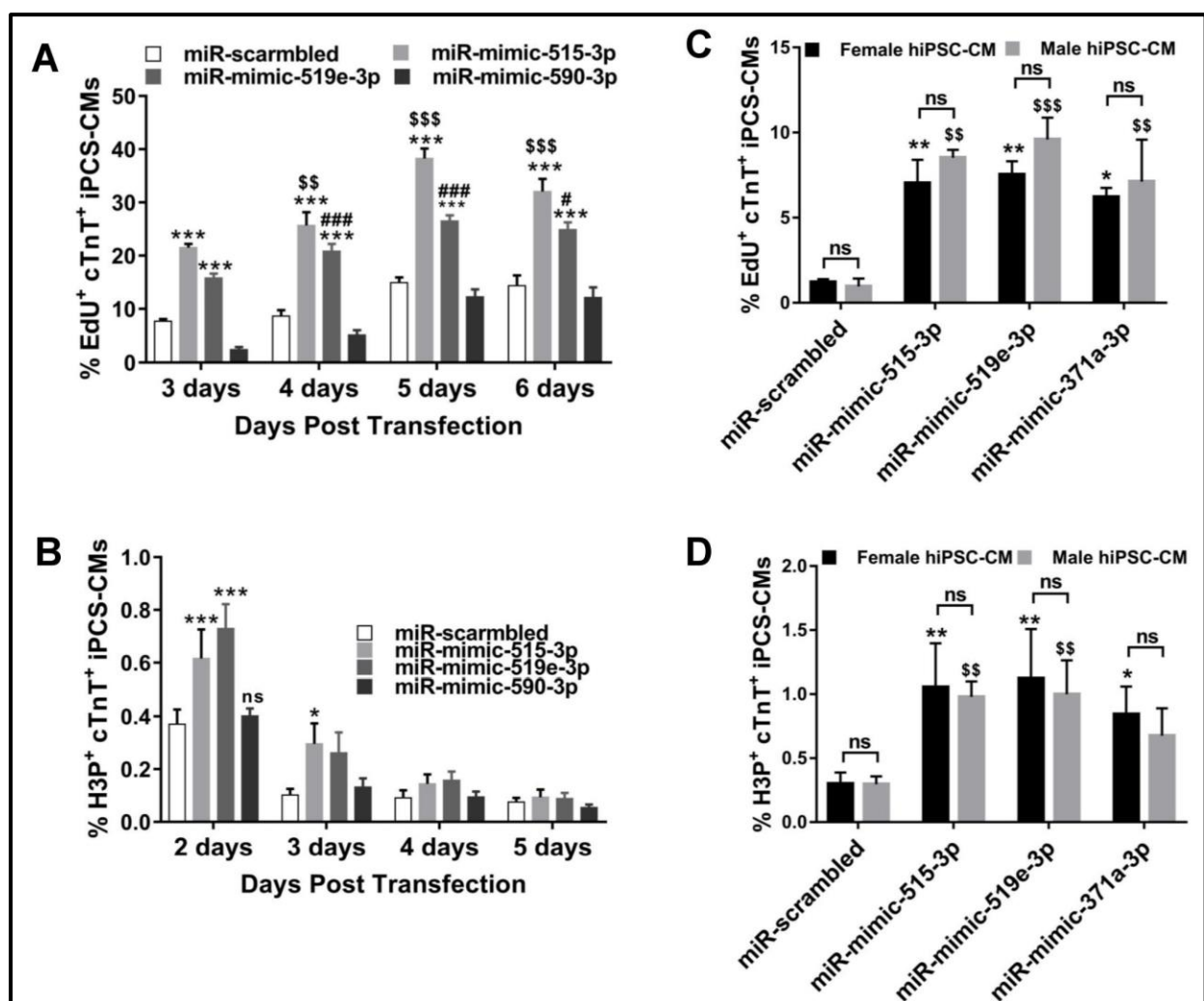


Figure 14: Prolonged effects of EdU Incorporation, and late G2 mitosis assessment after miRNA-transfection

Figure 14A: EdU-uptake, as assessed at day 3 to day 6-post transfection, in hiPSC-CMs treated with miR-scrambled, miR-mimic-515-3p, miR-mimic-519e-3p and miR-mimic-590 (n=3). *, vs. miR-

RESULTS

scrambled; \$, miR-515 from day 3 to 6; #, miR-519 from day 3 to 6. *, \$, #, P < 0.05, **, \$\$, ##, P < 0.01; ***, \$\$\$, ###, P < 0.001. **Figure 14B:** H3P-positive hiPSC-CMs, assessed at day 2 to day 5-post transfection, after treatment with miR-mimic-515-3p, miR-mimic-519e-3p and miR-mimic-590. (n=3). *, vs. miR- scrambled; *, P < 0.05, ***, P < 0.001. **Figure 14C:** Incorporation of EdU does not significantly differ in miRNA-mimic-transfected hiPSC-CMs from female as compared to male donors. (n=3). *, vs. miR-scrambled (female hiPSC-CMs). *, P < 0.05, **, P < 0.01. \$, vs. miR-scrambled (male hiPSC-CMs). \$\$, P < 0.01; \$\$\$, P < 0.001. **Figure 14D:** H3P-positive hiPSC-CMs transfected with miR-mimics in female as compared to male donors. (n=3). *, vs. miR-scrambled (female hiPSC-CMs). *, P < 0.05, **, P < 0.01. \$, vs miR-scrambled (male hiPSC-CMs). \$\$, P < 0.01.

Statistical Analysis 14:

Bars represent average of three biological experiments; data analysis conducted using Graph pad 7 software. Two-way ANOVA with Tukey multiple comparisons test was used for the analysis. Values are presented as mean \pm s.e.m. *P < 0.05, **P < 0.01, ***P < 0.001 relative to Control. A value of P \leq 0.05 was considered as statistically significant.

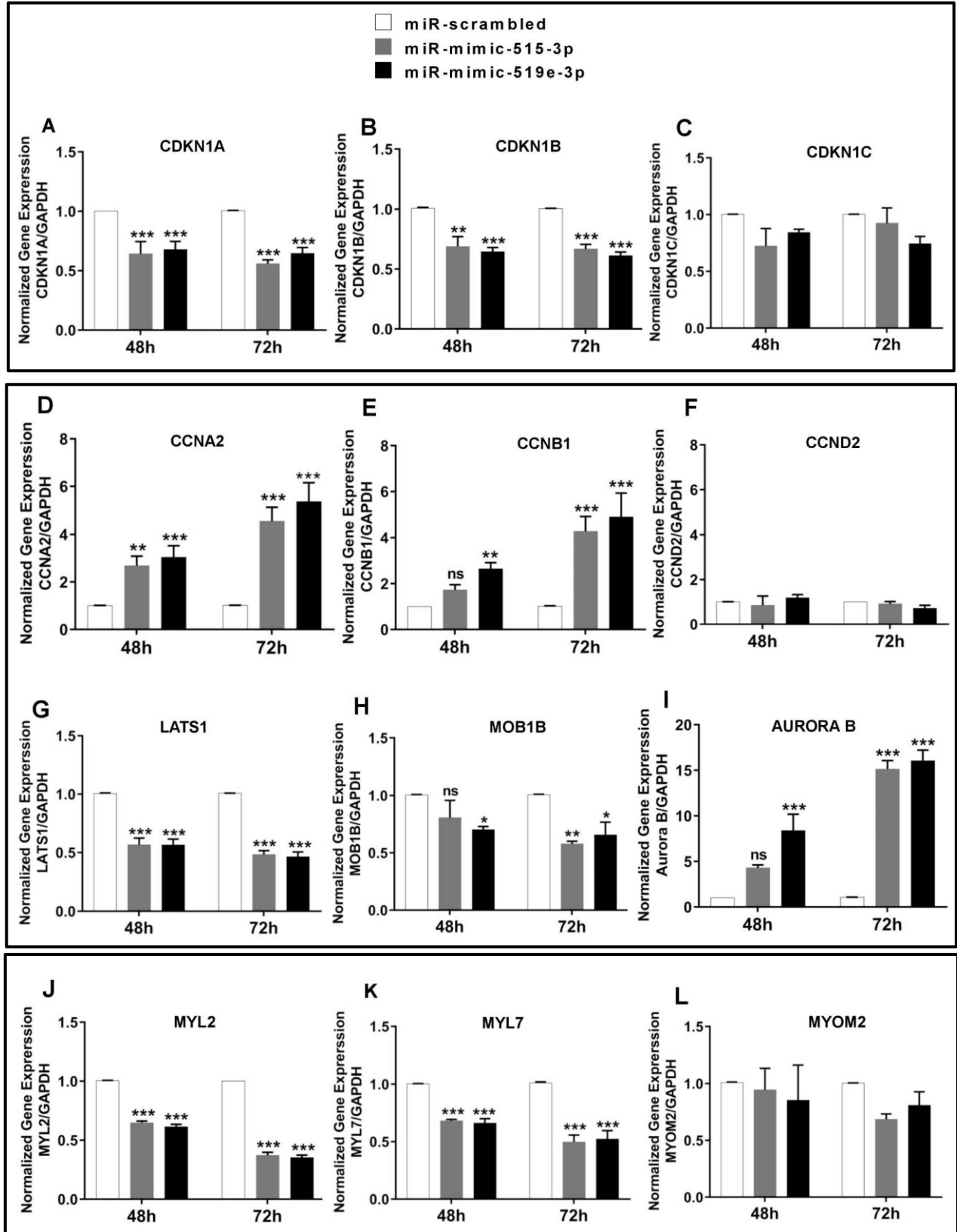
8.9 MiR-515-3p and miR-519e-3p markedly alter expression of genes involved in proliferation, dedifferentiation and hypertrophy

Cardiomyocyte proliferation is dependent on activation and repression of genes involved in cell-cycle reentry. Therefore, we assessed positive and negative cell cycle regulators using qPCR after transfection of hiPSC-CM with miR-515-3p and miR-519e-3p (**Figure. 15A-O**). RNA was isolated 48 and 72 hours after transfection for reverse transcription and qPCR for genes related to cell-cycle inhibition (*CDKN1A*, *CDKN1B*, and *CDKN1C*) (**Figure. 15A-C**) and cell-cycle activation (*CCNA2*, *CCNB1*, and *CCND2*) (**Figure. 15D-F**). Moreover, Hippo pathway activators (*LATS1* and *MOB1B*, **Figure. 15G-H**), cytokinesis marker (Aurora B, **Figure. 15I**), sarcomeric genes involved in maturation/differentiation (*MYL2*, *MYL7*, *MYOM2*, and *MYOM3*, **Figure. 15J-M**) and genes involved in cardiomyocyte hypertrophy (*NPPA*, *NPPB*, **Figure. 15N, O**) were also assessed.

As show in the **Figure. 15**, cell cycle inhibitors, hippo pathway activators, cardiac maturation markers and hypertrophy markers are down regulated, were as genes involving the cell cycle activation are upregulated, upon treatment with miR-515 and miR-

RESULTS

519e. This suggests that microRNA-515 and microRNA-519e play an important role genes involved in cardiomyocyte cell cycle activity.



RESULTS

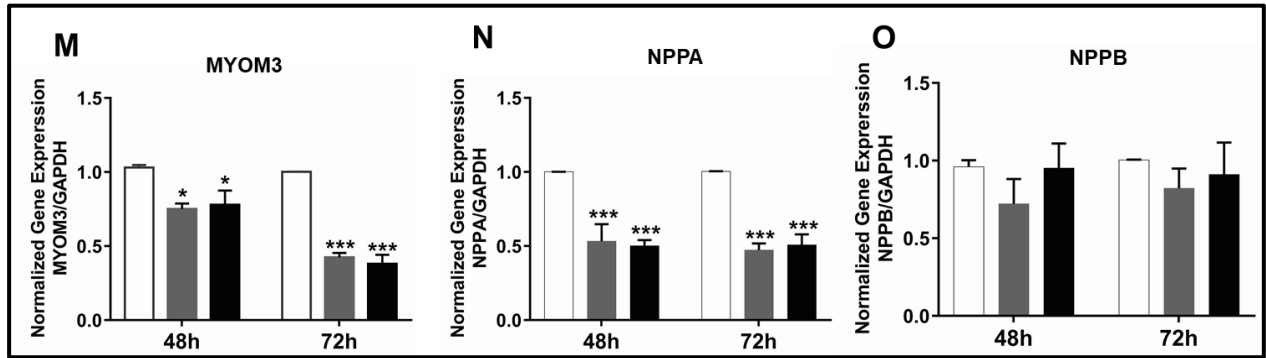


Figure 15: Overexpression of hsa-miR-515-3p and hsa-miR-519e-3p modulates genes involved in cardiomyocyte proliferation, hypertrophy and dedifferentiation

Figures 15A-C: Quantitative real-time PCR (qPCR) of cell-cycle inhibitors (CDKN1A, CDKN1B, and CDKN1C) in hiPSC-CMs after transfection with miR-scrambled, miR-mimic-515-3p or miR-mimic-519e-3p. (n=4-5). *, vs. miR-scrambled. ***, P < 0.001. **Figures 15D-F:** Quantitative real-time PCR (qPCR) of cell-cycle activators (CCNA2, CCNB1, and CCND2) in hiPSC-CMs after transfection with miR-scrambled, miR-mimic-515-3p or miR-mimic-519e-3p. (n=4-5). *, vs. miR-scrambled. **, P < 0.01; ***, P < 0.001. **Figures 15G-H:** Quantitative real-time PCR (qPCR) of Hippo pathway activators (LATS1 and MOB1B) in hiPSC-CMs after transfection with miR-scrambled, miR-mimic-515-3p or miR-mimic-519e-3p. (n=4-5). *, vs. miR-scrambled. *, P < 0.05, **, P < 0.01; ***, P < 0.001. **Figure 15I:** Quantitative real-time PCR (qPCR) of cytokinesis marker Aurora B in hiPSC-CMs after transfection with miR-scrambled, miR-mimic-515-3p or miR-mimic-519e-3p. *, vs. miR-scrambled. (n=4-5). **, P < 0.01; ***, P < 0.001. **Figures 15J-M:** Quantitative real-time PCR (qPCR) of sarcomeric genes involved in maturation/differentiation (MYL2, MYL7, MYOM2, and MYOM3) in hiPSC-CMs after transfection with miR-scrambled, miR-mimic-515-3p or miR-mimic-519e-3p. (n=4-5). *, vs. miR-scrambled. *, P < 0.05, ***, P < 0.001. **Figures 15N-O:** Quantitative real-time PCR (qPCR) of genes involved in cardiomyocyte hypertrophy in hiPSC-CMs after transfection with miR-scrambled, miR-mimic-515-3p or miR-mimic-519e-3p. (n=4-5). *, vs. miR-scrambled. ***, P < 0.001.

Statistical Analysis for Figure 15:

Bars represent average of four to five biological experiments; data analysis conducted using Graph pad 7 software. Two-way ANOVA with Tukey multiple comparisons test was used for the analysis. Values are presented as mean \pm s.e.m. *P < 0.05, **P < 0.01, ***P < 0.001 relative to Control. A value of P \leq 0.05 was considered as statistically significant.

RESULTS

8.10 Hsa-miR-515-3p, hsa-miR-519e-3p and hsa-miR-371a-3p regulate cell-cycle genes on protein level

To further corroborate the actions of miRNA mediated effects on translation and expression of proteins, we validated our results by Western blots (**Figure. 16**). After transfection of miR-515-3p, miR-519e-3p-mimics in hiPSC-CMs, a marked downregulation of cell cycle inhibitor *p21/CDKN1A* (**Figure. 16A-B**) and upregulation of cell cycle activator Cyclin A2/ *CCNA2* (**Figure. 16A-C**) and *AIM 1/ Aurora B* (*AURKB*), (**Figure. 16A-D**) at protein level was confirmed. This suggests that microRNA-515 and microRNA-519 modulate genes involved in cardiomyocyte proliferation.

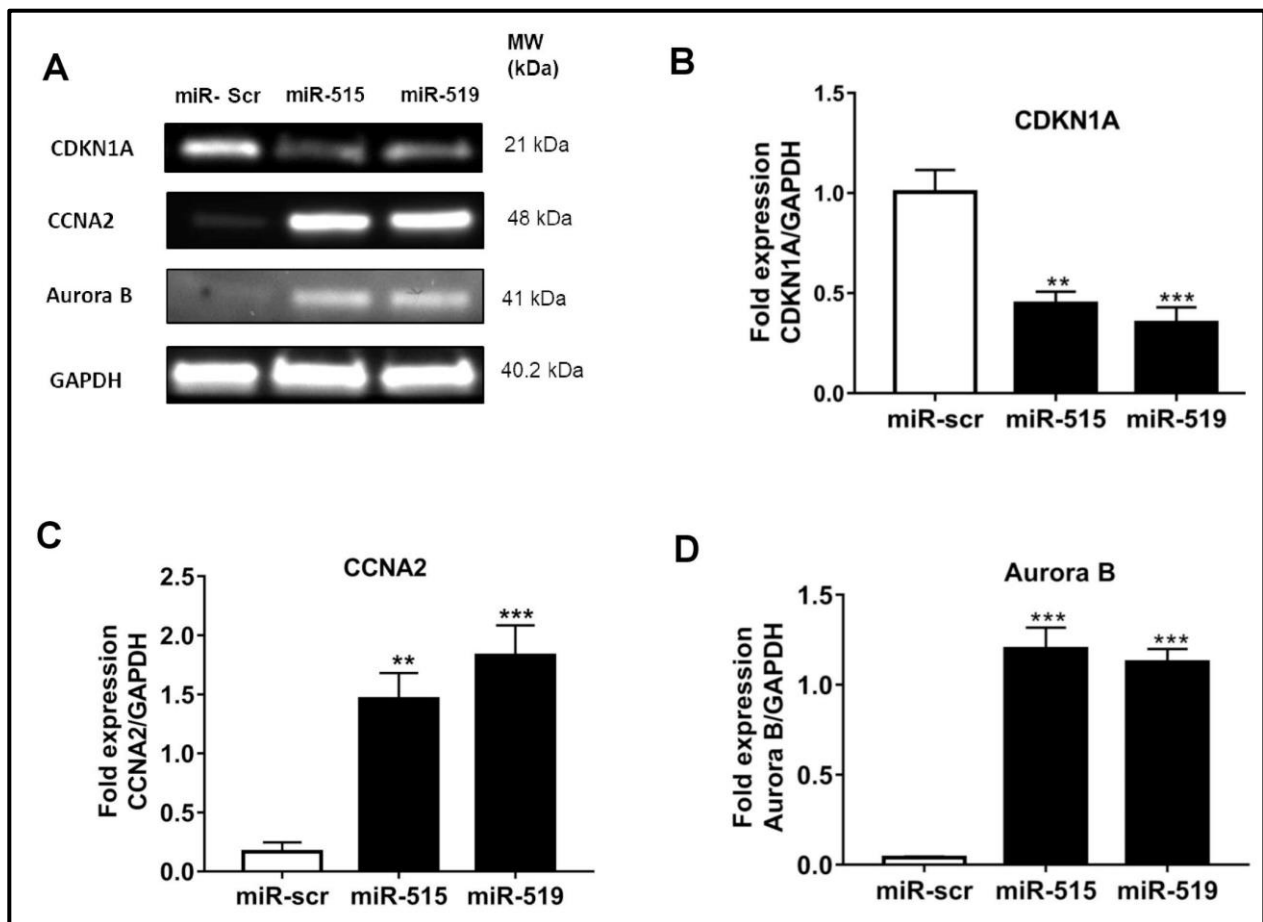


Figure 16: Overexpression of hsa-miR-515-3p and hsa-miR-519e-3p regulate cell-cycle genes on protein level

Figure 16A: Western blot analysis from hiPSC-CMs after transfection with miR-scr, miR-mimic-515-3p or miR-mimic-519e-3p using indicated antibodies. **Figure 16B:** Cell-cycle inhibitor CDKN1A (*p21*) is significantly reduced after miR-mimic 515-3p or miR-mimic-519e-3p treatment. (n=3-4). *, vs. miR-scr. **, P < 0.01; ***, P < 0.001. **Figure 16C:** Cell-cycle activator CCNA2 is substantially increased after miR-mimic-515-3p or miR-mimic-519e-3p treatment. (n=3-4). *, vs. miR-scr. **, P < 0.01; ***, P < 0.001.

RESULTS

P < 0.01; ***, P < 0.001. **Figure 16D:** Cytokinesis marker Aurora B show a substantially increased expression after miR-mimic-515-3p or miR-mimic-519e-3p treatment. (n=3-4). *, vs. miR-scrambled. ***, P < 0.001.

Statistical Analysis for Figure 16:

Bars represent average of three to four biological experiments; data analysis conducted using Graph pad 7 software. Ordinary One-way ANOVA with Sidak multiple comparisons test was used for the analysis. Values are presented as mean \pm s.e.m. *P < 0.05, **P < 0.01, ***P < 0.001 relative to Control. A value of P \leq 0.05 was considered as statistically significant.

8.11 The primate specific miRNAs - miR-515-3p and miR-519e-3p are effective in mouse cardiomyocytes

Notably, the investigated miRNAs - miR-515-3p and miR-519e-3p – are primate-specific and therefore not expressed in rodents. With regard to a potential pre-clinical model in vivo, we tested hsa-miR-515-3p and hsa-miR-519e-3p in mouse cardiomyocytes. Cardiomyocytes were isolated from mice at day three after birth (P3). In line with our findings in human iPSC-CM, transfection of P3 mouse cardiomyocytes with miR-515-3p and miR-519e-3p-mimics markedly enhanced incorporation of EdU (**Figure. 17A-B**) and H3P, a mitosis marker of late G2 phase (**Figure. 17C-D**). Immunocytochemistry was performed for the representative immunofluorescence images showing the increase in EdU positive (**Figure. 17B**) and H3P positive (**Figure. 17D**) hiPSC-CMs after transfection with miR-scrambled, miR-mimic-515-3p, miR-mimic-519e-3p. Together, these data indicate that human miR-515-3p and miR-519e-3p substantially enhance cardiomyocyte proliferation that is not restricted to primates.

RESULTS

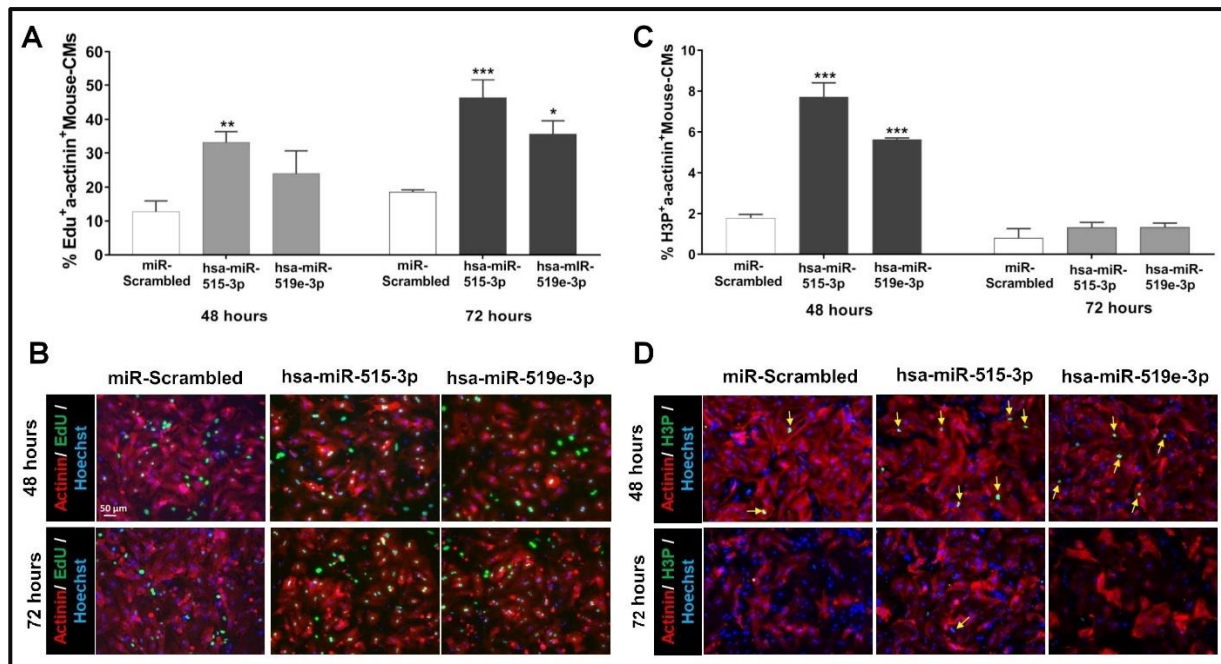


Figure 17: Hsa-miR-515-3p and hsa-miR-519e-3p induce proliferation in mouse cardiomyocytes

Figure 17A: Incorporation of EdU in mouse cardiomyocytes after transfection with hsa-miR-mimic-515-3p and hsa-miR-mimic-519e-3p. (n=3). *, vs. miR- scrambled. *, P < 0.05, **, P < 0.01; ***, P < 0.001.

Figure 17B: Representative immunofluorescence images of mouse cardiomyocytes showing Hoechst (blue; nuclei), Sarcomeric-Alpha Actinin (red) and EdU (green). **Scale bar: 50 μm.**

Figure 17C: H3P-positive cells in mouse cardiomyocytes after transfection with hsa-miR-mimic-515-3p and hsa-miR-mimic-519e-3p, *, vs. miR-scrambled. **Figure 17D:** Representative immunofluorescence images of mouse cardiomyocytes showing Hoechst (blue; nuclei), Sarcomeric-Alpha Actinin (red) and H3P (green).

Yellow arrows point to cardiomyocytes positive for H3P. **Scale bar: 50 μm.**

Statistical Analysis for Figure 17:

Bars represent average of three biological experiments; data analysis conducted using Graph pad 7 software. Two-way ANOVA with Tukey multiple comparisons test was used for the analysis. Values are presented as mean ± s.e.m. *P < 0.05, **P < 0.01, ***P < 0.001 relative to Control. A value of P ≤ 0.05 was considered as statistically significant.

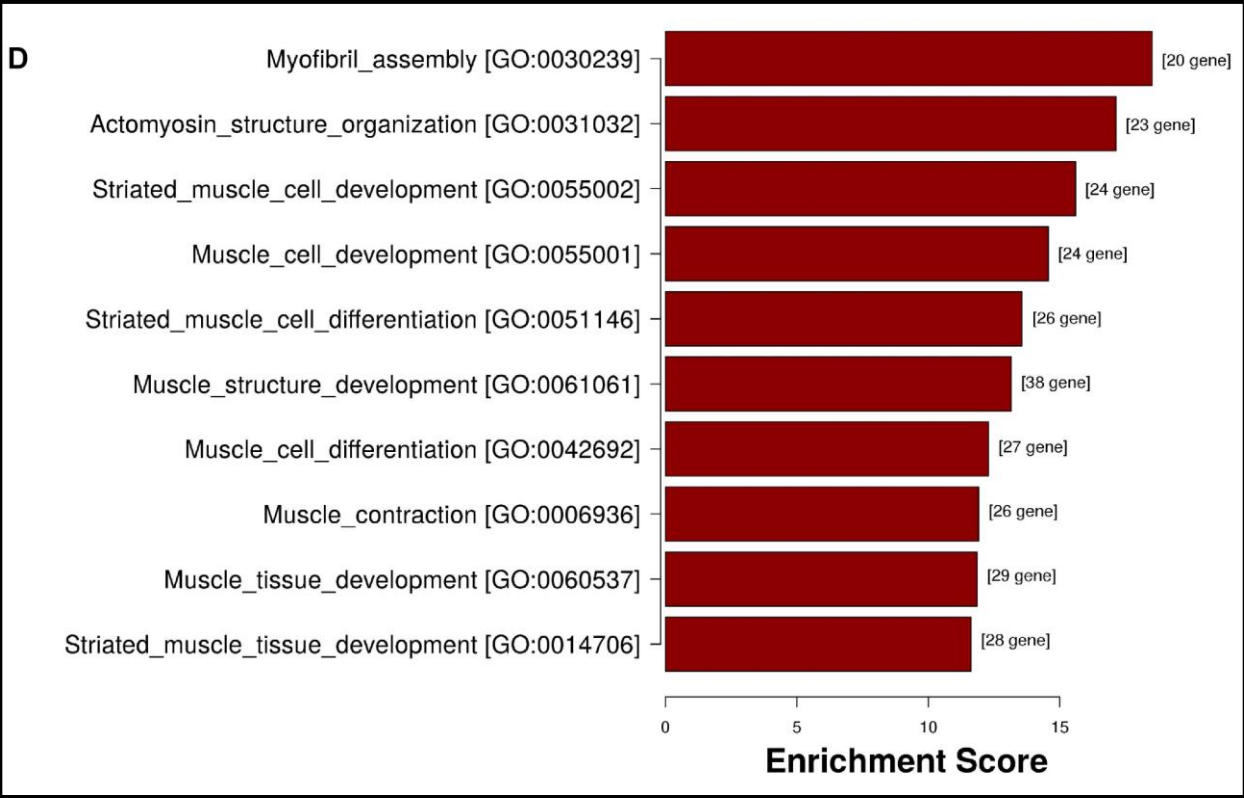
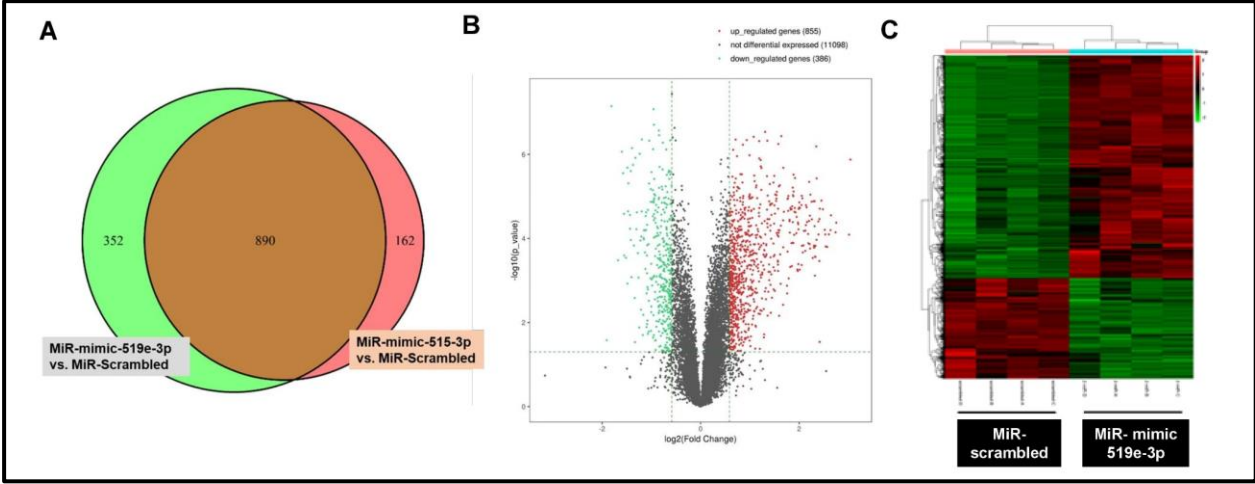
8.12 Transcriptome analysis after overexpression of miR-515-3p and miR-519e-3p in human iPSC-CMs reveals substantial changes on structural organization and proliferation pathways

To further understand pathways involved in the observed regenerative potential, we performed RNA-Sequencing (RNA-Seq) after overexpression of miR-515-3p and miR-519e-3p in hiPSC-CM (**Figure. 18**).

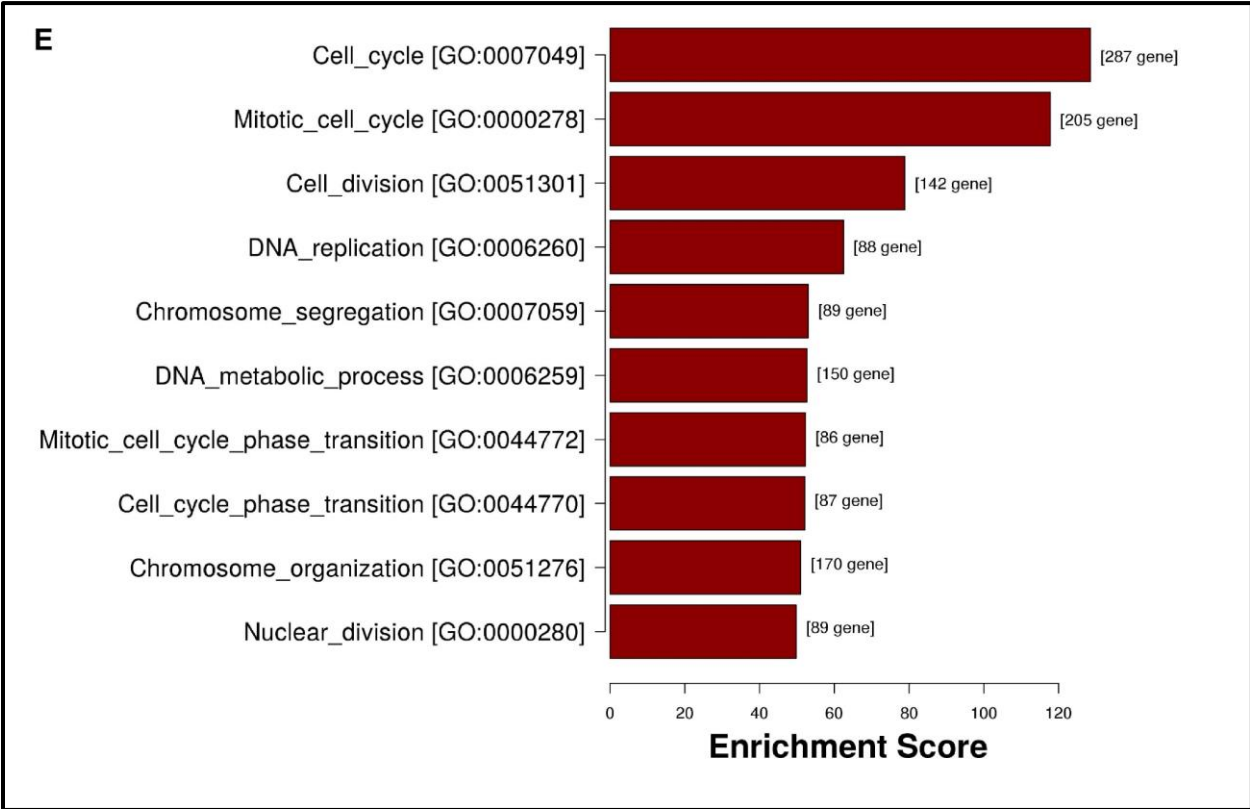
RESULTS

As expected, regulated genes after miR-515-3p and miR-519-3p transfection show an extensive overlap, with 890-shared genes (**Figure. 18A**). Volcano plot of differentially expressed genes after transfection with miR-519e-3p as compared to miR-scrambled transfected hiPSC-CMs (**Figure. 18B**). Heat map, arranged by hierarchical clustering, of differentially expressed genes (miR-519e-3p (right rows) vs. miR-scrambled (left rows)) (**Figure. 18C**). We used gene ontology (GO) enrichment analysis to investigate whether specific GO terms are associated with differentially expressed genes after miR-519-3p mimic treatment (**Figure. 18D-G**). Downregulated gene pathways are strongly involved in sarcomeric organization signalling (**Figure. 18D-F**). In contrary, upregulated enriched gene pathways comprise processes involved in cell-cycle regulation, specifically mitosis, cell division, nuclear division, DNA replication and chromosome assembly (**Figure. 18 E-G**). As expected, cell cycle genes such as cyclins (*CCNB1*, *CCNB2*, *CCNA2*), Klf family members (*KIF4a*, *KIF20A*, *KIFC1*, *KIF2C*, *KIF11*) and cytokinesis genes such as Aurora (*AURKA*, *AURKB*) and *NUSAP1* belong to the most significantly upregulated genes derived from the RNA-Seq. These findings indicate that miR-515 of miR-519e-3p strongly induce signalling pathways involved in cardiomyocyte proliferation.

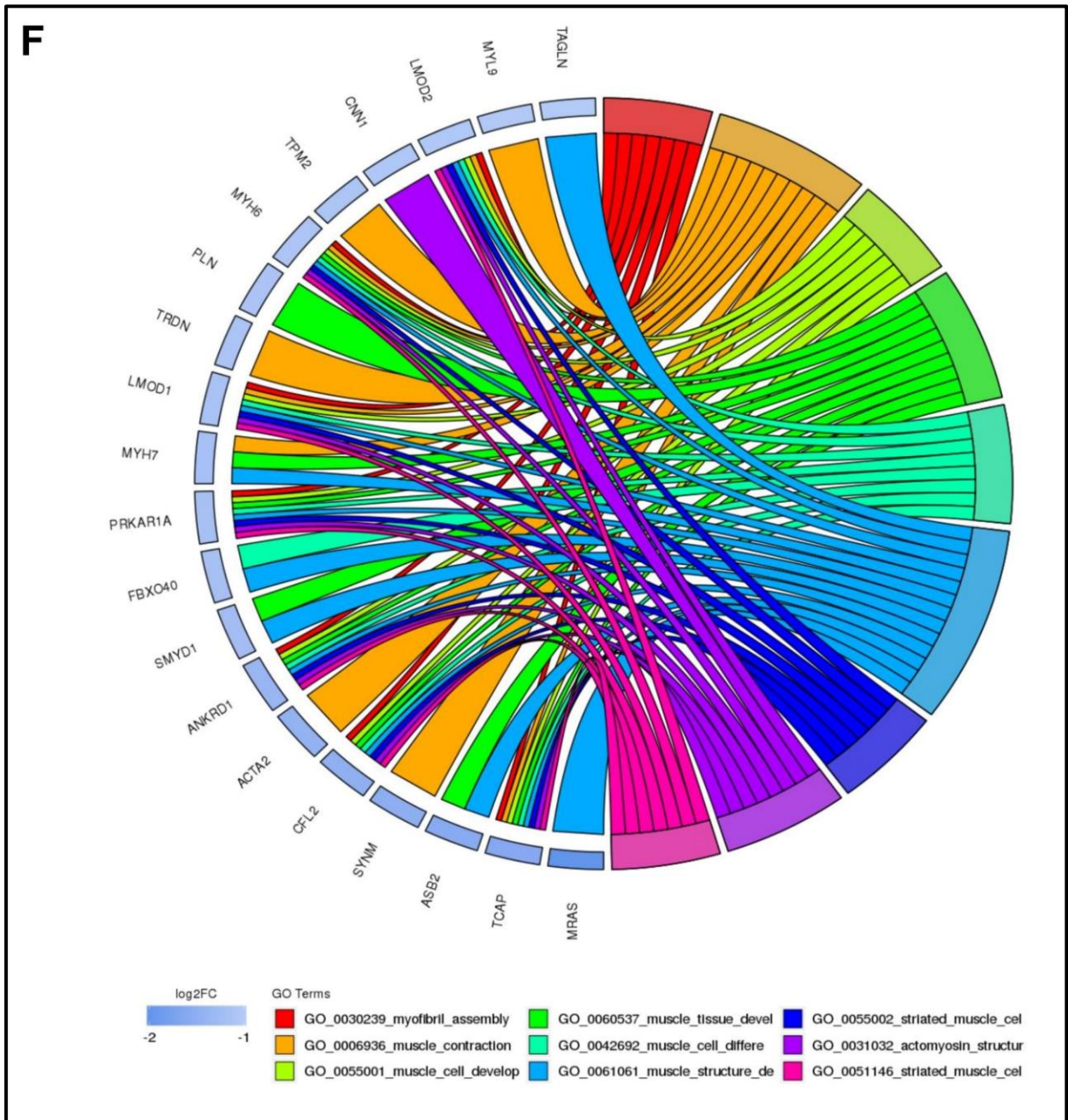
RESULTS



RESULTS



RESULTS



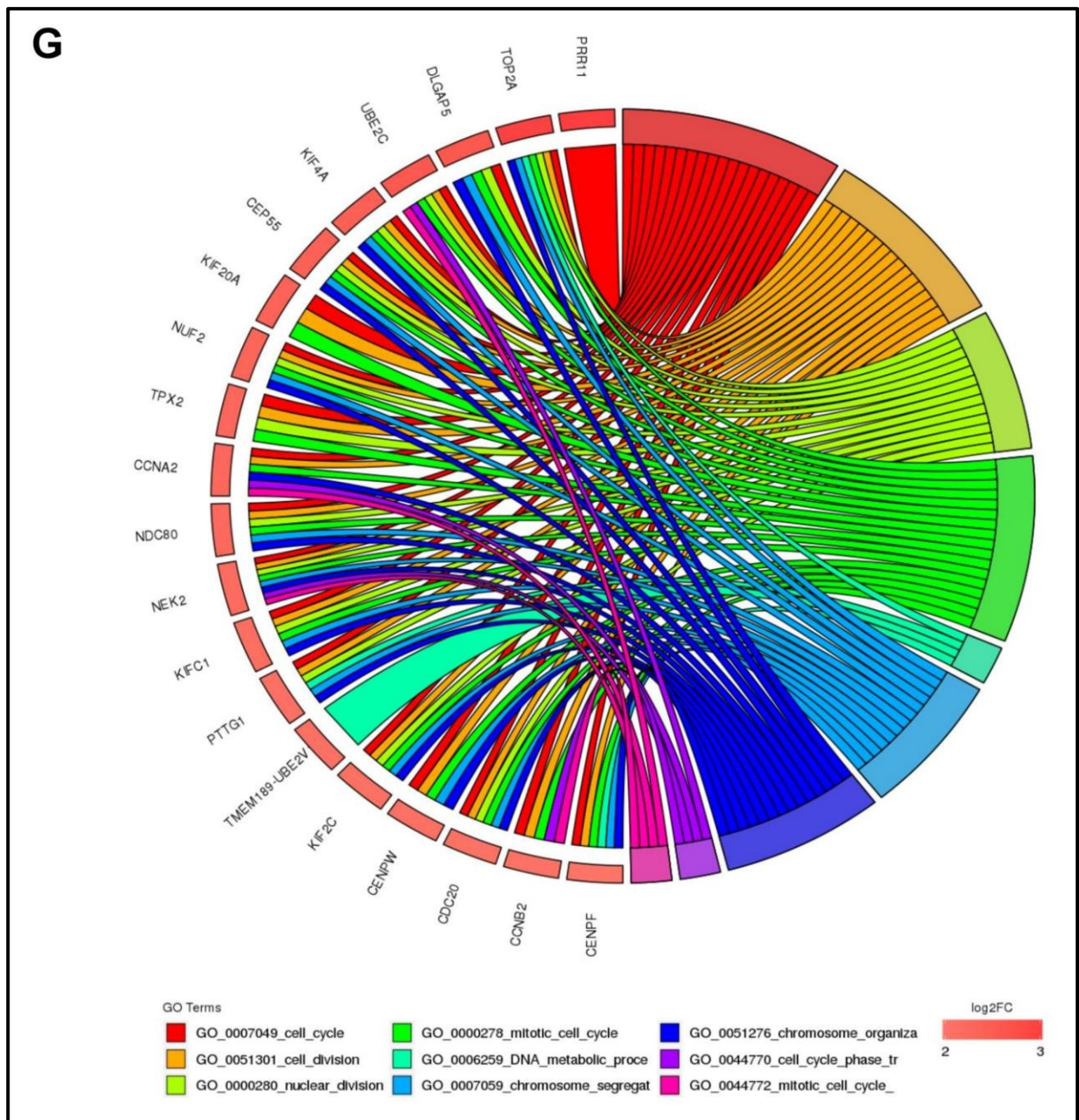


Figure 18: RNA-Seq reveals a strong regulation of hsa-miR-519e-3p for biological processes involved in cardiac muscle regeneration

Figure 18A: The Venn diagram shows overlapping and differentially expressed genes in hiPSC-CM after miR-mimic-519e-3p and miR-mimic-515-3p treatment as compared to miR-scrambled transfected hiPSC-CMs. **Figure 18B:** Volcano plot of differentially expressed genes after transfection with miR-519e-3p as compared to miR-scrambled transfected hiPSC-CMs. Green and red circles indicate statistically significant differentially expressed genes with fold change > 1.5 and p-value 0.05. Abscissa: Fold-change; vertical coordinates: p-value (n=4 per group). **Figure 18C:** Heat map, arranged by hierarchical clustering, of differentially expressed genes (miR-519e-3p (right rows) vs. miR-scrambled (left rows)). The color represents the relative expression level (log2 scaled FPKM). Red, increased

RESULTS

expression; green: reduced expression **Figure 18D:** Top ten enriched gene ontology (GO) terms of downregulated genes, ordered from top to bottom by p-value. **Figure 18E:** Top ten enriched gene ontology (GO) terms of upregulated genes, ordered from top to bottom by p-value. **Figure 18F:** Cord plots showing top nine GO biological process terms that are related to the top 20 significantly differentially downregulated genes. **Figure 18G:** Cord plots showing top nine GO biological process terms that are related to the top 20 significant differentially upregulated genes.

9. DISCUSSION

Ischemic heart disease (IHD) remains the leading cause of death in the world. In 2015, 110 million cases are estimated to suffer from IHD, with approximately 9 million deaths due to IHD¹³³ In addition, about 38 million patients suffer from heart failure that is associated with a high mortality.^{134, 135} Interventional and drug-based therapies may prevent the heart from extensive necrosis and remodelling, but do not address the underlying problem, cardiomyocyte loss. Cardiomyocyte proliferation is a key step in heart regeneration. In humans, cardiomyocyte withdrawal from the cell cycle is observed early after birth. Though it has been shown that in adolescence, a negligible count of cardiomyocytes within the human heart undergoes cell cycle re-entry.⁹ However, the low number of cardiomyocytes that re-enter cell cycle is insufficient to restore the non-contractile scar after myocardial infarction. In the last several years, many approaches targeted cardiac regeneration, through exosomes,^{136, 137} growth factors,^{138, 139} small molecules,^{64, 140} and recently with microRNAs. Of note, a recent publication of Giacca's research group has shown enhanced proliferation of cardiomyocytes and improved heart function in a large animal model¹¹⁶ after treatment with miRNA-mimics. As miRNAs have been shown to crucially regulate proliferative capacity in mammals,^{65, 66, 108, 112, 116, 125, 126} a high-throughput approach using a miRNA-library may identify miRNAs with the potential to rescue cardiomyocyte loss after myocardial infarction. To our best knowledge, our study for the first time describes a functional high-throughput screening in human iPSC-derived cardiomyocytes (hiPSC-CMs) to assess the proliferative capacity after hypoxia/reoxygenation using a human miRNA library consisting > 2000 microRNAs. 2019 miR-mimics and anti-miRs were used for individual overexpression and downregulation of endogenous miRNAs in human iPSC-CMs.

As a model system, to identify microRNAs in cardiomyocyte proliferation, human hiPSC-CMs were used. In 2007 Takahashi *et.al.*, for the first time generated human induced pluripotent stem cells from human dermal fibroblasts by transient overexpression of Yamanaka's factors (*OCT4*, *SOX2*, *KLF4* and *C-MYC*) and these human iPSCs can be utilized to differentiate into three embryonic germ layers (mesoderm, ectoderm, and endoderm).⁵¹ The mesodermal germ layer differentiations are used either by embryoid bodies (EBs) method or by monolayer cultures of cells to differentiate into cardiac lineages that include cardiomyocytes (hiPSC-CMs).^{53, 54}

DISCUSSION

hiPSC-CMs were used in the investigation of disease mechanisms especially in cardiovascular diseases (CVDs). As an example, to detect a disease-specific phenotype, hiPSC-CMs may be generated from patients suffering from hypertrophic cardiomyopathy (HCM) and compared to iPSC-CM from healthy subjects. The patient cells displayed specific altered properties, which are similar in HCM patients, such as cellular hypertrophy, abnormalities in sarcomere organization and altered calcium handling. These properties were not observed in the hiPSC-CMs derived from healthy subjects.¹⁴¹ In another study, healthy hiPSC-CMs were compared to the hiPSC-CMs obtained from patients with arrhythmogenic cardiomyopathy (ACM), which allowed in detecting plakophilin-2 (PKP2) gene mutations, by studying cell structure and morphology in hiPSC-CMs derived from patients, and these cells, showed the properties of altered Z-bands, larger cardiomyocytes, which are some of the typical ACM features.¹⁴² These cells can be used for high throughput screening approaches, by generating large-scale hiPSC cardiomyocytes,¹⁴³ that would be cost effective compared to the animal disease models used.¹⁴⁴

Several studies have utilized hiPSC-CMs to understand basic and translational aspects in cardiovascular regenerative medicine (*in-vitro* and *in-vivo*). In a study, hiPSC-CMs were transplanted into a mouse heart after myocardial infarction (MI). Transplantation of these cells improved left ventricular function and attenuated cardiac remodelling process, in mice. However, due to limited engraftment of cells, myocardial regeneration was not observed in mice, but rather stimulation of anti-apoptotic and pro-angiogenic effects.¹⁴⁵ Similarly in another study, left ventricular ejection fraction was improved and cardio protective effects were observed through paracrine factors in the damaged tissue after transplanting hiPSC-CMs in the mice post- myocardial infarction.¹⁴⁶ Large animal models were also tested using hiPSC; in a recent study, hiPSC-CMs sheets were transplanted following MI in a porcine heart, which underwent ischemia reperfusion injury. The CM sheets improved cardiac function and remodelling of the left ventricle. However, in a long-term trial, very few iPSC-CMs survived.¹⁴⁷ In a very recent study, iPSC-CMs injected in a cynomolgus monkey survived for a period of twelve weeks, without any immune rejections, and the function of cardiac contractility improved in between four and twelve weeks, but non-fatal-ventricular tachycardia, was observed resulting in arrhythmias.⁵⁸ These studies suggest that iPSC-CMs may be used as a regenerative cell-based therapy but also over major hurdles that have to be considered and improved. These include

DISCUSSION

homing and long-term survival in host tissue and maturation of hiPSC-CMs to efficiently integrate into the host myocardium. Therefore, further studies of hiPSC-CMs focussing on safety and feasibility are required to utilize these cells for treatment of cardiovascular diseases.^{63, 148, 149}

For our study, we used hiPSC-CMs to identify the role of microRNAs in cardiomyocyte proliferation. In order for the cells to have a more mature phenotype, we cultured hiPSC-CM for 40 days post differentiation (Figure. **8**). To verify miRNA-abundances after transfection, we performed qRT-PCR of miRNAs after microRNA-1825 overexpression (Figure. **9A**) and miR-195 downregulation (Figure. **9B**) using miR-mimics and anti-miRs, respectively. MiR-1825¹⁵⁰ and miR-195¹¹⁰ have been shown as positive and negative modulators of cardiomyocyte proliferation.^{110, 150} However overexpression of microRNA-1825 showed only modest effects in our hiPSC-CMs compared to the control groups (Figure. **9C,D,F**), which shows that proliferation of cardiomyocytes can be different in between species (i.e. murine cardiomyocytes vs human cardiomyocytes). We used transient hypoxia to mimic hypoxia reoxygenation such as present in patient with MI and as previous studies have shown that systemic gradual hypoxemia in 3-month-old adult mice reactivated the regenerative properties of the adult mammalian heart. In this experimental study, a group of mice were subjected to hypoxic conditions with and without myocardial infarction (MI) and another to normoxic conditions. Mice were exposed to systemic severe hypoxaemia (7% O₂) for a period of four weeks. During the initial two weeks, to avoid a rapid drop in oxygen pressure, the fraction of inspired oxygen (FiO₂) was dropped gradually by 1% per day, from ambient oxygen levels in the room 20.9% - to 7 % O₂. Once the oxygen levels reached 7%, the experimental approach was carried out for next two weeks. Similarly, another group of mice were subjected to MI. One week post-MI, these mice were exposed to hypoxic conditions as mentioned above. Histology assessment and cardiomyocytes isolated from the hearts after four weeks with and without MI showed a significant increase in the cell proliferation markers, such as DNA synthesis, G2/Mitosis and cytokinesis in hypoxic hearts compared to normoxia. However, exposure to 7% oxygen for 3 weeks increased the mortality rate in sham and MI-operated mice, demonstrating that mice do not tolerate prolonged severe exposure to hypoxia.^{25, 39} Similarly, in another recent study hiPSC-CMs were exposed to different levels of oxygen (5 %, 10 %, 15 %, and 20 %) for 7 days. Oxygen levels were dropped from 20 % to 5 %, in which moderate levels of hypoxia (15% and 10%) increased

DISCUSSION

cardiomyocyte proliferation.^{43 44} Altogether, these studies suggest that hypoxia can be used to induce cardiomyocyte proliferation as a new therapeutic approach. However, transcription factors and signalling pathways involved have to be studied to understand mechanisms involved in hypoxia-driven cardiac regeneration.²⁵

The screening method used in this study can also be widely applied to neonatal cardiomyocytes. Primarily, to screen large libraries, a pure culture of cardiomyocytes is a prerequisite, therefore in each experiment, we used a cardiomyocyte specific marker, human-cardiac Troponin T for human iPSC-CMs and sarcomeric-alpha Actinin for mouse CMs to distinguish positive cells. Due to a large number of microRNAs in the library, there might be some limitations with false positive or false negative readouts. To avoid this, we first performed the main screening with the human microRNA library (Figure. **10C, D, F, G**). Thereafter, hit candidates derived from the main screen were re-tested two times in a secondary screen (Figure. **10E, H**). Top candidates derived from the hit-picking screen were further validated for their proliferative capacity using markers for late mitosis and cytokinesis.

Importantly, overexpression of 28 miRNAs (miR-mimics) induced cell-cycle reentry in human iPSC-CMs. Of note, overexpression of miR-199b-5p, induced, the highest proliferative activity (Figure. **10G, H**). However, miR-199b reported to mitigate pathological remodelling and fibrosis and miR-199b expression is also increased in human and mouse heart in heart failure^{101, 151} and therefore was not considered for further investigation. Conversely, none of the anti-miRNAs, previously known to induce cardiomyocyte proliferation in mammals, such as anti-miR-99-5p,¹⁵² anti-miR-100-5p,¹⁵² anti-miR-195-5p,¹¹¹ and anti-miR-128¹⁵³ did yield a proliferative response in human iPSC-CMs. miR-195, a member of the miR-15-family, is highly up-regulated in mouse hearts between day 1 and 10 after birth. Delivery of artificial anti-miRs targeting miR-15-family members in neonatal mice increased cardiomyocyte proliferation by de-inhibiting cell cycle genes.^{110, 111} Of note, some of the miRNAs that were reported to induce cell-cycle in murine cardiomyocyte were confirmed in our screening, such as miR-1825 and miR-33b,⁶⁵ others did not show a significant proliferative effect in human iPSC-CMs after transient miRNA-overexpression, such as miR-590, miR-199a, the miR-302/367 cluster and the miR-17-92 family.^{65, 108, 109, 112} These findings suggest that cardiomyocyte proliferation is differentially regulated in human iPSC-CMs.

DISCUSSION

Interestingly, several pro-proliferating miRNAs identified in the high-throughput screening are members of miRNA-families, such as miR-148a-3p/miR-148b-3p (miRNA-148 family), miR-212-3p/miR-132-3p (miRNA 212 family) and miRNA-371a-3p/miR-371b (miR-371 family). Of note, five out of 28 miRNA-candidates derived from the screen belong to the imprinted chromosome 19 miR-cluster (C19MC, hsa-miR-515-3p, hsa-miR-519e-3p, and hsa-miR-517c-3p) and adjacent miR-371-3 cluster (hsa-miR-371a-3p, hsa-miR-371b-3p), located on chromosome 19q13.41^{154, 155} and they are expressed predominantly in placental tissue^{156, 157}. This primate-specific cluster represents one of the largest gene clusters of human miRNAs. Members of the C19MC are expressed in the placenta and undifferentiated cells.¹⁵⁴ In human embryonic stem cells (hESCs), this cluster is markedly upregulated compared to non-hESCs,¹⁵⁸ indicating an important role for dedifferentiation. Moreover, Wu et al.¹⁵⁹ has shown that several miRNAs of C19MC directly target cyclin-dependent kinase inhibitor 1A (*CDKN1A*) at its 3'-untranslated region in HEK 293 cells. *CDKN1A* is an important cell cyclin-dependent kinase (CDK)-inhibitor that regulates cell proliferation and G1/S transition. In addition, several experimental studies have investigated this family in the context of trophoblast differentiation, invasion and proliferation.^{160, 161} Of note, members of the C19MC are also involved in extracellular matrix composition¹⁶² that is known to impact on regenerative capacity of the heart¹⁶³ and antiviral immunity.^{164, 165} In placental-derived cells, miRNAs that belong to the C19MC cluster regulate proliferation, immunomodulation and extracellular matrix composition, biological features that are also highly relevant for cardiac regeneration. Therefore, we reasoned that these miRNAs are important for cardiomyocyte proliferation due to their involvement in biological processes that are key factors for cardiac regeneration.¹⁶⁶ Therefore, the three miRNAs with the highest proliferative activity in this group, namely hsa-miR-515-3p, hsa-miR-519e-3p and hsa-miR-371a-3p, were further investigated for the induction of human cardiomyocyte proliferation (Figure. 11 and Figure. 12).

In a recent study, overexpression of miR-199a or miR-590 using an Adeno-associated vector (AAV) was established in a pig model,¹¹⁶ which resulted in functional recovery post injury and increased cardiomyocyte proliferation. However, uncontrolled overexpression of miR-199a in pigs also caused ventricular arrhythmias resulting in sudden cardiac death. These results suggest that microRNAs can improve cardiac function post infarction in a large animal model. Notably, delivery method, dosage and

DISCUSSION

timeframe of overexpression of miRNAs seem to be critical steps in order to achieve translational aspects of microRNAs in human trials.^{116, 117} However, a therapeutic strategy using miRNAs to enhance cardiac regeneration in patients with MI or ICM may be feasible in the future. Most promising would be a miRNA-targeted therapy to direct human adult cardiomyocytes to re-enter the cell cycle and enhance proliferation, thereby compensating for the loss of myocardium after myocardial infarction. In our study, we used several concentrations of microRNAs to study the effects of toxicity (Figure. 13) and effects over several days after microRNA overexpression in hiPSC-CMs (Figure. 14).

As already reported in a study investigating the role of miRNAs in cyclin-dependent kinase inhibitor 1A (CDKN1A) suppression in HEK 293 cells,¹⁵⁹ that also represents an important negative regulator of cardiomyocyte cycling,¹⁶⁷ we could confirm a marked decrease in expression of this cyclin-dependent inhibitor after miR-515-3p and miR-519e-3p-mimic transfection. Similarly, downregulation of CDKN1B was observed. Importantly, miR-515-3p and miR-519e-3p-transfected hiPSC-CMs showed a substantial increase in cyclin A2 (CCNA2) expression. It has been reported that cyclin A2 is a key regulator of the cell cycle through G1-S and G2-M phase.^{168, 169} In addition, the cell-cycle activator cyclin B1 (CCNB1)^{19, 170} was markedly upregulated. Moreover, genes that are involved in the Hippo-signalling pathway, such as LATS1 and MOB1B¹¹² were significantly downregulated after miR-515-3p and miR-519e-3p-mimic transfection. Importantly Aurora B kinase¹⁷¹, an important regulator of cytokinesis was upregulated in qRT-PCR and at protein level after treatment with miR-515-3p and miR-519e-3p. In line, sarcomeric genes that are involved in structural maturation, such as Myosin light chain-2 (MYL-2), Myosin light chain-7 (MYL-7) and Myomesin 3 (MYOM-3)^{172, 173} were markedly downregulated. As upregulation of cycling markers and downregulation of dedifferentiation markers may be associated with a hypertrophic response and adult cardiomyocyte remodelling,^{33, 174} we assessed Natriuretic Peptide A (NPPA) and Natriuretic Peptide B (NPPB). Importantly, NPPA was significantly downregulated after miR-515-3p and miR-519e-3p-mimics transfection and NPPB did not show altered expression, indicating miRNA-dependent cell-cycle reentry in the absence of hypertrophic growth (Figure. 15 and Figure. 16).

Indeed, we confirmed that miR-515-3p and miR-519e-3p substantially enhance expression of cell-cycling markers in human iPSC-CM. Importantly, transient hypoxia further increased incorporation and labeling of early and late mitosis markers. As

DISCUSSION

experimental studies suggest that a distinct population of adult cardiomyocytes maintain their proliferative capacity in a hypoxic environment^{39, 175} and activation of cell-cycle in cardiomyocytes is more prominent at the border zone of the infarcted myocardium, miR-515-3p and miR-519e-3p may enhance cardiogenesis in patients with myocardial infarction and heart failure. As these are primate specific microRNAs, we tested their effect in 3 days old mice cardiomyocytes and treatment with human hsa-miR-mimic-515 and has-miR-mimic-519 enhanced proliferation of neonatal mouse cardiomyocytes, which gives us a hope to study these microRNAs in small animal models (Figure. **17**). Later using an RNA-Seq approach, we further observed that genes involved in sarcomeric organization pathways are strongly downregulated, most probably reflecting sarcomeric disassembly required for cell division. Importantly, besides an upregulation of cyclins and genes involved in the Hippo pathway, we also observed a strong upregulation of genes involved in cytokinesis, cell abscission and cell division (Figure. **18**). This compelling evidence suggests that miR-515-3p and miR-519-3p can force human cardiomyocytes to divide and therefore be used as a potential therapy for cardiac regeneration.

10. CONCLUSION

Cardiovascular diseases remain a significant health burden and a leading cause of deaths across the world. Induction of cardiomyocyte proliferation, as observed in newborn mice, and adult zebrafish, significantly contribute to cardiac regeneration after myocardial injury. This response is mostly absent in human adults, and therefore, the development of novel therapies to improve the cardiac repair mechanisms through cardiomyocyte cell-cycle reentry is urgently needed.

In this project, we established a microRNA based high-throughput screening approach to identify potential inducers of human cardiomyocyte proliferation. We established an efficient lipid-based transfection method for transient overexpression and downregulation of miRNAs in hiPSC-CMs.

Later we screened a human microRNA library consisting of more than two thousand microRNA-mimics and anti-miRNAs. Hit-miRNAs derived from the main high-throughput screening were further validated in a secondary screening. In this project, the screening revealed two primate specific microRNA-mimics - miR-515 and miR-519e – that significantly increased proliferation in human cardiomyocytes as assessed by markers of DNA synthesis and G2/Mitosis without inducing toxic effects, which was assessed by LDH assay.

Interestingly both miRNAs are equally effective in inducing proliferation in female and male human iPSC-derived cardiomyocytes. We also found that overexpression of these two microRNAs substantially increased expression of cell cycle activators and downregulate cell cycle inhibitors at both RNA and protein level in human iPSC-CMs. To further gain mechanistic insights into relevant pathways modulated by these miRNAs, RNA-Sequencing of human iPSC-CMs after overexpression with miR-515-3p and miR-519e-3p was performed.

Furthermore, we found that overexpression of these two microRNA-mimics induced proliferation in 3-day-old neonatal mice cardiomyocytes indicating that these miRNAs are also effective in non-primate species.

Taken together our data suggests that the identified miRNAs from the functional high-throughput screening may represent potential novel therapeutic options for treatment of

CONCLUSION

patients with myocardial infarction and ischemic cardiomyopathy that are associated with loss of cardiomyocytes.

11. FUTURE PERSPECTIVES

Potentially, these miRNAs may have the therapeutic potential for cardiac repair in patients with myocardial infarction and reversal of heart failure progression.

Direct gene targets of the microRNAs will be identified through computational analysis with the data derived from the RNA-Seq. Target Validation of the identified genes and signalling pathways regulated by these miRNAs will provide an in-depth view in mechanisms that induce cycling of human cardiomyocytes. Validation will be performed, using dual luciferase assays after transfection of the miRNAs and a construct harbouring the 3' UTR Sequence.

In the future, we will explore miR-515 and miR-519 as therapeutics for functional recovery through cardiomyocytes proliferation using *in vivo* myocardial infarction models. Mice will undergo ligation of the left anterior descending artery (LAD) to induce myocardial infarction. Human hsa-miR-515-3p and has-miR-519e-3p will be injected in the infarct border zone to induce cardiomyocyte proliferation. Mice will be followed-up for 4 weeks using transthoracic echocardiography to assess left ventricular ejection fraction (LVEF). In addition, immunofluorescence staining of histological sections after 3 days and 14 days to identify enhanced expression of cycling genes after miRNA-treatment will be performed. The *in vivo* studies will reveal the potential of these miRNA to induce cardiac regeneration in the injured heart and pave the way for clinical translation.

12. REFERENCES

1. Mendis S, Puska P and Norrving B. Global atlas on cardiovascular disease prevention and control. WHO. *World Heart Federation and World Stroke Organization*. 2011.
2. Medicine Io. *Cardiovascular Disability: Updating the Social Security Listings*. Washington, DC: The National Academies Press; 2010.
3. Cahill TJ and Kharbanda RK. Heart failure after myocardial infarction in the era of primary percutaneous coronary intervention: Mechanisms, incidence and identification of patients at risk. *World J Cardiol*. 2017;9:407-415.
4. Mozaffarian D, Benjamin EJ, Go AS, Arnett DK, Blaha MJ, Cushman M, Das SR, de Ferranti S, Despres JP, Fullerton HJ, Howard VJ, Huffman MD, Isasi CR, Jimenez MC, Judd SE, Kissela BM, Lichtman JH, Lisabeth LD, Liu S, Mackey RH, Magid DJ, McGuire DK, Mohler ER, 3rd, Moy CS, Muntner P, Mussolino ME, Nasir K, Neumar RW, Nichol G, Palaniappan L, Pandey DK, Reeves MJ, Rodriguez CJ, Rosamond W, Sorlie PD, Stein J, Towfighi A, Turan TN, Virani SS, Woo D, Yeh RW and Turner MB. Heart Disease and Stroke Statistics-2016 Update: A Report From the American Heart Association. *Circulation*. 2016;133:e38-360.
5. Murry CE, Reinecke H and Pabon LM. Regeneration gaps: observations on stem cells and cardiac repair. *Journal of the American College of Cardiology*. 2006;47:1777-85.
6. Kajstura J, Leri A, Finato N, Di Loreto C, Beltrami CA and Anversa P. Myocyte proliferation in end-stage cardiac failure in humans. *Proceedings of the National Academy of Sciences of the United States of America*. 1998;95:8801-5.
7. Romyantsev PP. Interrelations of the proliferation and differentiation processes during cardiac myogenesis and regeneration. *Int Rev Cytol*. 1977;51:186-273.
8. Beltrami AP, Urbanek K, Kajstura J, Yan SM, Finato N, Bussani R, Nadal-Ginard B, Silvestri F, Leri A, Beltrami CA and Anversa P. Evidence that human cardiac myocytes divide after myocardial infarction. *The New England journal of medicine*. 2001;344:1750-7.
9. Bergmann O, Bhardwaj RD, Bernard S, Zdunek S, Barnabe-Heider F, Walsh S, Zupicich J, Alkass K, Buchholz BA, Druid H, Jovinge S and Frisen J. Evidence for cardiomyocyte renewal in humans. *Science (New York, NY)*. 2009;324:98-102.
10. Tane S, Ikenishi A, Okayama H, Iwamoto N, Nakayama KI and Takeuchi T. CDK inhibitors, p21(Cip1) and p27(Kip1), participate in cell cycle exit of mammalian cardiomyocytes. *Biochem Biophys Res Commun*. 2014;443:1105-9.
11. Glotzer M. The molecular requirements for cytokinesis. *Science (New York, NY)*. 2005;307:1735-9.
12. Bicknell KA and Brooks G. Reprogramming the cell cycle machinery to treat cardiovascular disease. *Curr Opin Pharmacol*. 2008;8:193-201.
13. Locatelli P, Gimenez CS, Vega MU, Crottogini A and Belaich MN. Targeting the Cardiomyocyte Cell Cycle for Heart Regeneration. *Curr Drug Targets*. 2019;20:241-254.
14. Brodsky V, Sarkisov DS, Arefyeva AM, Panova NW and Gvasava IG. Polyploidy in cardiac myocytes of normal and hypertrophic human hearts; range of values. *Virchows Arch*. 1994;424:429-35.
15. Soonpaa MH, Kim KK, Pajak L, Franklin M and Field LJ. Cardiomyocyte DNA synthesis and binucleation during murine development. *Am J Physiol*. 1996;271:H2183-9.

REFERENCES

16. Yoshizumi M, Lee WS, Hsieh CM, Tsai JC, Li J, Perrella MA, Patterson C, Endege WO, Schlegel R and Lee ME. Disappearance of cyclin A correlates with permanent withdrawal of cardiomyocytes from the cell cycle in human and rat hearts. *The Journal of clinical investigation*. 1995;95:2275-80.
17. Kang MJ and Koh GY. Differential and dramatic changes of cyclin-dependent kinase activities in cardiomyocytes during the neonatal period. *Journal of molecular and cellular cardiology*. 1997;29:1767-77.
18. Ponnusamy M, Li PF and Wang K. Understanding cardiomyocyte proliferation: an insight into cell cycle activity. *Cellular and molecular life sciences : CMLS*. 2017;74:1019-1034.
19. Mohamed TMA, Ang YS, Radzinsky E, Zhou P, Huang Y, Elfenbein A, Foley A, Magnitsky S and Srivastava D. Regulation of Cell Cycle to Stimulate Adult Cardiomyocyte Proliferation and Cardiac Regeneration. *Cell*. 2018;173:104-116.e12.
20. Pasumarthi KB, Nakajima H, Nakajima HO, Soonpaa MH and Field LJ. Targeted expression of cyclin D2 results in cardiomyocyte DNA synthesis and infarct regression in transgenic mice. *Circulation research*. 2005;96:110-8.
21. Campa VM, Gutierrez-Lanza R, Cerignoli F, Diaz-Trelles R, Nelson B, Tsuji T, Barcova M, Jiang W and Mercola M. Notch activates cell cycle reentry and progression in quiescent cardiomyocytes. *J Cell Biol*. 2008;183:129-41.
22. Mahmoud AI, Kocabas F, Muralidhar SA, Kimura W, Koura AS, Thet S, Porrello ER and Sadek HA. Meis1 regulates postnatal cardiomyocyte cell cycle arrest. *Nature*. 2013;497:249-253.
23. Nguyen NUN, Canseco DC, Xiao F, Nakada Y, Li S, Lam NT, Muralidhar SA, Savla JJ, Hill JA, Le V, Zidan KA, El-Feky HW, Wang Z, Ahmed MS, Hubbi ME, Menendez-Montes I, Moon J, Ali SR, Le V, Villalobos E, Mohamed MS, Elhelaly WM, Thet S, Anene-Nzulu CG, Tan WLW, Foo RS, Meng X, Kanchwala M, Xing C, Roy J, Cyert MS, Rothermel BA and Sadek HA. A calcineurin-Hoxb13 axis regulates growth mode of mammalian cardiomyocytes. *Nature*. 2020;582:271-276.
24. Mohamed TMA, Ang YS, Radzinsky E, Zhou P, Huang Y, Elfenbein A, Foley A, Magnitsky S and Srivastava D. Regulation of Cell Cycle to Stimulate Adult Cardiomyocyte Proliferation and Cardiac Regeneration. *Cell*. 2018;173:104-116 e12.
25. Kimura W, Nakada Y and Sadek HA. Hypoxia-induced myocardial regeneration. *J Appl Physiol (1985)*. 2017;123:1676-1681.
26. Halder G and Johnson RL. Hippo signaling: growth control and beyond. *Development (Cambridge, England)*. 2011;138:9-22.
27. Pocaterra A, Romani P and Dupont S. YAP/TAZ functions and their regulation at a glance. *Journal of cell science*. 2020;133.
28. Heallen T, Zhang M, Wang J, Bonilla-Claudio M, Klysik E, Johnson RL and Martin JF. Hippo pathway inhibits Wnt signaling to restrain cardiomyocyte proliferation and heart size. *Science (New York, NY)*. 2011;332:458-61.
29. Yamamoto S, Yang G, Zablocki D, Liu J, Hong C, Kim SJ, Soler S, Odashima M, Thaisz J, Yehia G, Molina CA, Yatani A, Vatner DE, Vatner SF and Sadoshima J. Activation of Mst1 causes dilated cardiomyopathy by stimulating apoptosis without compensatory ventricular myocyte hypertrophy. *The Journal of clinical investigation*. 2003;111:1463-74.
30. Matsui Y, Nakano N, Shao D, Gao S, Luo W, Hong C, Zhai P, Holle E, Yu X, Yabuta N, Tao W, Wagner T, Nojima H and Sadoshima J. Lats2 is a negative regulator of myocyte size in the heart. *Circulation research*. 2008;103:1309-18.

REFERENCES

31. Heallen T, Morikawa Y, Leach J, Tao G, Willerson JT, Johnson RL and Martin JF. Hippo signaling impedes adult heart regeneration. *Development (Cambridge, England)*. 2013;140:4683-90.
32. von Gise A, Lin Z, Schlegelmilch K, Honor LB, Pan GM, Buck JN, Ma Q, Ishiwata T, Zhou B, Camargo FD and Pu WT. YAP1, the nuclear target of Hippo signaling, stimulates heart growth through cardiomyocyte proliferation but not hypertrophy. *Proceedings of the National Academy of Sciences of the United States of America*. 2012;109:2394-9.
33. Leach JP, Heallen T, Zhang M, Rahmani M, Morikawa Y, Hill MC, Segura A, Willerson JT and Martin JF. Hippo pathway deficiency reverses systolic heart failure after infarction. *Nature*. 2017;550:260-264.
34. Giordano FJ. Oxygen, oxidative stress, hypoxia, and heart failure. *The Journal of clinical investigation*. 2005;115:500-8.
35. Puente BN, Kimura W, Muralidhar SA, Moon J, Amatruda JF, Phelps KL, Grinsfelder D, Rothermel BA, Chen R, Garcia JA, Santos CX, Thet S, Mori E, Kinter MT, Rindler PM, Zacchigna S, Mukherjee S, Chen DJ, Mahmoud AI, Giacca M, Rabinovitch PS, Aroumougame A, Shah AM, Szweda LI and Sadek HA. The oxygen-rich postnatal environment induces cardiomyocyte cell-cycle arrest through DNA damage response. *Cell*. 2014;157:565-79.
36. Dunwoodie SL. The role of hypoxia in development of the Mammalian embryo. *Developmental cell*. 2009;17:755-73.
37. Ng KM, Lee YK, Chan YC, Lai WH, Fung ML, Li RA, Siu CW and Tse HF. Exogenous expression of HIF-1 alpha promotes cardiac differentiation of embryonic stem cells. *Journal of molecular and cellular cardiology*. 2010;48:1129-37.
38. Guimaraes-Camboa N, Stowe J, Aneas I, Sakabe N, Cattaneo P, Henderson L, Kilberg MS, Johnson RS, Chen J, McCulloch AD, Nobrega MA, Evans SM and Zambon AC. HIF1alpha Represses Cell Stress Pathways to Allow Proliferation of Hypoxic Fetal Cardiomyocytes. *Developmental cell*. 2015;33:507-21.
39. Nakada Y, Canseco DC, Thet S, Abdisalaam S, Asaithamby A, Santos CX, Shah AM, Zhang H, Faber JE, Kinter MT, Szweda LI, Xing C, Hu Z, Deberardinis RJ, Schiattarella G, Hill JA, Oz O, Lu Z, Zhang CC, Kimura W and Sadek HA. Hypoxia induces heart regeneration in adult mice. *Nature*. 2017;541:222-227.
40. Poss KD, Wilson LG and Keating MT. Heart regeneration in zebrafish. *Science (New York, NY)*. 2002;298:2188-90.
41. Nikinmaa M. Oxygen-dependent cellular functions--why fishes and their aquatic environment are a prime choice of study. *Comp Biochem Physiol A Mol Integr Physiol*. 2002;133:1-16.
42. Savla JJ, Levine BD and Sadek HA. The Effect of Hypoxia on Cardiovascular Disease: Friend or Foe? *High Alt Med Biol*. 2018;19:124-130.
43. Ye L, Qiu L, Feng B, Jiang C, Huang Y, Zhang H, Zhang H, Hong H and Liu J. Role of Blood Oxygen Saturation During Post-Natal Human Cardiomyocyte Cell Cycle Activities. *JACC Basic Transl Sci*. 2020;5:447-460.
44. Ahmed MS and Sadek HA. Hypoxia Induces Cardiomyocyte Proliferation in Humans. *JACC Basic Transl Sci*. 2020;5:461-462.
45. Nasser BA, Ebell W, Dandel M, Kukucka M, Gebker R, Doltra A, Knosalla C, Choi YH, Hetzer R and Stamm C. Autologous CD133+ bone marrow cells and bypass grafting for regeneration of ischaemic myocardium: the Cardio133 trial. *European heart journal*. 2014;35:1263-74.

REFERENCES

46. Tongers J, Losordo DW and Landmesser U. Stem and progenitor cell-based therapy in ischaemic heart disease: promise, uncertainties, and challenges. *European heart journal*. 2011;32:1197-206.
47. Jakob P and Landmesser U. Current status of cell-based therapy for heart failure. *Curr Heart Fail Rep*. 2013;10:165-76.
48. Takahashi K and Yamanaka S. Induction of pluripotent stem cells from mouse embryonic and adult fibroblast cultures by defined factors. *Cell*. 2006;126:663-76.
49. Evans MJ and Kaufman MH. Establishment in culture of pluripotential cells from mouse embryos. *Nature*. 1981;292:154-156.
50. Yoshida Y and Yamanaka S. Induced Pluripotent Stem Cells 10 Years Later: For Cardiac Applications. *Circulation research*. 2017;120:1958-1968.
51. Takahashi K, Tanabe K, Ohnuki M, Narita M, Ichisaka T, Tomoda K and Yamanaka S. Induction of pluripotent stem cells from adult human fibroblasts by defined factors. *Cell*. 2007;131:861-72.
52. Thomson JA, Itskovitz-Eldor J, Shapiro SS, Waknitz MA, Swiergiel JJ, Marshall VS and Jones JM. Embryonic stem cell lines derived from human blastocysts. *Science (New York, NY)*. 1998;282:1145-7.
53. Ieda M, Fu JD, Delgado-Olguin P, Vedantham V, Hayashi Y, Bruneau BG and Srivastava D. Direct reprogramming of fibroblasts into functional cardiomyocytes by defined factors. *Cell*. 2010;142:375-86.
54. Burridge PW, Keller G, Gold JD and Wu JC. Production of de novo cardiomyocytes: human pluripotent stem cell differentiation and direct reprogramming. *Cell stem cell*. 2012;10:16-28.
55. Burridge PW, Matsa E, Shukla P, Lin ZC, Churko JM, Ebert AD, Lan F, Diecke S, Huber B, Mordwinkin NM, Plews JR, Abilez OJ, Cui B, Gold JD and Wu JC. Chemically defined generation of human cardiomyocytes. *Nat Methods*. 2014;11:855-60.
56. Tohyama S and Fukuda K. Future Treatment of Heart Failure Using Human iPSC-Derived Cardiomyocytes. In: T. Nakanishi, R. R. Markwald, H. S. Baldwin, B. B. Keller, D. Srivastava and H. Yamagishi, eds. *Etiology and Morphogenesis of Congenital Heart Disease: From Gene Function and Cellular Interaction to Morphology* Tokyo; 2016: 25-31.
57. Chong JJ, Yang X, Don CW, Minami E, Liu YW, Weyers JJ, Mahoney WM, Van Biber B, Cook SM, Palpant NJ, Gantz JA, Fugate JA, Muskheli V, Gough GM, Vogel KW, Astley CA, Hotchkiss CE, Baldessari A, Pabon L, Reinecke H, Gill EA, Nelson V, Kiem HP, Laflamme MA and Murry CE. Human embryonic-stem-cell-derived cardiomyocytes regenerate non-human primate hearts. *Nature*. 2014;510:273-7.
58. Shiba Y, Gomibuchi T, Seto T, Wada Y, Ichimura H, Tanaka Y, Ogasawara T, Okada K, Shiba N, Sakamoto K, Ido D, Shiina T, Ohkura M, Nakai J, Uno N, Kazuki Y, Oshimura M, Minami I and Ikeda U. Allogeneic transplantation of iPSC cell-derived cardiomyocytes regenerates primate hearts. *Nature*. 2016;538:388-391.
59. Vreeker A, van Stuijvenberg L, Hund TJ, Mohler PJ, Nikkels PG and van Veen TA. Assembly of the cardiac intercalated disk during pre- and postnatal development of the human heart. *PLoS one*. 2014;9:e94722.
60. Kamakura T, Makiyama T, Sasaki K, Yoshida Y, Wuriyanghai Y, Chen J, Hattori T, Ohno S, Kita T, Horie M, Yamanaka S and Kimura T. Ultrastructural maturation of human-induced pluripotent stem cell-derived cardiomyocytes in a long-term culture. *Circ J*. 2013;77:1307-14.
61. Lundy SD, Zhu WZ, Regnier M and Laflamme MA. Structural and functional maturation of cardiomyocytes derived from human pluripotent stem cells. *Stem Cells Dev*. 2013;22:1991-2002.

REFERENCES

62. Lewandowski J, Rozwadowska N, Kolanowski TJ, Malcher A, Zimna A, Rugowska A, Fiedorowicz K, Labeledz W, Kubaszewski L, Chojnacka K, Bednarek-Rajewska K, Majewski P and Kurpisz M. The impact of in vitro cell culture duration on the maturation of human cardiomyocytes derived from induced pluripotent stem cells of myogenic origin. *Cell Transplant*. 2018;27:1047-1067.
63. Ahmed RE, Anzai T, Chanthra N and Uosaki H. A Brief Review of Current Maturation Methods for Human Induced Pluripotent Stem Cells-Derived Cardiomyocytes. *Frontiers in cell and developmental biology*. 2020;8:178.
64. Magadum A, Ding Y, He L, Kim T, Vasudevarao MD, Long Q, Yang K, Wickramasinghe N, Renikunta HV, Dubois N, Weidinger G, Yang Q and Engel FB. Live cell screening platform identifies PPARdelta as a regulator of cardiomyocyte proliferation and cardiac repair. *Cell Res*. 2017;27:1002-1019.
65. Eulalio A, Mano M, Dal Ferro M, Zentilin L, Sinagra G, Zacchigna S and Giacca M. Functional screening identifies miRNAs inducing cardiac regeneration. *Nature*. 2012;492:376-81.
66. Diez-Cunado M, Wei K, Bushway PJ, Maurya MR, Perera R, Subramaniam S, Ruiz-Lozano P and Mercola M. miRNAs that Induce Human Cardiomyocyte Proliferation Converge on the Hippo Pathway. *Cell reports*. 2018;23:2168-2174.
67. Del Alamo JC, Lemons D, Serrano R, Savchenko A, Cerignoli F, Bodmer R and Mercola M. High throughput physiological screening of iPSC-derived cardiomyocytes for drug development. *Biochimica et biophysica acta*. 2016;1863:1717-27.
68. Kussauer S, David R and Lemcke H. hiPSCs Derived Cardiac Cells for Drug and Toxicity Screening and Disease Modeling: What Micro- Electrode-Array Analyses Can Tell Us. *Cells*. 2019;8.
69. McKeithan WL, Feyen DAM, Bruyneel AAN, Okolotowicz KJ, Ryan DA, Sampson KJ, Potet F, Savchenko A, Gomez-Galeno J, Vu M, Serrano R, George AL, Jr., Kass RS, Cashman JR and Mercola M. Reengineering an Antiarrhythmic Drug Using Patient hiPSC Cardiomyocytes to Improve Therapeutic Potential and Reduce Toxicity. *Cell stem cell*. 2020;27:813-821 e6.
70. Karakikes I, Ameen M, Termglinchan V and Wu JC. Human induced pluripotent stem cell-derived cardiomyocytes: insights into molecular, cellular, and functional phenotypes. *Circulation research*. 2015;117:80-8.
71. Paik DT, Chandy M and Wu JC. Patient and Disease-Specific Induced Pluripotent Stem Cells for Discovery of Personalized Cardiovascular Drugs and Therapeutics. *Pharmacol Rev*. 2020;72:320-342.
72. Harris K, Aylott M, Cui Y, Louttit JB, McMahon NC and Sridhar A. Comparison of electrophysiological data from human-induced pluripotent stem cell-derived cardiomyocytes to functional preclinical safety assays. *Toxicol Sci*. 2013;134:412-26.
73. Cambria E, Pasqualini FS, Wolint P, Gunter J, Steiger J, Bopp A, Hoerstrup SP and Emmert MY. Translational cardiac stem cell therapy: advancing from first-generation to next-generation cell types. *NPJ Regen Med*. 2017;2:17.
74. Barwari T, Joshi A and Mayr M. MicroRNAs in Cardiovascular Disease. *Journal of the American College of Cardiology*. 2016;68:2577-2584.
75. Poller W, Dimmeler S, Heymans S, Zeller T, Haas J, Karakas M, Leistner DM, Jakob P, Nakagawa S, Blankenberg S, Engelhardt S, Thum T, Weber C, Meder B, Hajjar R and Landmesser U. Non-coding RNAs in cardiovascular diseases: diagnostic and therapeutic perspectives. *European heart journal*. 2018;39:2704-2716.
76. Bartel DP. MicroRNAs: genomics, biogenesis, mechanism, and function. *Cell*. 2004;116:281-97.

REFERENCES

77. Lee RC, Feinbaum RL and Ambros V. The *C. elegans* heterochronic gene *lin-4* encodes small RNAs with antisense complementarity to *lin-14*. *Cell*. 1993;75:843-54.
78. Wightman B, Ha I and Ruvkun G. Posttranscriptional regulation of the heterochronic gene *lin-14* by *lin-4* mediates temporal pattern formation in *C. elegans*. *Cell*. 1993;75:855-62.
79. Horvitz HR and Sulston JE. Isolation and genetic characterization of cell-lineage mutants of the nematode *Caenorhabditis elegans*. *Genetics*. 1980;96:435-54.
80. Lee R, Feinbaum R and Ambros V. A short history of a short RNA. *Cell*. 2004;116:S89-92, 1 p following S96.
81. Ha M and Kim VN. Regulation of microRNA biogenesis. *Nature reviews Molecular cell biology*. 2014;15:509-24.
82. Gebert LFR and MacRae IJ. Regulation of microRNA function in animals. *Nature reviews Molecular cell biology*. 2019;20:21-37.
83. O'Brien J, Hayder H, Zayed Y and Peng C. Overview of MicroRNA Biogenesis, Mechanisms of Actions, and Circulation. *Front Endocrinol (Lausanne)*. 2018;9:402.
84. Chong MM, Zhang G, Cheloufi S, Neubert TA, Hannon GJ and Littman DR. Canonical and alternate functions of the microRNA biogenesis machinery. *Genes & development*. 2010;24:1951-60.
85. Bernstein E, Kim SY, Carmell MA, Murchison EP, Alcorn H, Li MZ, Mills AA, Elledge SJ, Anderson KV and Hannon GJ. Dicer is essential for mouse development. *Nature genetics*. 2003;35:215-7.
86. Burger K and Gullerova M. Swiss army knives: non-canonical functions of nuclear Drosha and Dicer. *Nature reviews Molecular cell biology*. 2015;16:417-30.
87. Lee Y, Ahn C, Han J, Choi H, Kim J, Yim J, Lee J, Provost P, Radmark O, Kim S and Kim VN. The nuclear RNase III Drosha initiates microRNA processing. *Nature*. 2003;425:415-9.
88. Denli AM, Tops BB, Plasterk RH, Ketting RF and Hannon GJ. Processing of primary microRNAs by the Microprocessor complex. *Nature*. 2004;432:231-5.
89. Lund E, Guttinger S, Calado A, Dahlberg JE and Kutay U. Nuclear export of microRNA precursors. *Science (New York, NY)*. 2004;303:95-8.
90. Du T and Zamore PD. microPrimer: the biogenesis and function of microRNA. *Development (Cambridge, England)*. 2005;132:4645-52.
91. Forman JJ, Legesse-Miller A and Collier HA. A search for conserved sequences in coding regions reveals that the *let-7* microRNA targets Dicer within its coding sequence. *Proceedings of the National Academy of Sciences of the United States of America*. 2008;105:14879-84.
92. Lytle JR, Yario TA and Steitz JA. Target mRNAs are repressed as efficiently by microRNA-binding sites in the 5' UTR as in the 3' UTR. *Proceedings of the National Academy of Sciences of the United States of America*. 2007;104:9667-72.
93. Appasani K. MicroRNAs : from basic science to disease biology. 2008.
94. Hata A. Functions of microRNAs in cardiovascular biology and disease. *Annu Rev Physiol*. 2013;75:69-93.
95. Olson EN. MicroRNAs as therapeutic targets and biomarkers of cardiovascular disease. *Science translational medicine*. 2014;6:239ps3.
96. van Rooij E and Kauppinen S. Development of microRNA therapeutics is coming of age. *EMBO molecular medicine*. 2014;6:851-64.
97. Wehbe N, Nasser SA, Pintus G, Badran A, Eid AH and Baydoun E. MicroRNAs in Cardiac Hypertrophy. *Int J Mol Sci*. 2019;20.
98. Chen C, Ponnusamy M, Liu C, Gao J, Wang K and Li P. MicroRNA as a Therapeutic Target in Cardiac Remodeling. *Biomed Res Int*. 2017;2017:1278436.

REFERENCES

99. Yin H, Zhao L, Zhang S, Zhang Y and Lei S. MicroRNA1 suppresses cardiac hypertrophy by targeting nuclear factor of activated T cells cytoplasmic 3. *Molecular medicine reports*. 2015;12:8282-8.
100. Care A, Catalucci D, Felicetti F, Bonci D, Addario A, Gallo P, Bang ML, Segnalini P, Gu Y, Dalton ND, Elia L, Latronico MV, Hoydal M, Autore C, Russo MA, Dorn GW, 2nd, Ellingsen O, Ruiz-Lozano P, Peterson KL, Croce CM, Peschle C and Condorelli G. MicroRNA-133 controls cardiac hypertrophy. *Nat Med*. 2007;13:613-8.
101. da Costa Martins PA, Salic K, Gladka MM, Armand AS, Leptidis S, el Azzouzi H, Hansen A, Coenen-de Roo CJ, Bierhuizen MF, van der Nagel R, van Kuik J, de Weger R, de Bruin A, Condorelli G, Arbones ML, Eschenhagen T and De Windt LJ. MicroRNA-199b targets the nuclear kinase Dyrk1a in an auto-amplification loop promoting calcineurin/NFAT signalling. *Nature cell biology*. 2010;12:1220-7.
102. Rane S, He M, Sayed D, Vashistha H, Malhotra A, Sadoshima J, Vatner DE, Vatner SF and Abdellatif M. Downregulation of miR-199a derepresses hypoxia-inducible factor-1alpha and Sirtuin 1 and recapitulates hypoxia preconditioning in cardiac myocytes. *Circulation research*. 2009;104:879-86.
103. Hu S, Huang M, Li Z, Jia F, Ghosh Z, Lijkwan MA, Fasanaro P, Sun N, Wang X, Martelli F, Robbins RC and Wu JC. MicroRNA-210 as a novel therapy for treatment of ischemic heart disease. *Circulation*. 2010;122:S124-31.
104. Ren XP, Wu J, Wang X, Sartor MA, Jones K, Qian J, Nicolaou P, Pritchard TJ and Fan GC. MicroRNA-320 is involved in the regulation of cardiac ischemia/reperfusion injury by targeting heat-shock protein 20. *Circulation*. 2009;119:2357-2366.
105. Chen JF, Murchison EP, Tang R, Callis TE, Tatsuguchi M, Deng Z, Rojas M, Hammond SM, Schneider MD, Selzman CH, Meissner G, Patterson C, Hannon GJ and Wang DZ. Targeted deletion of Dicer in the heart leads to dilated cardiomyopathy and heart failure. *Proceedings of the National Academy of Sciences of the United States of America*. 2008;105:2111-6.
106. Rao PK, Toyama Y, Chiang HR, Gupta S, Bauer M, Medvid R, Reinhardt F, Liao R, Krieger M, Jaenisch R, Lodish HF and Blelloch R. Loss of cardiac microRNA-mediated regulation leads to dilated cardiomyopathy and heart failure. *Circulation research*. 2009;105:585-94.
107. Borden A, Kurian J, Nickoloff E, Yang Y, Troupes C, Ibeti J, Lucchese AM, Gao E, Mohsin S, Koch WJ, Houser SR, Kishore R and Khan M. Transient Introduction of miR-294 in the Heart Promotes Cardiomyocyte Cell Cycle Reentry After Injury. *Circulation research*. 2019.
108. Chen J, Huang ZP, Seok HY, Ding J, Kataoka M, Zhang Z, Hu X, Wang G, Lin Z, Wang S, Pu WT, Liao R and Wang DZ. mir-17-92 cluster is required for and sufficient to induce cardiomyocyte proliferation in postnatal and adult hearts. *Circulation research*. 2013;112:1557-66.
109. Gao F, Kataoka M, Liu N, Liang T, Huang ZP, Gu F, Ding J, Liu J, Zhang F, Ma Q, Wang Y, Zhang M, Hu X, Kyselovic J, Hu X, Pu WT, Wang J, Chen J and Wang DZ. Therapeutic role of miR-19a/19b in cardiac regeneration and protection from myocardial infarction. *Nature communications*. 2019;10:1802.
110. Porrello ER, Johnson BA, Aurora AB, Simpson E, Nam YJ, Matkovich SJ, Dorn GW, 2nd, van Rooij E and Olson EN. MiR-15 family regulates postnatal mitotic arrest of cardiomyocytes. *Circulation research*. 2011;109:670-9.
111. Porrello ER, Mahmoud AI, Simpson E, Johnson BA, Grinsfelder D, Canseco D, Mammen PP, Rothermel BA, Olson EN and Sadek HA. Regulation of neonatal and adult mammalian heart regeneration by the miR-15 family. *Proceedings of the National Academy of Sciences of the United States of America*. 2013;110:187-92.

REFERENCES

112. Tian Y, Liu Y, Wang T, Zhou N, Kong J, Chen L, Snitow M, Morley M, Li D, Petrenko N, Zhou S, Lu M, Gao E, Koch WJ, Stewart KM and Morrissey EE. A microRNA-Hippo pathway that promotes cardiomyocyte proliferation and cardiac regeneration in mice. *Science translational medicine*. 2015;7:279ra38.
113. Wahlquist C, Jeong D, Rojas-Munoz A, Kho C, Lee A, Mitsuyama S, van Mil A, Park WJ, Sluijter JP, Doevendans PA, Hajjar RJ and Mercola M. Inhibition of miR-25 improves cardiac contractility in the failing heart. *Nature*. 2014;508:531-5.
114. Lesizza P, Prosdocimo G, Martinelli V, Sinagra G, Zacchigna S and Giacca M. Single-Dose Intracardiac Injection of Pro-Regenerative MicroRNAs Improves Cardiac Function After Myocardial Infarction. *Circulation research*. 2017;120:1298-1304.
115. Porrello ER, Mahmoud AI, Simpson E, Hill JA, Richardson JA, Olson EN and Sadek HA. Transient regenerative potential of the neonatal mouse heart. *Science (New York, NY)*. 2011;331:1078-80.
116. Gabisonia K, Prosdocimo G, Aquaro GD, Carlucci L, Zentilin L, Secco I, Ali H, Braga L, Gorgodze N, Bernini F, Burchielli S, Collesi C, Zandona L, Sinagra G, Piacenti M, Zacchigna S, Bussani R, Recchia FA and Giacca M. MicroRNA therapy stimulates uncontrolled cardiac repair after myocardial infarction in pigs. *Nature*. 2019;569:418-422.
117. Sadek H and Olson EN. Toward the Goal of Human Heart Regeneration. *Cell stem cell*. 2020;26:7-16.
118. Xin M, Kim Y, Sutherland LB, Murakami M, Qi X, McAnally J, Porrello ER, Mahmoud AI, Tan W, Shelton JM, Richardson JA, Sadek HA, Bassel-Duby R and Olson EN. Hippo pathway effector Yap promotes cardiac regeneration. *Proceedings of the National Academy of Sciences of the United States of America*. 2013;110:13839-44.
119. Torrini C, Cubero RJ, Dirx E, Braga L, Ali H, Prosdocimo G, Gutierrez MI, Collesi C, Licastro D, Zentilin L, Mano M, Zacchigna S, Vendruscolo M, Marsili M, Samal A and Giacca M. Common Regulatory Pathways Mediate Activity of MicroRNAs Inducing Cardiomyocyte Proliferation. *Cell reports*. 2019;27:2759-2771.e5.
120. Janssen HL, Reesink HW, Lawitz EJ, Zeuzem S, Rodriguez-Torres M, Patel K, van der Meer AJ, Patick AK, Chen A, Zhou Y, Persson R, King BD, Kauppinen S, Levin AA and Hodges MR. Treatment of HCV infection by targeting microRNA. *The New England journal of medicine*. 2013;368:1685-94.
121. Taubel J, Hauke W, Rump S, Viereck J, Batkai S, Poetsch J, Rode L, Weigt H, Genschel C, Lorch U, Theek C, Levin AA, Bauersachs J, Solomon SD and Thum T. Novel antisense therapy targeting microRNA-132 in patients with heart failure: results of a first-in-human Phase 1b randomized, double-blind, placebo-controlled study. *European heart journal*. 2021;42:178-188.
122. Abplanalp WT, Fischer A, John D, Zeiher AM, Gosgnach W, Darville H, Montgomery R, Pestano L, Allee G, Paty I, Fougereuse F and Dimmeler S. Efficiency and Target Derepression of Anti-miR-92a: Results of a First in Human Study. *Nucleic Acid Ther*. 2020;30:335-345.
123. Attene-Ramos MS, Austin CP and Xia M. High Throughput Screening. In: P. Wexler, ed. *Encyclopedia of Toxicology (Third Edition)* Oxford: Academic Press; 2014: 916-917.
124. Malo N, Hanley JA, Cerquozzi S, Pelletier J and Nadon R. Statistical practice in high-throughput screening data analysis. *Nature biotechnology*. 2006;24:167-75.
125. Heallen TR, Kadow ZA, Kim JH, Wang J and Martin JF. Stimulating Cardiogenesis as a Treatment for Heart Failure. *Circulation research*. 2019;124:1647-1657.
126. Borden A, Kurian J, Nickoloff E, Yang Y, Troupes CD, Ibeti J, Lucchese AM, Gao E, Mohsin S, Koch WJ, Houser SR, Kishore R and Khan M. Transient Introduction of miR-

REFERENCES

- 294 in the Heart Promotes Cardiomyocyte Cell Cycle Reentry After Injury. *Circulation research*. 2019;125:14-25.
127. Streckfuss-Bomeke K, Wolf F, Azizian A, Stauske M, Tiburcy M, Wagner S, Hubscher D, Dressel R, Chen S, Jende J, Wulf G, Lorenz V, Schon MP, Maier LS, Zimmermann WH, Hasenfuss G and Guan K. Comparative study of human-induced pluripotent stem cells derived from bone marrow cells, hair keratinocytes, and skin fibroblasts. *European heart journal*. 2013;34:2618-29.
128. Borchert T, Hubscher D, Guessoum CI, Lam TD, Ghadri JR, Schellinger IN, Tiburcy M, Liaw NY, Li Y, Haas J, Sossalla S, Huber MA, Cyganek L, Jacobshagen C, Dressel R, Raaz U, Nikolaev VO, Guan K, Thiele H, Meder B, Wollnik B, Zimmermann WH, Luscher TF, Hasenfuss G, Templin C and Streckfuss-Bomeke K. Catecholamine-Dependent beta-Adrenergic Signaling in a Pluripotent Stem Cell Model of Takotsubo Cardiomyopathy. *Journal of the American College of Cardiology*. 2017;70:975-991.
129. Kim D, Langmead B and Salzberg SL. HISAT: a fast spliced aligner with low memory requirements. *Nat Methods*. 2015;12:357-60.
130. Pertea M, Pertea GM, Antonescu CM, Chang TC, Mendell JT and Salzberg SL. StringTie enables improved reconstruction of a transcriptome from RNA-seq reads. *Nature biotechnology*. 2015;33:290-5.
131. Mortazavi A, Williams BA, McCue K, Schaeffer L and Wold B. Mapping and quantifying mammalian transcriptomes by RNA-Seq. *Nat Methods*. 2008;5:621-8.
132. Frazee AC, Pertea G, Jaffe AE, Langmead B, Salzberg SL and Leek JT. Ballgown bridges the gap between transcriptome assembly and expression analysis. *Nature biotechnology*. 2015;33:243-6.
133. Roth GA, Johnson C, Abajobir A, Abd-Allah F, Abera SF, Abyu G, Ahmed M, Aksut B, Alam T, Alam K, Alla F, Alvis-Guzman N, Amrock S, Ansari H, Arnlov J, Asayesh H, Atey TM, Avila-Burgos L, Awasthi A, Banerjee A, Barac A, Barnighausen T, Barregard L, Bedi N, Belay Ketema E, Bennett D, Berhe G, Bhutta Z, Bitew S, Carapetis J, Carrero JJ, Malta DC, Castaneda-Orjuela CA, Castillo-Rivas J, Catala-Lopez F, Choi JY, Christensen H, Cirillo M, Cooper L, Jr., Criqui M, Cundiff D, Damasceno A, Dandona L, Dandona R, Davletov K, Dharmaratne S, Dorairaj P, Dubey M, Ehrenkranz R, El Sayed Zaki M, Faraon EJA, Esteghamati A, Farid T, Farvid M, Feigin V, Ding EL, Fowkes G, Gebrehiwot T, Gillum R, Gold A, Gona P, Gupta R, Habtewold TD, Hafezi-Nejad N, Hailu T, Hailu GB, Hankey G, Hassen HY, Abate KH, Havmoeller R, Hay SI, Horino M, Hotez PJ, Jacobsen K, James S, Javanbakht M, Jeemon P, John D, Jonas J, Kalkonde Y, Karimkhani C, Kasaeian A, Khader Y, Khan A, Khang YH, Khera S, Khoja AT, Khubchandani J, Kim D, Kolte D, Kosen S, Krohn KJ, Kumar GA, Kwan GF, Lal DK, Larsson A, Linn S, Lopez A, Lotufo PA, El Razek HMA, Malekzadeh R, Mazidi M, Meier T, Meles KG, Mensah G, Meretoja A, Mezgebe H, Miller T, Mirrakhimov E, Mohammed S, Moran AE, Musa KI, Narula J, Neal B, Ngalesoni F, Nguyen G, Obermeyer CM, Owolabi M, Patton G, Pedro J, Qato D, Qorbani M, Rahimi K, Rai RK, Rawaf S, Ribeiro A, Safiri S, Salomon JA, Santos I, Santric Milicevic M, Sartorius B, Schutte A, Sepanlou S, Shaikh MA, Shin MJ, Shishehbor M, Shore H, Silva DAS, Sobngwi E, Stranges S, Swaminathan S, Tabares-Seisdedos R, Tadele Atnafu N, Tesfay F, Thakur JS, Thrift A, Topor-Madry R, Truelsen T, Tyrovolas S, Ukwaja KN, Uthman O, Vasankari T, Vlassov V, Vollset SE, Wakayo T, Watkins D, Weintraub R, Werdecker A, Westerman R, Wiysonge CS, Wolfe C, Workicho A, Xu G, Yano Y, Yip P, Yonemoto N, Younis M, Yu C, Vos T, Naghavi M and Murray C. Global, Regional, and National Burden of Cardiovascular Diseases for 10 Causes, 1990 to 2015. *Journal of the American College of Cardiology*. 2017;70:1-25.
134. Braunwald E. The war against heart failure: the Lancet lecture. *Lancet (London, England)*. 2015;385:812-24.

REFERENCES

135. Ambrosy AP, Fonarow GC, Butler J, Chioncel O, Greene SJ, Vaduganathan M, Nodari S, Lam CSP, Sato N, Shah AN and Gheorghiade M. The global health and economic burden of hospitalizations for heart failure: lessons learned from hospitalized heart failure registries. *Journal of the American College of Cardiology*. 2014;63:1123-1133.
136. Barile L, Lionetti V, Cervio E, Matteucci M, Gherghiceanu M, Popescu LM, Torre T, Siclari F, Moccetti T and Vassalli G. Extracellular vesicles from human cardiac progenitor cells inhibit cardiomyocyte apoptosis and improve cardiac function after myocardial infarction. *Cardiovascular research*. 2014;103:530-41.
137. Foglio E, Puddighinu G, Fasanaro P, D'Arcangelo D, Perrone GA, Mocini D, Campanella C, Coppola L, Logozzi M, Azzarito T, Marzoli F, Fais S, Pieroni L, Marzano V, Germani A, Capogrossi MC, Russo MA and Limana F. Exosomal clusterin, identified in the pericardial fluid, improves myocardial performance following MI through epicardial activation, enhanced arteriogenesis and reduced apoptosis. *Int J Cardiol*. 2015;197:333-47.
138. Bersell K, Arab S, Haring B and Kuhn B. Neuregulin1/ErbB4 signaling induces cardiomyocyte proliferation and repair of heart injury. *Cell*. 2009;138:257-70.
139. Kuhn B, del Monte F, Hajjar RJ, Chang YS, Lebeche D, Arab S and Keating MT. Periostin induces proliferation of differentiated cardiomyocytes and promotes cardiac repair. *Nat Med*. 2007;13:962-9.
140. Xie S, Fu W, Yu G, Hu X, Lai KS, Peng X, Zhou Y, Zhu X, Christov P, Sawyer L, Ni TT, Sulikowski GA, Yang Z, Lee E, Zeng C, Wang WE and Zhong TP. Discovering small molecules as Wnt inhibitors that promote heart regeneration and injury repair. *J Mol Cell Biol*. 2020;12:42-54.
141. Lan F, Lee AS, Liang P, Sanchez-Freire V, Nguyen PK, Wang L, Han L, Yen M, Wang Y, Sun N, Abilez OJ, Hu S, Ebert AD, Navarrete EG, Simmons CS, Wheeler M, Pruitt B, Lewis R, Yamaguchi Y, Ashley EA, Bers DM, Robbins RC, Longaker MT and Wu JC. Abnormal calcium handling properties underlie familial hypertrophic cardiomyopathy pathology in patient-specific induced pluripotent stem cells. *Cell stem cell*. 2013;12:101-13.
142. Ma D, Wei H, Lu J, Ho S, Zhang G, Sun X, Oh Y, Tan SH, Ng ML, Shim W, Wong P and Liew R. Generation of patient-specific induced pluripotent stem cell-derived cardiomyocytes as a cellular model of arrhythmogenic right ventricular cardiomyopathy. *European heart journal*. 2013;34:1122-33.
143. Hamad S, Derichsweiler D, Papadopoulos S, Nguemo F, Saric T, Sachinidis A, Brockmeier K, Hescheler J, Boukens BJ and Pfannkuche K. Generation of human induced pluripotent stem cell-derived cardiomyocytes in 2D monolayer and scalable 3D suspension bioreactor cultures with reduced batch-to-batch variations. *Theranostics*. 2019;9:7222-7238.
144. Sacchetto C, Vitiello L, de Windt LJ, Rampazzo A and Calore M. Modeling Cardiovascular Diseases with hiPSC-Derived Cardiomyocytes in 2D and 3D Cultures. *Int J Mol Sci*. 2020;21.
145. Ong SG, Huber BC, Lee WH, Kodo K, Ebert AD, Ma Y, Nguyen PK, Diecke S, Chen WY and Wu JC. Microfluidic Single-Cell Analysis of Transplanted Human Induced Pluripotent Stem Cell-Derived Cardiomyocytes After Acute Myocardial Infarction. *Circulation*. 2015;132:762-771.
146. Tachibana A, Santoso MR, Mahmoudi M, Shukla P, Wang L, Bennett M, Goldstone AB, Wang M, Fukushi M, Ebert AD, Woo YJ, Rulifson E and Yang PC. Paracrine Effects of the Pluripotent Stem Cell-Derived Cardiac Myocytes Salvage the Injured Myocardium. *Circulation research*. 2017;121:e22-e36.

REFERENCES

147. Kawamura M, Miyagawa S, Miki K, Saito A, Fukushima S, Higuchi T, Kawamura T, Kuratani T, Daimon T, Shimizu T, Okano T and Sawa Y. Feasibility, safety, and therapeutic efficacy of human induced pluripotent stem cell-derived cardiomyocyte sheets in a porcine ischemic cardiomyopathy model. *Circulation*. 2012;126:S29-37.
148. Jung G and Bernstein D. hiPSC Modeling of Inherited Cardiomyopathies. *Curr Treat Options Cardiovasc Med*. 2014;16:320.
149. Yang C, Al-Aama J, Stojkovic M, Keavney B, Trafford A, Lako M and Armstrong L. Concise Review: Cardiac Disease Modeling Using Induced Pluripotent Stem Cells. *Stem cells (Dayton, Ohio)*. 2015;33:2643-51.
150. Pandey R, Velasquez S, Durrani S, Jiang M, Neiman M, Crocker JS, Benoit JB, Rubinstein J, Paul A and Ahmed RP. MicroRNA-1825 induces proliferation of adult cardiomyocytes and promotes cardiac regeneration post ischemic injury. *American journal of translational research*. 2017;9:3120-3137.
151. Duygu B, Poels EM, Juni R, Bitsch N, Ottaviani L, Olieslagers S, de Windt LJ and da Costa Martins PA. miR-199b-5p is a regulator of left ventricular remodeling following myocardial infarction. *Non-coding RNA research*. 2017;2:18-26.
152. Aguirre A, Montserrat N, Zacchigna S, Nivet E, Hishida T, Krause MN, Kurian L, Ocampo A, Vazquez-Ferrer E, Rodriguez-Esteban C, Kumar S, Moresco JJ, Yates JR, 3rd, Campistol JM, Sancho-Martinez I, Giacca M and Izpisua Belmonte JC. In vivo activation of a conserved microRNA program induces mammalian heart regeneration. *Cell stem cell*. 2014;15:589-604.
153. Huang W, Feng Y, Liang J, Yu H, Wang C, Wang B, Wang M, Jiang L, Meng W, Cai W, Medvedovic M, Chen J, Paul C, Davidson WS, Sadayappan S, Stambrook PJ, Yu XY and Wang Y. Loss of microRNA-128 promotes cardiomyocyte proliferation and heart regeneration. *Nature communications*. 2018;9:700.
154. Bentwich I, Avniel A, Karov Y, Aharonov R, Gilad S, Barad O, Barzilai A, Einat P, Einav U, Meiri E, Sharon E, Spector Y and Bentwich Z. Identification of hundreds of conserved and nonconserved human microRNAs. *Nature genetics*. 2005;37:766-70.
155. Noguer-Dance M, Abu-Amero S, Al-Khtib M, Lefevre A, Coullin P, Moore GE and Cavaille J. The primate-specific microRNA gene cluster (C19MC) is imprinted in the placenta. *Human molecular genetics*. 2010;19:3566-82.
156. de Rie D, Abugessaisa I, Alam T, Arner E, Arner P, Ashoor H, Astrom G, Babina M, Bertin N, Burroughs AM, Carlisle AJ, Daub CO, Detmar M, Deviatiiarov R, Fort A, Gebhard C, Goldowitz D, Guhl S, Ha TJ, Harshbarger J, Hasegawa A, Hashimoto K, Herlyn M, Heutink P, Hitchens KJ, Hon CC, Huang E, Ishizu Y, Kai C, Kasukawa T, Klinken P, Lassmann T, Lecellier CH, Lee W, Lizio M, Makeev V, Mathelier A, Medvedeva YA, Mejhert N, Mungall CJ, Noma S, Ohshima M, Okada-Hatakeyama M, Persson H, Rizzu P, Roudnicky F, Saetrom P, Sato H, Severin J, Shin JW, Swoboda RK, Tarui H, Toyoda H, Vitting-Seerup K, Winteringham L, Yamaguchi Y, Yasuzawa K, Yoneda M, Yumoto N, Zabierowski S, Zhang PG, Wells CA, Summers KM, Kawaji H, Sandelin A, Rehli M, Hayashizaki Y, Carninci P, Forrest ARR and de Hoon MJL. An integrated expression atlas of miRNAs and their promoters in human and mouse. *Nature biotechnology*. 2017;35:872-878.
157. Ludwig N, Leidinger P, Becker K, Backes C, Fehlmann T, Pallasch C, Rheinheimer S, Meder B, Stahler C, Meese E and Keller A. Distribution of miRNA expression across human tissues. *Nucleic acids research*. 2016;44:3865-77.
158. Laurent LC, Chen J, Ulitsky I, Mueller FJ, Lu C, Shamir R, Fan JB and Loring JF. Comprehensive microRNA profiling reveals a unique human embryonic stem cell signature dominated by a single seed sequence. *Stem cells (Dayton, Ohio)*. 2008;26:1506-16.

REFERENCES

159. Wu S, Huang S, Ding J, Zhao Y, Liang L, Liu T, Zhan R and He X. Multiple microRNAs modulate p21Cip1/Waf1 expression by directly targeting its 3' untranslated region. *Oncogene*. 2010;29:2302-8.
160. Zhang M, Muralimanoharan S, Wortman AC and Mendelson CR. Primate-specific miR-515 family members inhibit key genes in human trophoblast differentiation and are upregulated in preeclampsia. *Proceedings of the National Academy of Sciences of the United States of America*. 2016;113:E7069-e7076.
161. Donker RB, Mouillet JF, Chu T, Hubel CA, Stolz DB, Morelli AE and Sadovsky Y. The expression profile of C19MC microRNAs in primary human trophoblast cells and exosomes. *Molecular human reproduction*. 2012;18:417-24.
162. Kim KH, Jung JY, Son ED, Shin DW, Noh M and Lee TR. miR-526b targets 3' UTR of MMP1 mRNA. *Experimental & molecular medicine*. 2015;47:e178.
163. Xu S, Webb SE, Lau TCK and Cheng SH. Matrix metalloproteinases (MMPs) mediate leukocyte recruitment during the inflammatory phase of zebrafish heart regeneration. *Scientific reports*. 2018;8:7199.
164. Bayer A, Lennemann NJ, Ouyang Y, Sadovsky E, Sheridan MA, Roberts RM, Coyne CB and Sadovsky Y. Chromosome 19 microRNAs exert antiviral activity independent from type III interferon signaling. *Placenta*. 2018;61:33-38.
165. Mouillet JF, Ouyang Y, Bayer A, Coyne CB and Sadovsky Y. The role of trophoblastic microRNAs in placental viral infection. *The International journal of developmental biology*. 2014;58:281-9.
166. Sereti KI, Nguyen NB, Kamran P, Zhao P, Ranjbarvaziri S, Park S, Sabri S, Engel JL, Sung K, Kulkarni RP, Ding Y, Hsiai TK, Plath K, Ernst J, Sahoo D, Mikkola HKA, Iruela-Arispe ML and Ardehali R. Analysis of cardiomyocyte clonal expansion during mouse heart development and injury. *Nature communications*. 2018;9:754.
167. Di Stefano V, Giacca M, Capogrossi MC, Crescenzi M and Martelli F. Knockdown of cyclin-dependent kinase inhibitors induces cardiomyocyte re-entry in the cell cycle. *The Journal of biological chemistry*. 2011;286:8644-54.
168. Pagano M, Pepperkok R, Verde F, Ansorge W and Draetta G. Cyclin A is required at two points in the human cell cycle. *The EMBO journal*. 1992;11:961-71.
169. Shapiro SD, Ranjan AK, Kawase Y, Cheng RK, Kara RJ, Bhattacharya R, Guzman-Martinez G, Sanz J, Garcia MJ and Chaudhry HW. Cyclin A2 induces cardiac regeneration after myocardial infarction through cytokinesis of adult cardiomyocytes. *Science translational medicine*. 2014;6:224ra27.
170. Bicknell KA, Coxon CH and Brooks G. Forced expression of the cyclin B1-CDC2 complex induces proliferation in adult rat cardiomyocytes. *The Biochemical journal*. 2004;382:411-6.
171. Wu Q, Zhang W, Mu T, Song T and Li D. Aurora B kinase is required for cytokinesis through effecting spindle structure. *Cell Biol Int*. 2013;37:436-42.
172. Bassat E, Mutlak YE, Genzelinakh A, Shadrin IY, Baruch Umansky K, Yifa O, Kain D, Rajchman D, Leach J, Riabov Bassat D, Udi Y, Sarig R, Sagi I, Martin JF, Bursac N, Cohen S and Tzahor E. The extracellular matrix protein agrin promotes heart regeneration in mice. *Nature*. 2017;547:179-184.
173. Piccini I, Rao J, Seebohm G and Greber B. Human pluripotent stem cell-derived cardiomyocytes: Genome-wide expression profiling of long-term in vitro maturation in comparison to human heart tissue. *Genomics data*. 2015;4:69-72.
174. Sassi Y, Avramopoulos P, Ramanujam D, Gruter L, Werfel S, Giosele S, Brunner AD, Esfandyari D, Papadopoulou AS, De Strooper B, Hubner N, Kumarswamy R, Thum T, Yin X, Mayr M, Laggerbauer B and Engelhardt S. Cardiac myocyte miR-29 promotes

REFERENCES

pathological remodeling of the heart by activating Wnt signaling. *Nature communications*. 2017;8:1614.

175. Kimura W, Xiao F, Canseco DC, Muralidhar S, Thet S, Zhang HM, Abderrahman Y, Chen R, Garcia JA, Shelton JM, Richardson JA, Ashour AM, Asaithamby A, Liang H, Xing C, Lu Z, Zhang CC and Sadek HA. Hypoxia fate mapping identifies cycling cardiomyocytes in the adult heart. *Nature*. 2015;523:226-30.

13. STATUTORY DECLARATION

“I, Harsha Vardhan Renikunta, by personally signing this document in lieu of an oath, hereby affirm that I prepared the submitted dissertation on the topic, **“Identifizierung von microRNAs für die Proliferation von humanen Kardiomyozyten (iPSC-CM) mittels funktionellem Hochdurchsatzverfahren.”**. **“Identification of microRNAs promoting proliferation in human induced pluripotent stem cell-derived cardiomyocytes using a functional high-throughput screening”** independently and without the support of third parties, and that I used no other sources and aids than those stated.

All parts, which are based on the publications or presentations of other authors, either in letter or in spirit, are specified as such in accordance with the citing guidelines. The sections on methodology (in particular regarding practical work, laboratory regulations, statistical processing) and results (in particular regarding figures, charts and tables) are exclusively my responsibility.

Furthermore, I declare that I have correctly marked all of the data, the analyses, and the conclusions generated from data obtained in collaboration with other persons, and that I have correctly marked my own contribution and the contributions of other persons. I have correctly marked all texts or parts of texts that were generated in collaboration with other persons.

My contributions to any publications to this dissertation correspond to those stated in the below joint declaration made together with the supervisor. All publications created within the scope of the dissertation comply with the guidelines of the ICMJE (International Committee of Medical Journal Editors (www.icmje.org)) on authorship. In addition, I declare that I shall comply with the regulations of Charité – Universitätsmedizin Berlin on ensuring good scientific practice.

I declare that I have not yet submitted this dissertation in identical or similar form to another Faculty.

The significance of this statutory declaration and the consequences of a false statutory declaration under criminal law (Sections 156, 161 of the German Criminal Code) are known to me.”

Date

Signature

14. CURRICULUM VITAE

"My curriculum vitae does not appear in the electronic version of my paper for reasons of data protection."

CURRICULUM VITAE

"My curriculum vitae does not appear in the electronic version of my paper for reasons of data protection."

CURRICULUM VITAE

"My curriculum vitae does not appear in the electronic version of my paper for reasons of data protection."

15. ACKNOWLEDGEMENTS

First and foremost, I would like to thank my supervisors, Dr. med. Philipp Jakob, and Prof. Dr. med. Ulf Landmesser for their constant support and guidance throughout my project. I sincerely express my gratitude to Prof. Landmesser, for providing me an opportunity to perform my PhD thesis in his research laboratory at the Department of Cardiology, Charité- University Medicine Berlin.

My greatest admiration to my co-supervisor, Dr. med. Philipp Jakob. It is my privilege to work under Dr. P. Jakob, who guided me through the entire path of my PhD, teaching and helping me to gain more exposure in the field of regenerative cardiovascular medicine. This thesis would never have been accomplished without his reassurance and encouragement. I am extremely grateful for his empathy, his friendliness, and his great sense of humor.

I feel honored to be a student of the very prestigious graduate school “Berlin-Brandenburg School for Regenerative Therapies” (BSRT). Especially, I want to express my gratitude to Dr. Sabine Bartosch and Bianca Kühn, who supported me throughout the structured courses, and for guiding through the application process to receive a doctoral stipend.

I am very grateful to Prof. Felix B. Engel, Dr. Katina Lazarow, PD Dr. rer. nat. Katrin Streckfuß-Bömeke, and Dr. Ajit Magadum for their constant support in my project during the last years. I would thank all my colleagues for their support.

My special thanks to Prof. Dr. Praphulla Chandra Shukla, Dr. Rajkumar Vutukuri, Dr. Hector Giral Arnal and Dr. Adelheid Kratzer, for their constant support, with special coffee breaks, and helping me to explore more possibilities in my career.

Finally, I would like to thank my parents Dr. Rajesh Kumar Renikunta, Anjali Renikunta, and my friends for their loving support, encouragement, and understanding.